

Aims and Scope: The "Cell Journal (Yakhteh)" is a peer review and monthly English publication of Royan Institute of Iran. The aim of the journal is to disseminate information through publishing the most recent scientific research studies on exclusively Cellular, Molecular and other related topics. **Cell J**, has been certified by the Ministry of Culture and Islamic Guidance since 1999 and also accredited as a scientific and research journal by HBI (Health and Biomedical Information) Journal Accreditation Commission since 2000 which is an open access journal. **This journal holds the membership of the Committee on Publication Ethics (COPE).**

1. Types of articles

The articles in the field of Cellular and Molecular can be considered for publications in **Cell J**. These articles are as below:

A. Original articles

Original articles are scientific reports of the original research studies. The article consists of English Abstract (structured), Introduction, Materials and Methods, Results, Discussion, Conclusion, Acknowledgements, Author's Contributions, and References (**Up to 40**).

B. Review articles

Review articles are the articles written by well experienced authors and those who have excellence in the related fields. The corresponding author of the review article must be one of the authors of at least three published articles appearing in the references. The review article consists of English Abstract (unstructured), Introduction, Conclusion, Author's Contributions, and References (**Up to 70**).

C. Systematic Reviews

Systematic reviews are a type of literature review that collect and critically analyzes multiple research studies or papers. The Systematic reviews consist of English Abstract (unstructured), Introduction, Materials and Methods, Results, Discussion, Conclusion, Acknowledgements, Author's Contributions, and References (**Up to 70**).

D. Short communications

Short communications are articles containing new findings. Submissions should be brief reports of ongoing researches. The short communication consists of English Abstract (unstructured), the body of the manuscript (should not hold heading or sub-heading), Acknowledgements, Author's Contributions, and References (**Up to 30**).

E. Case reports

Case reports are short discussions of a case or case series with unique features not previously described which make an important teaching point or scientific observation. They may describe novel techniques or use equipment, or new information on diseases of importance. It consists of English Abstracts (Unstructured), Introduction, Case Report, Discussion, Acknowledgements, Author's Contributions, and References (**Up to 30**).

F. Editorial

Editorials are articles should be written in relevant and new data of journals' filed by either the editor in chief or the editorial board.

G. Imaging in biology

Images in biology should focus on a single case with an interesting illustration such as a photograph, histological specimen or investigation. Color images are welcomed. The text should be brief and informative.

H. Letter to the editors

Letter to the editors are in response to previously published **Cell J** articles, and may also include interesting cases that do not meet the requirement of being truly exceptional, as well as other brief technical or clinical notes of general interest.

I. Debate

Debates are articles which show a discussion of the positive and negative view of the author concerning all aspect of the issue relevant to scientific research.

2. Submission process

It is recommended to see the guidelines for reporting different kinds of manuscripts. This guide explains how to prepare the

manuscript for submission. Before submitting, we suggest authors to familiarize themselves with **Cell J** format and content by reading the journal via the website (www.celljournal.org). The corresponding author ensures that all authors are included in the author list and agree with its order, and they must be aware of the manuscript submission.

A. Author contributions statements

It is essential for authors to include a statement of responsibility in the manuscript that specifies the contribution of every one of them. This participation must include conception and design of the manuscript, data acquisition or data analysis and interpretation, drafting of the manuscript and/or revising it for critically important intellectual content, revision and final approval of the manuscript and statistical analysis, obtaining funding, administrative, technical, or material support, or supervision. Authors who do not meet the above criteria should be acknowledged in the **Acknowledgments section**.

B. Cover letter and copyright

Each manuscript should be accompanied by a cover letter, signed by all authors specifying the following statement: "The manuscript has been seen and approved by all authors and is not under active consideration for publication. It has neither been accepted for publication nor published in another journal fully or partially (except in abstract form). **Also, no manuscript would be accepted in case it has been pre-printed or submitted to other websites.** I hereby assign the copyright of the enclosed manuscript to **Cell J**." Corresponding author must confirm the proof of the manuscript before online publishing. Also, it is needed to suggest three peer reviewers in the field of their manuscript.

C. Manuscript preparation

Authors whose first language is not English encouraged to consult a native English speaker in order to confirm his manuscripts to American or British (not a mixture) English usage and grammar. It is necessary to mention that we will check the plagiarism of your manuscript by iThenticate Software. The manuscript should be prepared in accordance with the "International Committee of Medical Journal Editors (ICMJE)". Please send your manuscript in two formats word and PDF (including: title, name of all the authors with their degree, abstract, full text, references, tables and figures) and also send tables and figures separately in the site. The abstract and text pages should have consecutive line numbers in the left margin beginning with the title page and continuing through the last page of the written text. Each abbreviation must be defined in the abstract and text when they are mentioned for the first time. Avoid using abbreviation in the title. Please use the international and standard abbreviations and symbols

It should be added that an essential step toward the integration and linking of scientific information reported in published literature is using standardized nomenclature in all fields of science and medicine. Species names must be italicized (*e.g.*, *Homo sapiens*) and also the full genus and species written out in full, both in the title of the manuscript and at the first mention of an organism in a paper.

It is necessary to mention that genes, mutations, genotypes, and alleles must be indicated in italics. Please use the recommended name by consulting the appropriate genetic nomenclature database, *e.g.*, HUGO for human genes. In another words; if it is a human gene, you must write all the letters in capital and italic (*e.g.*, *OCT4*, *c-MYC*). If not, only write the first letter in capital and italic (*e.g.*, *Oct4*, *c-Myc*). **In addition, protein designations are the same as the gene symbol but are not italicized.**

Of note, Cell J will only consider publishing genetic association study papers that are novel and statistically robust. Authors are advised to adhere to the recommendations outlined in the STREGA statement (<http://www.strega-statement.org>). The following criteria must be met for all submissions:

1. Hardy-Weinberg Equilibrium (HWE) calculations must be carried out and reported along with the P-values if applicable [see Namipashaki et al. 2015 (Cell J, Vol 17, N 2, Pages: 187-192) for a discussion].
2. Linkage disequilibrium (LD) structure between SNPs (if multiple SNPs are reported) must be presented.
3. Appropriate multiple testing correction (if multiple independent SNPs are reported) must be included.

Submissions that fail to meet the above criteria will be rejected before being sent out for review.

Each of the following manuscript components should begin in the following sequence:

Authors' names and order of them must be carefully considered (full name(s), highest awarded academic degree(s), email(s), and institutional affiliation(s) of all the authors in English. Also, you must send mobile number and full postal address of the corresponding author).

Changes to Authorship such as addition, deletion or rearrangement of author names must be made only before the manuscript has been accepted in the case of approving by the journal editor. In this case, the corresponding author must explain the reason of changing and confirm them (which has been signed by all authors of the manuscript). If the manuscript has already been published in an online issue, an erratum is needed.

Title is providing the full title of the research (do not use abbreviations in title).

Running title is providing a maximum of 7 words (no more than 50 characters).

Abstract must include Objective, Materials and Methods, Results, and Conclusion (no more than 300 words).

Keywords, three to five, must be supplied by the authors at the foot of the abstract chosen from the Medical Subject Heading (MeSH). Therefore; they must be specific and relevant to the paper.

The following components should be identified after the abstract:

Introduction: The Introduction should provide a brief background to the subject of the paper, explain the importance of the study, and state a precise study question or purpose.

Materials and Methods: It includes the exact methods or observations of experiments. If an apparatus is used, its manufacturer's name and address should be stipulated in parenthesis. If the method is established, give reference but if the method is new, give enough information so that another author can perform it. If a drug is used, its generic name, dose, and route of administration must be given. Standard units of measurements and chemical symbols of elements do not need to be defined.

Statistical analysis: Type of study and statistical methods should be mentioned and specified by any general computer program used.

Ethical considerations: Please state that informed consent was obtained from all human adult participants and from the parents or legal guardians of minors and include the name of the appropriate institutional review board that approved the project. It is necessary to indicate in the text that the maintenance and care of experimental animals complies with National Institutes of Health guidelines for the humane use of laboratory animals, or those of your Institute or agency.

Clinical trial registration: All of the Clinical Trials performing in Iran must be registered in Iranian Registry of Clinical Trials (www.irct.ir). The clinical trials performed abroad, could be considered for publication if they register in a registration site approved by WHO or www.clinicaltrials.gov. If you are reporting phase II or phase III randomized controlled trials, you must refer to the CONSORT Statement for recommendations to facilitate the complete and transparent reporting of trial findings. Reports that do not conform to the CONSORT guidelines may need to be revised before peer-reviewing.

Results: They must be presented in the form of text, tables, and figures. Take care that the text does not repeat data that are presented in tables and/or figures. Only emphasize and summarize the essential features of the main results. Tables and figures must be numbered consecutively as appeared in the text and should be organized in separate pages at the end of the manuscript while their location should be mentioned in the main text.

Tables and figures: If the result of your manuscript is too short, it is better to use the text instead of tables & figures. Tables should have a short descriptive heading above them and also any footnotes. Figure's caption should contain a brief title for the whole figure and continue with a short explanation of each part and also the symbols used (no more than 100 words). All figures must be prepared based on cell journal's guideline in color (no more than 6 Figures and Tables) and also in TIF format with 300 DPI resolution.

Of Note: Please put the tables & figures of the result in the results section not any other section of the manuscript.

Supplementary materials would be published on the online version of the journal. This material is important to the understanding and interpretation of the report and should not repeat material within the print article. The amount of supplementary material should be limited. Supplementary material should be original and not previously published and will undergo editorial and peer review with the main manuscript. Also, they must be cited in the manuscript text in parentheses, in a similar way as when citing a figure or a table. Provide a caption for each supplementary material submitted.

Discussion: It should emphasize the present findings and the variations or similarities with other researches done by other researchers. The detailed results should not be repeated in the discussion again. It must emphasize the new and important aspects of the study.

Conclusion: It emphasizes the new and important aspects of the study. All conclusions are justified by the results of the study.

Acknowledgements: This part includes a statement thanking those who contributed substantially with work relevant to the study but does not have authorship criteria. It includes those who provided technical help, writing assistance and name of departments that provided only general support. You must mention financial support in the study. Otherwise; write this sentence "There is no financial support in this study".

Conflict of interest: Any conflict of interest (financial or otherwise) and sources of financial support must be listed in the Acknowledgements. It includes providers of supplies and services from a commercial organization. Any commercial affiliation must be disclosed, regardless of providing the funding or not.

Of Note: If you have already any patent related to the subject of your manuscript, or you are going to apply for such a patent, it must be mentioned in this part.

References: The references must be written based on the Vancouver style. Thus the references are cited numerically in the text and listed in the bibliography by the order of their appearance. The titles of journals must be abbreviated according to the style used in the list of Journals Indexed in PubMed. Write surname and initials of all authors when there are six or less. In the case of seven or more authors, the names of the first six authors followed by "et al." must be listed. You can download Endnote file for Journal references style: endnote file

The reference of information must be based on the following order:

Article:

Surname(s) and first letter of name & middle name(s) of author(s). Manuscript title. Journal title (abbr). publication date (year); Volume & Issue: Page number.

Example: Manicardi GC, Bianchi PG, Pantano S, Azzoni P, Bizzaro D, Bianchi U, et al. Presence of endogenous nicks in DNA of ejaculated human spermatozoa and its relationship to chromomycin A3 accessibility. *Biol Reprod.* 1995; 52(4): 864-867.

Book:

Surname(s) and first letter of name & middle name(s) of author(s). Book title. Edition. Publication place: publisher name; publication date (year); Page number.

Example: Edelman CL, Mandle CL. Health promotion throughout the lifespan. 2nd ed. ST Louis: Mosby; 1998; 145-163.

Chapter of book:

Surname(s) and first letter of name & middle name(s) of author(s). Chapter title. In: Surname(s) and first letter of name & middle name(s) of editor(s), editors. Book title. Edition. Publication place: publisher name; publication date (year); Page number.

Example: Phillips SJ, Whisnant JP. Hypertension and stroke. In: Laragh JH, Brenner BM, editors. Hypertension: pathophysiology, diagnosis, and management. 2nd ed. New York: Raven Press; 1995; 465-478.

Abstract book:

Example: Amini rad O. The antioxidant effect of pomegranate juice on sperm parameters and fertility potential in mice. *Cell J.* 2008;10 Suppl 1:38.

Thesis:

Name of author. Thesis title. Degree. City name. University. Publication date (year).

Example: Eftekhari Yazdi P. Comparison of fragment removal and co-culture with Vero cell monolayers on development of human fragmented embryos. Presented for the Ph.D., Tehran. Tarbiyat Modarres University. 2004.

Internet references

Article:

Example: Jahanshahi A, Mirnajafi-Zadeh J, Javan M, Mohammad-Zadeh M, Rohani M. Effect of low-frequency stimulation on adenosine A1 and A2A receptors gene expression in dentate gyrus of perforant path kindled rats. *Cell J.* 2008; 10 (2): 87-92. Available from: <http://www.celljournal.org>. (20 Oct 2008).

Book:

Example: Anderson SC, Poulsen KB. Anderson's electronic atlas of hematology.[CD-ROM]. Philadelphia: Lippincott Williams & Wilkins; 2002.

D. Proofs are sent by email as PDF files and should be checked and returned within 72 hours of receipt. It is the authors' responsibility to check that all the text and data as contained in the page proofs are correct and suitable for publication. **We are requested to pay particular attention to author's names and affiliations as it is essential that these details be accurate when the article is published.**

E. Pay for publication: Publishing an article in **Cell J** requires Article Processing Charges (APC) that will be billed to the submitting author following the acceptance of an article for publication. For more information please see www.celljournal.org.

F. Ethics of scientific publication: Manuscripts that have been published elsewhere with the same intellectual material will refer to duplicate publication. If authors have used their own previously published work or work that is currently under review, as the basis for a submitted manuscript, they are required to cite the previous work and indicate how their submitted manuscript offers novel contributions beyond those of the previous work. Research and publication misconduct is considered a serious breach of ethics.

The Journal systematically employs iThenticate, plagiarism detection and prevention software designed to ensure the originality of written work before publication. Plagiarism of text from a previously published manuscript by the same or another author is a serious publication offence. Some parts of text may be used, only where the source of the quoted material is clearly acknowledged.

3. General information

A. You can send your manuscript via online submission system which is available on our website. If the manuscript is not prepared according to the format of **Cell J**, it will be returned to authors.

B. The order of article appearance in the Journal is not demonstrating the scientific characters of the authors.

C. **Cell J** has authority to accept or reject the manuscript.

D. The received manuscript will be evaluated by associate editor. **Cell J** uses a single-blind peer review system and if the manuscript suits the journal criteria, we select the reviewers. If three reviewers pass their judgments on the manuscript, it will be presented to the editorial board of **Cell J**. If the editorial board has a positive judgment about the manuscript, reviewers' comments will be presented to the corresponding author (the identification of the reviewers will not be revealed). The executive member of journal will contact the corresponding author directly within 3-4 weeks by email. If authors do not receive any reply from journal office after the specified time, they can contact journal office. Finally, executive manager will respond promptly to authors' request.

The Final Checklist

The authors must ensure that before submitting the manuscript for publication, they have to consider the following parts:

1. The first page of manuscript should contain title, name of the author/coauthors, their academic qualifications, designation & institutions they are affiliated with, mailing address for future correspondence, email address, phone, and fax number.
2. Text of manuscript and References prepared as stated in the "guide for authors" section.
3. Tables should be on a separate page. Figures must be sent in color and also in JPEG (Jpg) format.
4. Cover Letter should be uploaded with the signature of all authors.
5. An ethical committee letter should be inserted at the end of the cover letter.

The Editor-in-Chief: Ahmad Hosseini, Ph.D.

Cell Journal (Yakhteh)

P.O. Box: 16635-148, Iran

Tel/Fax: + 98-21-22510895

Emails: Celljournal@royaninstitute.org

info@celljournal.org





IN THE NAME OF GOD

Gone But not Forgotten

In the memory of the late Director of Royan Institute,
Founder of Stem Cells Research in Iran and Chairman of
Cell Journal (Yakhteh). May he rest in peace.

Dr. Saeed Kazemi Ashtiani

OWNED:

Royan Institute, Iranian Academic Center for Education Culture and Research (ACECR)

CHAIRMAN:

Hamid Gourabi, Ph.D., (Professor, Royan Institute, Tehran, Iran)

EDITOR IN CHIEF:

Ahmad Hosseini, Ph.D., (Professor, Shahid Beheshti Medical University, Tehran, Iran)

EDITOR ASSOCIATE:

Saeid Abroun, Ph.D., (Professor, Tarbiat Modares University, Tehran, Iran)

EDITORIAL BOARD:

Saeid Abroun, Ph.D., (Professor, Tarbiat Modares University, Tehran, Iran)

Kamran Alimoghdam, M.D., (Associate Professor, Tehran Medical University, Tehran, Iran)

Alireza Asgari, Ph.D., (Professor, Baghyatallah University, Tehran, Iran)

Mohammad Kazem Aghaee Mazaheri, D.D.S., (Assistant Professor, ACECR, Tehran, Iran)

Mohamadreza Baghaban Eslaminejad, Ph.D., (Professor, Royan Institute, Tehran, Iran)

Gila Behzadi, Ph.D., (Professor, Shahid Beheshti Medical University, Tehran, Iran)

Hossein Baharvand, Ph.D., (Professor, Royan Institute, Tehran, Iran)

Marzieh Ebrahimi, Ph.D., (Professor, Royan Institute, Tehran, Iran)

Mary Familiar, Ph.D., (Senior Lecturer, University of Melbourne, Melbourne, Australia)

Hamid Gourabi, Ph.D., (Professor, Royan Institute, Tehran, Iran)

Jurgen Hescheler, M.D., (Professor, Institute of Neurophysiology of University Zu Koln, Germany)

Ghasem Hosseini Salekdeh, Ph.D., (Professor, Agricultural Biotechnology Research Institute, Karaj, Iran)

Esmail Jabbari, Ph.D., (Associate Professor, University of South Carolina, Columbia, USA)

Suresh Jesuthasan, Ph.D., (Associate Professor, National University of Singapore, Singapore)

Bahram Kazemi, Ph.D., (Professor, Shahid Beheshti Medical University, Tehran, Iran)

Saadi Khochbin, Ph.D., (Professor, Inserm/Grenoble University, France)

Ali Khademhosseini, Ph.D., (Professor, Harvard Medical School, USA)

Kun Ping Lu, M.D., Ph.D., (Professor, Harvard Medical School, Boston, USA)

Navid Manuchehrabadi, Ph.D., (Angio Dynamics, Marlborough, USA)

Hossein Ali Mehrani, Ph.D., (Professor, Baghyatallah University, Tehran, Iran)

Marcos Meseguer, Ph.D., (Clinical Embryology Laboratory IVI Valencia, Valencia, Spain)

Seyed Javad Mowla, Ph.D., (Professor, Tarbiat Modares University, Tehran, Iran)

Mohammad Hossein Nasr Esfahani, Ph.D., (Professor, Royan Institute, Tehran, Iran)

Toru Nakano, M.D., Ph.D., (Professor, Osaka University, Osaka, Japan)

Donald Newgreen, Ph.D., (Professor, Murdoch Children Research Institute, Melbourne, Australia)

Mojtaba Rezazadeh Valojerdi, Ph.D., (Professor, Tarbiat Modares University, Tehran, Iran)

Mohammad Hossein Sanati, Ph.D., (Associate Professor, National Institute for Genetic Engineering and Biotechnology, Tehran, Iran)

Eimei Sato, Ph.D., (Professor, Tohoku University, Sendai, Japan)

Andreas Serra, M.D., (Professor, University of Zurich, Zurich, Switzerland)

Abdolhossein Shahverdi, Ph.D., (Professor, Royan Institute, Tehran, Iran)

Michele Catherine Studer, Ph.D., (Institute of Biology Valrose, IBV University of Nice Sophia-Antipolis, France)

Peter Timashev, Ph.D., (Sechenov University, Moscow, Russia)

Daniela Toniolo, Ph.D., (Head, Unit of Common Disorders, San Raffaele Research Institute, Milano, Italy)

Christian van den Bos, Ph.D., Managing Director MARES Ltd, Greven, Germany

Catherine Verfaillie, Ph.D., (Professor, Katholie Universiteit Leuven, Leuven, Belgium)

Gianpaolo Zerbini, M.D., Ph.D., (San Raffaele Scientific Institute, Italy)

Shubing Zhang, Ph.D., (Associate Professor, Central South University, China)

Daniele Zink, Ph.D., (Institute of Bioengineering and Nanotechnology, Agency for Science Technology & Science, Singapore)

EXECUTIVE MANAGER:

Farideh Malekzadeh, M.Sc., (Royan Institute, Tehran, Iran)

EXECUTIVE BOARD:

Parvaneh Afsharian, Ph.D., (Royan Institute, Tehran, Iran)
Reza Azimi, B.Sc., (Royan Institute, Tehran, Iran)
Reza Omani-Samani, M.D., (Royan Institute, Tehran, Iran)
Elham Amirchaghmaghi, M.D., Ph.D., (Royan Institute, Tehran, Iran)
Leila Daliri, M.Sc., (Royan Institute, Tehran, Iran)
Mahdi Lotfipanah, M.Sc., (Royan Institute, Tehran, Iran)
Faezeh Shekari, Ph.D., (Royan Institute, Tehran, Iran)

ENGLISH EDITOR:

Mitra Amiri Khabooshan, Ph.D., (Monash University, Victoria, Australia)
Sima Binaafar, M. Sc., (Royan Institute, Tehran, Iran)
Saman Eghtesad, Ph.D., (Royan Institute, Tehran, Iran)
Jane Elizabeth Ferrie, Ph.D., (University College of London, London, UK)
Vahid Ezzatizadeh, Ph.D., (Royan Institute, Tehran, Iran)
Kiana Kakavand, Ph.D., (University of Melbourne, Melbourne, Australia)
Farnaz Shapouri, Ph.D., (Memphasys Limited, NSW, Australia)
Kim Vagharfard, M.Sc., (Royan Institute, Tehran, Iran)
Maryam Vatani, M.Sc., (University of Calgary, Canada)

GRAPHICS:

Laleh Mirza Ali Shirvani, B.Sc., (Royan Institute, Tehran, Iran)

PUBLISHED & SPONSORED BY:

Publication of Royan Institute (ACECR)

Indexed in:

1. Thomson Reuters (ISI)
2. PubMed
3. PubMed Central (PMC)
4. National Library Medicine (NLM)
5. Biosis Preview
6. Index Medicus for the Eastern Mediterranean Region (IMEMR)
7. Regional Information Center for Sciences and Technology (RICeST)
8. Index Copernicus International
9. Cambridge Scientific Abstract (CSA)
10. EMBASE
11. Scopus
12. Cinahl Database
13. Google Scholar
14. Chemical Abstract Service (CAS)
15. Proquest
16. Directory of Open Access Journals (DOAJ)
17. Open Academic Journals Index (OAJI)
18. Directory of Research Journals Indexing (DRJI)
19. Scientific Information Database (SID)
20. Iranmedex
21. Islamic World Science Citation Center (ISC)
22. Magiran
23. Science Library Index
24. Biological Abstracts
25. Essential Science Indicators
26. EuroPub

ACECR**Copyright and license information:**

The **Cell Journal**^(Yakhteh) is an open access journal which means the articles are freely available online for any individual author to download and use the providing address. The journal is licensed under a Creative Commons Attribution-Non Commercial 3.0 Unported License which allows the author(s) to hold the copyright without restrictions that is permitting unrestricted non-commercial use, distribution, and reproduction in any medium provided the original work is properly cited.

Editorial Office Address (Dr. Ahmad Hosseini):

Royan Institute, P.O.Box: 16635-148,
Tehran, Iran
Tel & Fax: (+9821)22510895
Website: www.celljournal.org
Emails: info@celljournal.org
celljournal@royaninstitute.org

Printing Company:

Naghshe e Johar Co.
No. 103, Fajr alley, Tehranpars Street,
Tehran, Iran.



CONTENTS

Review Articles

• **Vulnerability of The Male Reproductive System to SARS-CoV-2 Invasion: Potential Role for The Endoplasmic Reticulum Chaperone Grp78/HSPA5/BiP**

Niloofer Sadeghi, Marziyeh Tavalaei, Abdolhossein Shahverdi, Pallav Sengupta, Kristian Leisegang, Ramadan Saleh, Ashok Agarwal, Mohammad Hossein Nasr-Esfahani 427

• **Strategies for Mammalian Mesenchymal Stem Cells Differentiation into Primordial Germ Cell-Like Cells: A Review**

Shabnam Fayezi, Parisa Fayyazpour, Zahra Norouzi, Amir Mehdizadeh 434

Original Articles

• **The Effect of miR-106b-5p Expression in The Production of iPS-Like Cells from Mice SSCs during The Formation of Teratoma and The Three Embryonic Layers**

Amir Hossein Hasani Fard, Fatemeh Kamalipour, Zohreh Mazaheri, Seyed Jalil Hosseini 442

• **Differentiation of Alginate-Encapsulated Wharton Jelly-Derived Mesenchymal Stem Cells into Insulin Producing Cells**

Zahra Poursafavi, Saeid Abroun, Saeid Kaviani, Nasim Hayati Roodbari 449

• **Investigation of Signals and Transcription Factors for The Generation of Female Germ-Like Cells**

Saman Ebrahimi, Alireza Shams, Parvaneh Maghami, Azadeh Hekmat 458

• **Endothelin-1 Stimulates PAI-1 Protein Expression via Dual Transactivation Pathway Dependent ROCK and Phosphorylation of Smad2L**

Hossein Babaahmadi-Rezaei, Alireza Kheirollah, Faezeh Seif 465

• **MiRNA-16-1 Suppresses Mcl-1 and Bcl-2 and Sensitizes Chronic Lymphocytic Leukemia Cells to BH3 Mimetic ABT-199**

Nooshin Ashofteh, Amir Sayed Ali Mehdod, Mohammad Bayat, Hadi Karami 473

• **Genetic and Epigenetic Evaluation of Human Spermatogonial Stem Cells Isolated by MACS in Different Two and Three-Dimensional Culture Systems**

Maria Zahiri, Mansoureh Movahedin, Seyed Javad Mowla, Mehrdad Noruzinia, Morteza Koruji, Mohammad Reza Nowroozi, Fatemeh Asgari 481

• **Front page of Cell Journal_(Yakhteh): Figure 3, Page: 445**

Vulnerability of The Male Reproductive System to SARS-CoV-2 Invasion: Potential Role for The Endoplasmic Reticulum Chaperone Grp78/HSPA5/BiP

Niloofer Sadeghi, Ph.D.^{1, 2}, Marziyeh Tavalaei, Ph.D.¹, Abdolhossein Shahverdi, Ph.D.³, Pallav Sengupta, Ph.D.⁴, Kristian Leisegang Ph.D.⁵, Ramadan Saleh, M.D., Ph.D.^{6, 7}, Ashok Agarwal, Ph.D.^{8*},
Mohammad Hossein Nasr-Esfahani, Ph.D.^{1*}

1. Department of Animal Biotechnology, Reproductive Biomedicine Research Center, Royan Institute for Biotechnology, ACECR, Isfahan, Iran
2. Department of Biochemistry and Functional Genomics, Université de Sherbrooke, Sherbrooke, QC J1K 2R1, Canada
3. Department of Embryology, Reproductive Biomedicine Research Center, Royan Institute for Reproductive Biomedicine, ACECR, Tehran, Iran
4. Department of Physiology, Faculty of Medicine, Bioscience and Nursing, MAHSA University, Bandar Saujana Putra, Malaysia
5. School of Natural Medicine, Faculty of Community and Health Sciences, University of the Western Cape, Cape Town, South Africa
6. Department of Dermatology, Venereology and Andrology, Faculty of Medicine, Sohag University, Sohag, Egypt
7. Ajyal IVF Center, Ajyal Hospital, Sohag, Egypt
8. American Center for Reproductive Medicine, Cleveland Clinic, Cleveland, OH, USA

*Corresponding Addresses: American Center for Reproductive Medicine, Cleveland Clinic, Cleveland, OH, USA

P.O.Box: 8165131378, Department of Animal Biotechnology, Reproductive Biomedicine Research Center, Royan Institute for Biotechnology, ACECR, Isfahan, Iran

Emails: agarwaa@ccf.org, mh.nasr-esfahani@royaninstitute.org

Received: 12/October/2021, Accepted: 24/May/2022

Abstract

Severe acute respiratory syndrome coronavirus-2 (SARS-CoV-2) may adversely affect male reproductive tissues and male fertility. This concern is elicited by the higher susceptibility and mortality rate of men to the SARS-CoV-2 mediated coronavirus disease-19 (COVID-19), compared to the women. SARS-CoV-2 enters host cells after binding to a functional receptor named angiotensin-converting enzyme-2 (ACE2) and then replicates in the host cells and gets released into the plasma. SARS-CoVs use the endoplasmic reticulum (ER) as a site for viral protein synthesis and processing, as well as glucose-regulated protein 78 (Grp78) is a key ER chaperone involved in protein folding by preventing newly synthesized proteins from aggregation. Therefore, we analyzed Grp78 expression in various human organs, particularly male reproductive organs, using Broad Institute Cancer Cell Line Encyclopedia (CCLE), the Genotype-Tissue Expression (GTEx), and Human Protein Atlas online datasets. Grp78 is expressed in male reproductive tissues such as the testis, epididymis, prostate, and seminal vesicle. It can facilitate the coronavirus entry into the male reproductive tract, providing an opportunity for its replication. This link between the SARS-CoV-2 and the Grp78 protein could become a therapeutic target to mitigate its harmful effects on male fertility.

Keywords: COVID-19, Endoplasmic Reticulum, Grp78, Male Infertility, SARS-CoV-2

Cell Journal (Yakhteh), Vol 24, No 8, August 2022, Pages: 427-433

Citation: Sadeghi N, Tavalaei M, Shahverdi AH, Sengupta P, Leisegang K, Saleh R, Agarwal A, Nasr-Esfahani MH. Vulnerability of the male reproductive system to SARS-CoV-2 invasion: potential role for the endoplasmic reticulum chaperone Grp78/HSPA5/BiP. Cell J. 2022; 24(8): 427-433. doi: 10.22074/cellj.2022.8312.

This open-access article has been published under the terms of the Creative Commons Attribution Non-Commercial 3.0 (CC BY-NC 3.0).

Introduction

The World Health Organization declared coronavirus disease 2019 (COVID-19), caused by the severe acute respiratory syndrome coronavirus 2 (SARS-CoV-2), as a global pandemic on March 11, 2020 (1). According to data from Johns Hopkins University's Center for Systems Science and Engineering, there have been >400 million reported cases of COVID-19 worldwide, with >5 million deaths until July 2021 (<https://coronavirus.jhu.edu/map.html>) (2). Interestingly, clinical data emerging from COVID-19 demonstrate that male patients constitute 56-73% of the infected population (3). In addition, higher morbidity and mortality rates of SARS-CoV-2-infected males than age-matched females suggest sex-based differences in COVID-19 outcomes (4).

Severe acute respiratory syndrome coronavirus (SARS-CoV) and SARS-CoV-2 invade human cells through the angiotensin-converting enzyme-2 (ACE2) receptor and

transmembrane serine protease 2 (TMPRSS2) (5, 6). As the 79% amino acid sequence identity of SARS-CoV-2 is similar to SARS-CoV (7), both viruses are thought to utilize the same receptor, ACE2, as a gate to mediate virus entry to target host cells (5, 8, 9). The higher affinity of SARS-CoV-2 spike protein for binding to ACE2 (approximately 10 to 15 folds) compared to that of SARS-CoV, which is one of the reasons for the more impactful pathogenicity of the latter (10). The subunit S1 of the S protein, which includes the receptor-binding domain, directly attaches to the peptidase domain of ACE2, while the membrane fusion is in control of the S2 subunit (11). In addition to ACE2, TMPRSS2, the cell-surface membrane protein, is required to integrate the virus with the cell membrane through cleaving SARS-CoV spike proteins (10).

ACE2 is a metallopeptidase enzyme attached to the membranes of cells located in different

organs, particularly the lungs, heart, kidneys, and testes. Interestingly, ACE2 protein expression is evident only in specific tissues despite the demonstration of ACE2 mRNA in virtually all body organs (5). The physiological relevance of ACE2 in most tissues is yet unknown. However, ACE2 is regarded to be an important regulator of cardiac function and blood pressure control (12), probably through functioning as a natural counterpart to ACE1 (13). The testis is also one of the few organs with high levels of ACE2 expression (14, 15). ACE2 functions to convert Angiotensin II to Angiotensin 1-7 in Leydig cells and adjust testosterone production and consequently contribute to spermatogenesis modulation, which reveals their influence on male fertility (16). Overall, ACE2 mediates the activation of the Renin-Angiotensin-Aldosterone System (RAAS) (5) as a cell signaling system to regulate spermatogenesis (17).

Human spermatozoa include a number of RAAS family ligand enzymes and receptors, including the angiotensin receptor type 1 and 2 and the angiotensin mitochondrial assembly receptor (18). SARS-CoV-2 binding to this sperm surface signaling system may impair the functional capacity of the affected sperm. Specifically, the virus's impact on spermatozoa ACE2 activity may enhance angiotensin II levels and increase reactive oxygen species (ROS) production resulting in oxidative stress (19). Excessive ROS production may cause sperm membrane and DNA damage and ultimately affect the sperm's fertilizing potential (20).

Viruses such as human immunodeficiency virus (HIV), mumps, hepatitis B virus (HBV), influenza A virus subtype H1N1 (A/H1N1), and Ebola virus (21) had been incriminated in the pathogenesis of orchitis, infertility, and testicular tumors (22, 23). Orchitis was also reported as a complication of SARS, an outbreak in 2003 caused by another member of the coronavirus family known as SARS-CoV-1. In another study, histopathological evaluation of testicular biopsy specimens from six men infected with SARS-CoV-1 indicated the findings of increased thickness of the basement membrane, destruction of germ cells, and low density of sperm in the seminiferous tubules (24). In this regard, a systematic review on the presence of SARS-CoV-2 in semen, including fourteen studies, suggested that the virus is rarely found in the semen of infected men and probably COVID-19 affects male fertility by making a deleterious effect on testicular structure (25). In line with this study, Khalili et al. (26) explained that despite the limited data on the detection of SARS-CoV-2 in the semen of infected patients, there is some evidence that the virus may play a role in testicular damage, abnormal sex hormone secretion, and infertility, which could be due to direct viral invasion through receptors or secondary immunological and inflammatory effects (26, 27). Hence, more studies are needed to evaluate all the possibilities.

The endoplasmic reticulum (ER) is the intracellular site where almost one-third of protein synthesis and protein folding occurs. Increased protein synthesis and excessive accumulation of unfolded/misfolded proteins

in the ER lumen activate the unfolded protein response (UPR) and consequently drive the cell into ER stress (28). Under these circumstances, glucose-regulated protein 78 (Grp78), an ER chaperon protein, cooperates with three types of ER stress sensors such as Activating Transcription Factor 6 (ATF6), Protein Kinase R-like ER Kinase (PERK), and Inositol-requiring enzyme 1 (IRE1) to decrease unfolded/misfolded protein levels and avoid unfolded protein accumulation, thereby promoting cell survival. However, UPR may also activate the apoptotic response if ER homeostasis could not be regained (29). Therefore, Grp78 is more likely found within the ER lumen (30).

Under some circumstances, Grp78 can be moved towards the cell surface and act as a receptor to adjust different pathways (31). Grp78, also known as a binding immunoglobulin protein (BiP) or heat shock protein A5 (HSPA5) that is a member of the heat shock protein 70 (HSP70) family. This protein plays an essential role in resistance to apoptotic death in somatic cells and the response to chemical or physical cellular stress induced by cancer, malnutrition, and hypoxia (32, 33). Grp78 is highly expressed in human testicular tissue and mature spermatozoa, contributing to the physiology of spermatogenesis and fertilization (34, 35). Interestingly, previous results have confirmed that Grp78 protein contributes to the intrusion of different viruses like Ebola virus, dengue virus, influenza virus (36), Middle East respiratory syndrome coronavirus (MERS-CoV), Zika virus (37), and coronaviruses (38) into host cells. Moreover, recently the first experimental study proved that in addition to ACE2, the main receptor for virus entry, Grp78 as a host auxiliary factor for SAR-CoV-2 can simplify control virus entry (39).

Spike proteins of SARS-CoV-2 are one of the most important virulent factors of viruses to attach and penetrate host cells. For this purpose, host cell receptors like ACE2 and Grp78 are considered the target for viruses (5). Ibrahim et al. (40) have reported that the attachment of Grp78 Substrate Binding Domain β (SBD β) with the receptor-binding domain of the coronavirus spike protein is required to identify and help the virus to enter the host cells.

It has also been demonstrated that Grp78 protein expression increases in SARS-CoV infection, reflecting its role in virus entry into cells (41, 42). The present study aims to investigate the Grp78 expression in male reproductive organs using the findings of recent studies up to July 2021 and discuss the potential implications for SARS-CoV-2 invasion of the male reproductive tract.

In order to investigate the Grp78 expression in the male reproductive system, RNA and protein expression data of HSPA5/Grp78 in various human tissues and cancer, particularly male reproductive organs such as the testis and prostate were retrieved online using The Human Protein Atlas (<http://www.proteinatlas.org/>), Genotype-Tissue Expression (GTEx) (<https://www.gtexportal.org/>), and

the Broad Institute Cancer Cell Line Encyclopedia (CCLE) (<https://www.portals.broadinstitute.org/ccle>) portals. All the data is available online. Protein expression scores are based on the best estimate of the “true” protein expression from a knowledge-based annotation. Immunohistochemistry (IHC) images of normal and cancer tissue of male reproductive organs such as testes, epididymis, and accessory sex glands from the tissue and pathology atlas on the Human Protein Atlas portal were used to evaluate the protein expression of HSPA5/Grp78 in the specific cells of these organs.

Data obtained from CCLE and the GTEx portal showed a high level of Grp78 mRNA expression in the male tissues such as the testis and prostate. The mRNA expression is also relatively high in the upper respiratory, digestive tracts, and lungs (Figs.1, 2). Data obtained from the Human Protein Atlas portal showed highly expressed in male tissues, including testis, epididymis, seminal vesicle, and prostate (Fig.3A, B). Moreover, IHC staining shows an increased level of Grp78 expression in cells of testis seminiferous tubules and the glandular cells of the epididymis, seminal vesicle, and prostate (Fig.3C). Data obtained from the Human Protein Atlas portal to assess Grp78 expression in various cancer organs, including the testis and prostate, showed high levels of this protein in these cancer organs (Fig.4).

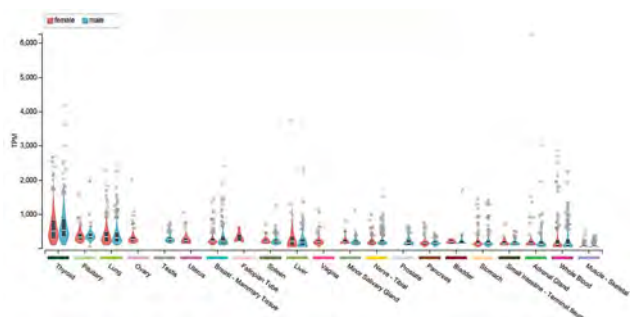


Fig.1: Male and female gene expression for heat shock protein A5 (HSPA5)/ glucose-regulated protein 78 (Grp78) (ENSG00000044574.7) obtained from the genotype-tissue expression (GTEx) portal in different tissues (<https://www.gtexportal.org>).

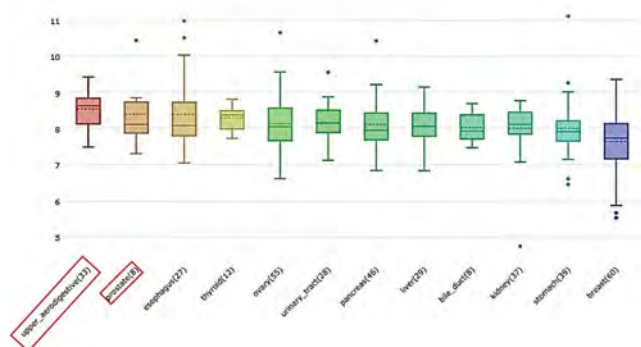


Fig.2: The mRNA expression level of HSPA5/Grp78 in diverse human tissues from the broad institute cancer cell line encyclopedia (CCLE) shows the expression of GRP78 in the upper aerodigestive tract and prostate (<https://www.portals.broadinstitute.org/ccle>).

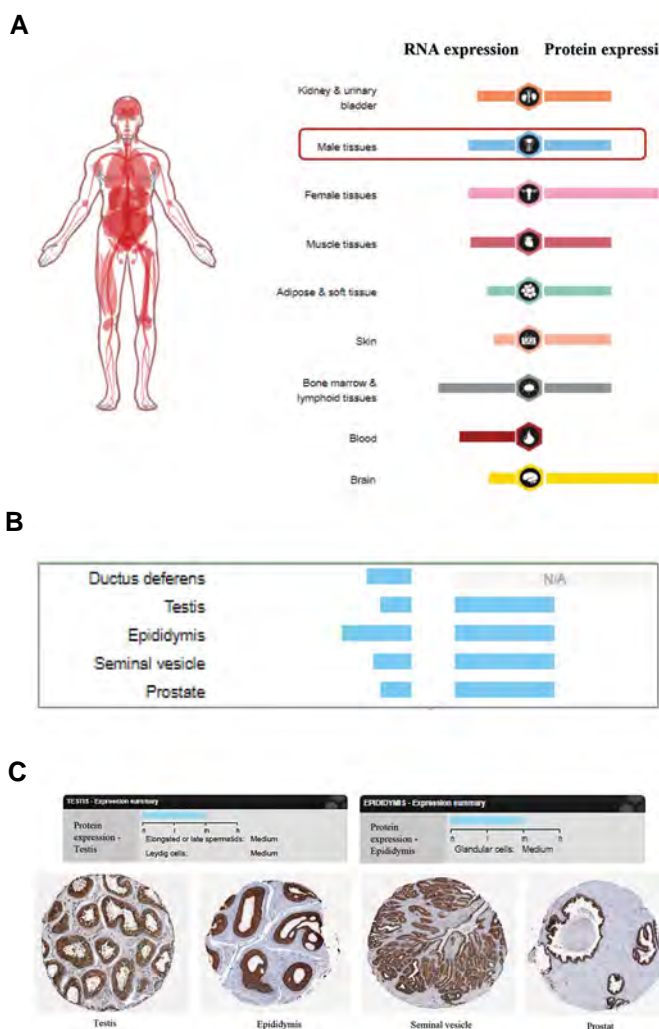


Fig.3: Data of HSPA5/Grp78 protein expression level in different human tissues from HPA portal. **A.** Each bar shows the highest expression score found in a particular group of tissues. Note the notable protein expression of HSPA5/Grp78 in male tissues (red box). **B.** HSPA5/Grp78 protein expression level in different part of male tissues (Human Protein Atlas portal). **C.** IHC staining of HSPA5/Grp78 in normal testis, epididymis, seminal vesicle, and prostate (Human Protein Atlas portal) (<https://www.portals.broadinstitute.org/ccle>).

Grp78 is overexpressed under pathological stresses like cancer, cellular malnutrition, hypoxia, and viral infections and is translocated from the ER to the plasma membrane (31, 32). This protein acts as a multifunctional receptor to interact with various proteins (29); therefore, it may be a gate for viruses to penetrate host cells (43, 44). In this regard, Grp78 has been introduced as a receptor to facilitate coronaviruses’ entrance into host cells in humans and bats (38). Thus, Grp78 seems to be an essential factor in helping virus protein folding, and its internalization to the host cells as well as protecting them from host immunity (Fig.5).

Recent studies proposed interaction between host cell Grp78 and the particular region of the COVID-19 spike model and considered this receptor a probable vaccination target (40, 45, 46). A series of recent studies have indicated that Pep42, a cyclic peptide, binds to the overexpressed Grp78 in the cancer cell membrane and by which enters the cancer cell (47, 48).

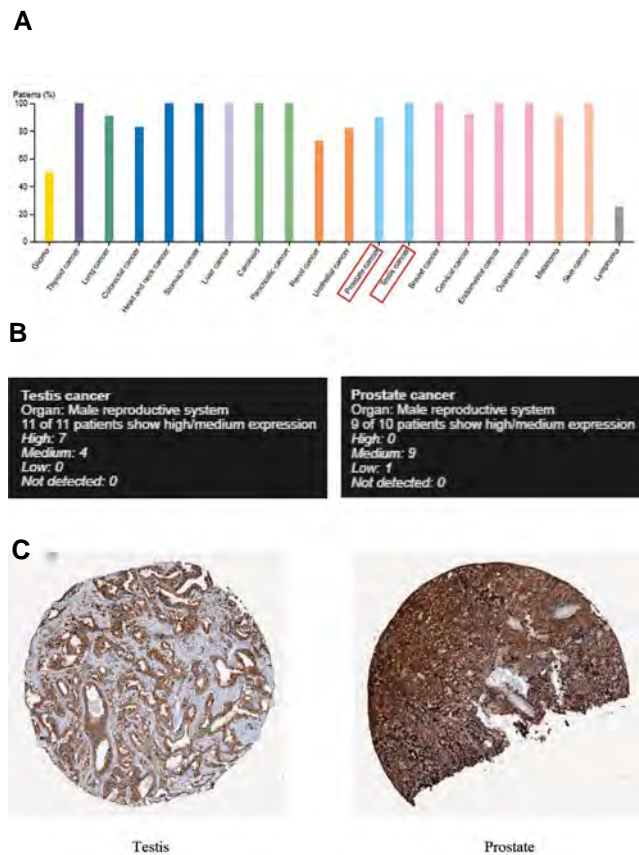


Fig.4: Data of HSPA5/Grp78 protein expression level in cancers. **A.** For each cancer, color-coded bars represent the percentage of patients (maximum 12 patients) with high and medium protein expression levels. **B.** Note the black box showing 100 percent of patients with testis cancer indicate high/medium expression and 90 percentage of patients with prostate shows a medium expression of GRP78. **C.** IHC staining of GRP78 in the testicular and prostatic cancer (IHC staining, Human Protein Atlas portal).

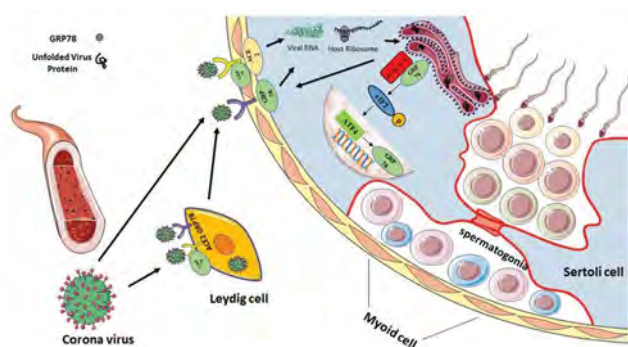


Fig.5: Hypothesized model for SARS-CoV-2 testicular infection. In addition to Leydig cell as one of the main targets for SARS-CoV-2 due to high expression of ACE2, Sertoli cell contributes to virus infection. The virus binds to the ACE2 receptor of the Sertoli cell and releases the viral RNA genome into the cytoplasm. Released and uncoated RNA is translated by the host ribosome to produce viral fundamental protein. Translated proteins are inserted into the endoplasmic reticulum for processing. Accumulation of unfolded SARS-CoV proteins in the lumen of E.R activates E.R. stress, UPR, and consequently PERK pathway by enhancing GRP78 expression as an important E.R. chaperon for folding of SARS-CoV proteins. Increased GRP78 expression and pathological stress induced by virus translocate GRP78 from E.R lumen to cell membrane and act either as a direct receptor or a host co-factor for ACE2 to accelerate virus entry genome.

That is why Pep42 is considered a vehicle for tumor cell-specific chemotherapy (48). Ibrahim et al. (40) assessed the binding features of spike proteins of SARS-CoV-2 with Grp78. Interestingly, he also encountered 13 different cyclic regions in this spike model that were matched with the cyclic Pep42 structure and demonstrated the contribution of the spike protein model (regions III and IV) to binding with Grp78. Furthermore, a recent experimental study by Carlos et al. (39) revealed a new aspect of Grp78 role in the coronavirus infection. They presented some evidence that Grp78 functions not only as a cofactor to aid viral spike binding to ACE2, but also as a regulator of ACE2 protein expression, which highlight the great contribution of this protein to viral entry.

In the context of male reproduction, Grp78 expression has been confirmed by various studies in germ cells of humans and mice during spermatogenesis (49, 50). Investigation of Grp78 cellular localization in human testis revealed its expression in spermatocytes, round spermatids, and neck region of ejaculated spermatozoa as well as principal cells of the epididymis (51). A similar observation was found using an animal model to measure the Grp78 gene expression in testicular tissue of two groups of 2-month and 4-month-old rats (52).

Based on the high level of Grp78 expression in male tissues, including spermatogenesis cells, epididymis cells, vesicle seminal, and prostate (Fig.3), we speculate that in addition to ACE2 and TMPRSS2, Grp78 can act as a receptor to intermediate coronavirus entrance to male reproductive cells. Leydig and Sertoli cells may be considered a target for SARS-CoV-2 due to the high expression of ACE-2 (8, 15). This may result in testicular destruction depending on the disease's severity as immune and inflammatory responses (25). In this case, the virus attaches to the ACE2 receptor of the Sertoli cell and releases the viral RNA genome into the cytoplasm. The host ribosome translates the released RNA to produce fundamental viral protein and is finally inserted into the ER for processing (53).

On the other hand, several studies failed to demonstrate SARS-CoV-2 in the semen of COVID-19 patients, whether those patients were tested during an acute attack of the disease (54) or at different stages of recovery (55, 56). Pan et al. (55), and Stanley et al. (57), attributed the lack of SARS-Co-2 in the semen of COVID-19 patients to the fact that less than 1% of testis cells (spermatozoa, spermatogonia, and Leydig and Sertoli cells) express both ACE2 and TMPRSS2 receptors, which may reduce the virus's ability to penetrate these cells. Accordingly, SARS-CoV-2 is unlikely to be sexually transmitted by men. However, it is difficult to rely on those observations to exclude the potential of sexual transmission of SARS-Cov-2 due to: i. Small sample of COVID-19 patients included in those studies and the heterogeneity of inclusion criteria, ii. Lack of data regarding the viral load of COVID-19- infected patients, iii. Difficulties

that surround the collection of semen samples from COVID-19 patients during acute attacks, and iv. lack of a standard protocol of RT-PCR technique that is used for detection of seminal SARS-CoV-2.

The genome of SARS-CoV, like other coronaviruses, replicates in the host cell cytoplasm and is highly dependent on ER function for the preparation of proteins. This induces ER stress owing to the accumulation of unfolded yet synthesized SARS-CoV proteins in the ER lumen (28). Under these circumstances, UPR is activated by multiple cell-signaling pathways to maintain cellular homeostasis. However, if this condition continues and damages ER function severely, the UPR triggers cellular apoptosis (30). Interestingly, viruses apply various strategies to regulate UPR for ER preservation. In the case of SARS-CoV, UPR modulation is accomplished by the PERK pathway and eIF2 α phosphorylation. This leads to the transcriptional activation of Grp78 as the intraluminal ER chaperones increase the processing and folding of expressed SARS-CoV proteins through viral replication and protect cells from apoptosis, at least in the early stage of infection (Fig.5) (41, 58).

Moreover, upon ER stress activation, IRE1as an ER transmembrane sensor, starts generating X box-binding protein 1 (XBP1), acting as a transcriptional activator of genes involved in UPR to maintain ER and cellular function (30). It has been reported that SARS-CoV has been shown to cause a slight increase in XBP1 expression, which is likely important for increased virus protein folding and avoiding the harmful effects of ER stress-induced apoptosis (41). Therefore, SARS-CoV by selective modulation of the ER stress pathways provides the time and opportunity for viral replication before the infected host cell is sensitized to apoptosis.

It is notable that, *in vitro* treatment of lung epithelial cells with a humanized monoclonal antibody (hMAb159) with high affinity and specificity against GRP78, caused decreased cell surface GRP78 and cell surface ACE2 expression, as well as viral entry and SARS-CoV-2 infection. This finding showed that targeting host chaperones such as GRP78, which are necessary for viral entry and even production, might provide novel techniques for repressing SARS-CoV-2 and perhaps future coronavirus strains (39).

The connection between reproductive tissue cancers and increased Grp78 expression as a central part of UPR has been explored in prior studies. The results indicate a role of Grp78 in protein folding to guarantee survival, proliferation, and invasion of various cancer cells (59, 60) like the endometrial, gastric, renal cell, pancreatic, and prostate cancer (29, 61). These observations agree with our data extracted from the Human Protein Atlas portal (Fig.4). This may explain the relation of blocking Grp78 in different types of cancer cells and their apoptosis (62). Also, recently, some literature has proved the association

between up-regulation and relocation of Grp78 to the tumor cell surface and some features like aggressive and invasive growth patterns of these cells (63, 64). This feature of cancer cells has turned the Grp78 at the cell surface into a useful prognostic marker and a target for cancer therapy (31).

A recent study by Liang et al. (65) concluded that patients with cancer have a higher risk of getting infected with SARS-CoV-2 compared to individuals without cancer. Although cancer patients are at a higher risk of getting infected as a result of immunocompromised states (66), the observation that Grp78 is overexpressed and translocated to the cancer cell membrane (67) may explain why tumor cells are more likely vulnerable to virus entrance and thereby virus propagation in cancer patients. Similarly, in diabetic and obese individuals, Grp78 is translocated to the cell membrane due to cellular glucose starvation (68), thus explaining why those individuals are at higher risk and severely affected (69). Based on these reports, increased Grp78 at the cell membrane may increase the severity of viral infection in specific tissue and individuals with higher Grp78 in their serum. Furthermore, it has been demonstrated that dysregulation of male hormonal sex can result from acute SARS-CoV-2 infection (70). Since Grp78 can play a prominent role in the steroidogenesis regulation of various reproductive mammalian cells (60), It seems that the hormonal defect is dependent on Grp78 function in testicular tissues infected with SARS-CoV-2.

Conclusion

In this study, we reviewed the present studies regarding the possible role of Grp78/HSPA5/BiP to facilitate the virus entry into host cells. However, it remains unclear how and when SARS-CoV-2 can impair male fertility potential. Given the global importance of fertility, all aspects of the impact of SARS-CoV-2 infection on the male reproductive system should be further assessed. A better understanding of the infection routes and target cells of the male reproductive system is critical for predicting some effective methods to treat or avoid likely consequences of infection in the male reproductive system.

Acknowledgments

This study was supported by the Royan Institute. We would like to express our gratitude to the staff of the Biotechnology Department of Royan Institute, Isfahan, Iran and the American Center for Reproductive Medicine, Cleveland, USA, for their full support. The authors declare that they have no competing interests.

Authors' Contributions

N.S.; Main search, collection, and study of published papers, writing, and approval of the manuscript. M.T., A.Sh., P.S., K.L., R.S., A.A., M.H.N.-E.; Reviewed the

manuscript, provided comments and suggestions, and finally approved the manuscript.

References

- Zanke AA, Thenge RR, Adhao VS. COVID-19: A pandemic declared by world health organization. *IP Int J Compr Adv Pharmacol*. 2020; 5(2): 49-57.
- Dong E, Du H, Gardner L. An interactive web-based dashboard to track COVID-19 in real time. *Lancet Infect Dis*. 2020; 20(5): 533-534.
- Xu XW, Wu XX, Jiang XG, Xu KJ, Ying LJ, Ma CL, et al. Clinical findings in a group of patients infected with the 2019 novel coronavirus (SARS-CoV-2) outside of Wuhan, China: retrospective case series. *BMJ*. 2020; 368: m606.
- Teixeira TA, Bernardes FS, Oliveira YC, Hsieh MK, Esteves SC, Duarte Neto AN, et al. SARS-CoV-2 and multi-organ damage—what men's health specialists should know about the COVID-19 pathophysiology. *Int Braz J Urol*. 2021; 47(3): 637-646.
- Hoffmann M, Kleine-Weber H, Schroeder S, Krüger N, Herrler T, Eichsen S, et al. SARS-CoV-2 cell entry depends on ACE2 and TMPRSS2 and is blocked by a clinically proven protease inhibitor. *Cell*. 2020; 181(2): 271-280.
- Abdel-Moneim A. COVID-19 pandemic and male fertility: Clinical manifestations and pathogenic mechanisms. *Biochemistry (Mosc)*. 2021; 86(4): 389-396.
- Lu R, Zhao X, Li J, Niu P, Yang B, Wu H, et al. Genomic characterisation and epidemiology of 2019 novel coronavirus: implications for virus origins and receptor binding. *Lancet*. 2020; 395(10224): 565-574.
- Wang Z, Xu X. scRNA-seq profiling of human testes reveals the presence of the ACE2 receptor, a target for SARS-CoV-2 infection in spermatogonia, leydig and sertoli cells. *Cells*. 2020; 9(4): 920.
- Tian Y, Zhou LQ. Evaluating the impact of COVID-19 on male reproduction. *Reproduction*. 2021; 161(2): R37-R44.
- Stopsack KH, Mucci LA, Antonarakis ES, Nelson PS, Kantoff PW. TMPRSS2 and COVID-19: Serendipity or opportunity for intervention? *Cancer Discov*. 2020; 10(6): 779-782.
- Hallak J, Teixeira TA, Bernardes FS, Carneiro F, Duarte SA, Pariz JR, et al. SARS-CoV-2 and its relationship with the genitourinary tract: Implications for male reproductive health in the context of COVID-19 pandemic. *Andrology*. 2021; 9(1):73-79.
- Crackower MA, Sarao R, Oudit GY, Yagil C, Koziarzki I, Scanga SE, et al. Angiotensin-converting enzyme 2 is an essential regulator of heart function. *Nature*. 2002; 417(6891): 822-828.
- Yagil Y, Yagil C. Hypothesis: ACE2 modulates blood pressure in the mammalian organism. *Hypertension*. 2003; 41: 871-873.
- Hezavehei M, Shokohian B, Nasr-Esfahani MH, Shpichka A, Timashev P, Shahverdi AH, et al. Possible male reproduction complications after coronavirus pandemic. *Cell J*. 2021; 23(4): 382-388.
- Tabar AN, Sojoudi K, Henduei H, Azizi H. Review of sertoli cell dysfunction caused by COVID-19 that could affect male fertility. *Zygote*. 2021; 30(1): 17-24.
- Lee W, Mok A, Chung JP. Potential effects of COVID-19 on reproductive systems and fertility; assisted reproductive technology guidelines and considerations: a review. *Hong Kong Med J*. 2021; 27: 118-126.
- Edenfield RC, Easley CA. Implications of testicular ACE2 and the renin-angiotensin system for SARS-CoV-2 on testis function. *Nat Rev Urol*. 2022; 19(2): 116-127.
- Valdivia A, Cortés L, Beitia M, Totorikaguena L, Agirregoitia N, Corcostegui B, et al. Role of angiotensin-(1-7) via MAS receptor in human sperm motility and acrosome reaction. *Reprod*. 2020; 159(3): 241-249.
- Aitken RJ. COVID-19 and human spermatozoa-Potential risks for infertility and sexual transmission? *Andrology*. 2021; 9(1): 48-52.
- Agarwal A, Saleh RA, Bedaiwy MA. Role of reactive oxygen species in the pathophysiology of human reproduction. *Fertil Steril*. 2003; 79(4): 829-843.
- Roychoudhury S, Das A, Sengupta P, Dutta S, Roychoudhury S, Choudhury AP, et al. Viral pandemics of the last four decades: pathophysiology, health impacts and perspectives. *Int J Environ Res Public Health*. 2020; 17(24): 9411.
- Schuppe HC, Meinhardt A, Allam JP, Bergmann M, Weidner W, Haidl G. Chronic orchitis: a neglected cause of male infertility? *Andrologia*. 2008; 40(2): 84-91.
- Mahé D, Matusali G, Deleage C, Alvarenga RL, Satie AP, Pagliuzza A, et al. Potential for virus endogenization in humans through testicular germ cell infection: the case of HIV. *J Virol*. 2020; 94(24): e01145-20.
- Xu J, Qi L, Chi X, Yang J, Wei X, Gong E, et al. Orchitis: a complication of severe acute respiratory syndrome (SARS). *Biol Reprod*. 2006; 74(2): 410-416.
- Yao Y, Yuan X, Wu L, Guo N, Yin L, Li Y. COVID-19 and male reproduction: Current research and unknown factors. *Andrology*. 2021; 9(4): 1027-1037.
- Khalili MA, Leisegang K, Majzoub A, Finelli R, Selvam MK, Henkel R, et al. Male fertility and the COVID-19 pandemic: systematic review of the literature. *World J Mens Health*. 2020; 38(4): 506-520.
- Rastrelli G, Di Stasi V, Inglese F, Beccaria M, Garuti M, Di Costanzo D, et al. Low testosterone levels predict clinical adverse outcomes in SARS-CoV-2 pneumonia patients. *Andrology*. 2021; 9(1): 88-98.
- Almanza A, Carlesso A, Chintha C, Creedican S, Doultosinos D, Leuzzi B, et al. Endoplasmic reticulum stress signalling—from basic mechanisms to clinical applications. *FEBS J*. 2019; 286(2): 241-278.
- Ibrahim IM, Abdelmalek DH, Elfiky AA. GRP78: a cell's response to stress. *Life Sci*. 2019; 226: 156-163.
- Karna KK, Shin YS, Choi BR, Kim HK, Park JK. The role of endoplasmic reticulum stress response in male reproductive physiology and pathology: a review. *World J Mens Health*. 2020; 38(4): 484-494.
- Casas C. GRP78 at the centre of the stage in cancer and neuroprotection. *Front Neurosci*. 2017; 11: 177.
- Ni M, Zhang Y, Lee AS. Beyond the endoplasmic reticulum: atypical GRP78 in cell viability, signalling and therapeutic targeting. *Biochem J*. 2011; 434(2): 181-188.
- Xing X, Lai M, Wang Y, Xu E, Huang Q. Overexpression of glucose-regulated protein 78 in colon cancer. *Clin Chim Acta*. 2006; 364(1-2): 308-315.
- Boiland M, Reyes-Moreno C, Lachance C, Massicotte L, Bailey JL, Sirard MA, et al. Localization of the chaperone proteins GRP78 and HSP60 on the luminal surface of bovine oviduct epithelial cells and their association with spermatozoa. *Biol Reprod*. 2004; 71(6): 1879-1889.
- Lachance C, Bailey JL, Leclerc P. Expression of Hsp60 and Grp78 in the human endometrium and oviduct, and their effect on sperm functions. *Hum Reprod*. 2007; 22(10): 2606-2614.
- Booth L, Roberts JL, Cash DR, Tavallai S, Jean S, Fidanza A, et al. GRP78/BiP/HSPA5/Dna K is a universal therapeutic target for human disease. *J Cell Physiol*. 2015; 230(7): 1661-1676.
- Turpin J, Frumence E, Harrabi W, Haddad JG, El Kalamouni C, Desprès P, et al. Zika virus subversion of chaperone GRP78/BiP expression in A549 cells during UPR activation. *Biochimie*. 2020; 175: 99-105.
- Chu H, Chan CM, Zhang X, Wang Y, Yuan S, Zhou J, et al. Middle East respiratory syndrome coronavirus and bat coronavirus HKU9 both can utilize GRP78 for attachment onto host cells. *J Biol Chem*. 2018; 293(30): 11709-11726.
- Carlos AJ, Ha DP, Yeh DW, Van Krieken R, Tseng CC, Zhang P, et al. The chaperone GRP78 is a host auxiliary factor for SARS-CoV-2 and GRP78 depleting antibody blocks viral entry and infection. *J Biol Chem*. 2021; 296: 100759.
- Ibrahim IM, Abdelmalek DH, Elshahat ME, Elfiky AA. COVID-19 spike-host cell receptor GRP78 binding site prediction. *J Infect*. 2020; 80(5): 554-562.
- Chan CP, Siu KL, Chin KT, Yuen KY, Zheng B, Jin DY. Modulation of the unfolded protein response by the severe acute respiratory syndrome coronavirus spike protein. *J Virol*. 2006; 80(18): 9279-9287.
- Elgohary AM, Elfiky AA, Barakat K. GRP78: A possible relationship of COVID-19 and the mucormycosis; in silico perspective. *Comput Biol Med*. 2021; 139: 104956.
- Jindadamrongwech S, Theparit C, Smith DR. Identification of GRP 78 (BiP) as a liver cell expressed receptor element for dengue virus serotype 2. *Arch Virol*. 2004; 149(5): 915-927.
- Honda T, Horie M, Daito T, Ikuta K, Tomonaga K. Molecular chaperone BiP interacts with Borna disease virus glycoprotein at the cell surface. *J Virol*. 2009; 83(23): 12622-12625.
- Elfiky AA. SARS-CoV-2 spike-heat shock protein A5 (GRP78) recognition may be related to the immersed human coronaviruses. *Front Pharmacol*. 2020; 11: 577467.
- Sabirli R, Koseler A, Goren T, Turkcuer I, Kurt O. High GRP78 levels in Covid-19 infection: a case-control study. *Life Sci*. 2021; 265: 118781.
- Kim Y, Lillo AM, Steiniger SC, Liu Y, Ballatore C, Anichini A, et al.

- Targeting heat shock proteins on cancer cells: selection, characterization, and cell-penetrating properties of a peptidic GRP78 ligand. *Biochemistry*. 2006; 45(31): 9434-9444.
48. Yoneda Y, Steiniger SC, Čapková K, Mee JM, Liu Y, Kaufmann GF, et al. A cell-penetrating peptidic GRP78 ligand for tumor cell-specific prodrug therapy. *Bio Med Chem Lett*. 2008; 18(5): 1632-1636.
 49. Huo R, Zhu YF, Ma X, Lin M, Zhou ZM, Sha JH. Differential expression of glucose-regulated protein 78 during spermatogenesis. *Cell Tissue Res*. 2004; 316(3): 359-367.
 50. Aguilar-Mahecha A, Hales BF, Robaire B. Expression of stress response genes in germ cells during spermatogenesis. *Biol Reprod*. 2001; 65(1): 119-127.
 51. Wang W, Wang X, Zhu P, Sun CM, Jin S, Liu J, et al. Expression and location of glucose-regulated protein 78 in testis and epididymis. *WIMJ Open*. 2014; 1: 14-7.
 52. Rahmani M, Tavalaei M, Hosseini M, Eskandari A, Shaygannia E, Sadeghi N, et al. Deferasirox, an iron-chelating agent, improves testicular morphometric and sperm functional parameters in a rat model of varicocele. *Oxid Med Cell Longev*. 2021; 2021: 6698482.
 53. Yesudhas D, Srivastava A, Gromiha MM. COVID-19 outbreak: history, mechanism, transmission, structural studies and therapeutics. *Infection*. 2021; 49(2): 199-213.
 54. Song C, Wang Y, Li W, Hu B, Chen G, Xia P, et al. Absence of 2019 novel coronavirus in semen and testes of COVID-19 patients. *Biol Reprod*. 2020; 103(1): 4-6.
 55. Pan F, Xiao X, Guo J, Song Y, Li H, Patel DP, et al. No evidence of severe acute respiratory syndrome–coronavirus 2 in semen of males recovering from coronavirus disease 2019. *Ferti Steril*. 2020; 113(6): 1135-1139.
 56. Ma L, Xie W, Li D, Shi L, Ye G, Mao Y, et al. Evaluation of sex-related hormones and semen characteristics in reproductive-aged male COVID-19 patients. *J Med Virol*. 2021; 93(1):456-462.
 57. Stanley KE, Thomas E, Leaver M, Wells D. Coronavirus disease-19 and fertility: viral host entry protein expression in male and female reproductive tissues. *Fertil Steril*. 2020; 114(1):33-43.
 58. Luo S, Baumeister P, Yang S, Abcouwer SF, Lee AS. Induction of Grp78/BiP by translational block: activation of the Grp78 promoter by ATF4 through an upstream ATF/CRE site independent of the endoplasmic reticulum stress elements. *J Biol Chem*. 2003; 278(39): 37375-37385.
 59. Guzel E, Arlier S, Guzeloglu-Kayisli O, Tabak MS, Ekiz T, Semerci N, et al. Endoplasmic reticulum stress and homeostasis in reproductive physiology and pathology. *Int J Mol Sci*. 2017; 18(4): 792.
 60. Hebert-Schuster M, Rotta BE, Kirkpatrick B, Guibourdenche J, Cohen M. The interplay between glucose-regulated protein 78 (GRP78) and steroids in the reproductive system. *Int J Mol Sci*. 2018; 19(7): 1842.
 61. Gifford JB, Huang W, Zeleniak AE, Hindoyan A, Wu H, Donahue TR, et al. Expression of GRP78, master regulator of the unfolded protein response, increases chemoresistance in pancreatic ductal adenocarcinoma. *Mol Cancer Ther*. 2016; 15(5): 1043-1052.
 62. Rasche L, Duell J, Morgner C, Chatterjee M, Hensel F, Rosenwald A, et al. The natural human IgM antibody PAT-SM6 induces apoptosis in primary human multiple myeloma cells by targeting heat shock protein GRP78. *PLoS One*. 2013; 8(5): e63414.
 63. Lee AS. Glucose-regulated proteins in cancer: molecular mechanisms and therapeutic potential. *Nat Rev Cancer*. 2014; 14(4): 263-276.
 64. Ferrara F, Staquicini DI, Driessen WH, D'Angelo S, Dobroff AS, Barry M, et al. Targeted molecular-genetic imaging and ligand-directed therapy in aggressive variant prostate cancer. *Proc Natl Acad Sci USA*. 2016; 113(45): 12786-12791.
 65. Liang W, Guan W, Chen R, Wang W, Li J, Xu K, et al. Cancer patients in SARS-CoV-2 infection: a nationwide analysis in China. *Lancet Oncol*. 2020; 21(3): 335-337.
 66. Gosain R, Abdou Y, Singh A, Rana N, Puzanov I, Ernstoff MS. COVID-19 and cancer: a comprehensive review. *Curr Oncol Rep*. 2020; 22(5): 1-5.
 67. Toyoda Y, Akarlar B, Sarov M, Ozlu N, Saitoh S. Extracellular glucose level regulates dependence on GRP 78 for cell surface localization of multipass transmembrane proteins in HeLa cells. *FEBS Lett*. 2018; 592(19): 3295-3304.
 68. Girona J, Rodríguez-Borjabad C, Ibarretxe D, Vallvé JC, Ferré R, Heras M, et al. The circulating GRP78/BiP is a marker of metabolic diseases and atherosclerosis: bringing endoplasmic reticulum stress into the clinical scenario. *J Clin Med*. 2019; 8(11):1793.
 69. Santos A, Magro DO, Evangelista-Poderoso R, Saad MJ. Diabetes, obesity, and insulin resistance in COVID-19: molecular interrelationship and therapeutic implications. *Diabetol Metab Syndr*. 2021; 13(1): 23.
 70. Verma S, Saksena S, Sadri-Ardekani H. ACE2 receptor expression in testes: implications in coronavirus disease 2019 pathogenesis. *Biol Reprod*. 2020; 103(3): 449-451.

Strategies for Mammalian Mesenchymal Stem Cells Differentiation into Primordial Germ Cell-Like Cells: A Review

Shabnam Fayezi, Ph.D.^{1,2}, Parisa Fayyazpour, M.Sc.^{3,4}, Zahra Norouzi, M.Sc.⁵, Amir Mehdizadeh, Ph.D.^{6*}

1. Department of Reproductive Biology, Faculty of Advanced Medical Sciences, Tabriz University of Medical Sciences, Tabriz, Iran
2. Department of Gynecologic Endocrinology and Fertility Disorders, Women's Hospital, Ruprecht-Karls University of Heidelberg, Heidelberg, Germany
3. Hematology and Oncology Research Center, Tabriz University of Medical Sciences, Tabriz, Iran
4. Department of Biochemistry and Clinical Laboratories, Faculty of Medicine, Tabriz University of Medical Sciences, Tabriz, Iran
5. Student's Research Committee, Tabriz University of Medical Sciences, Tabriz, Iran
6. Endocrine Research Center, Tabriz University of Medical Sciences, Tabriz, Iran

*Corresponding Address: P.O.Box: 5166614756, Endocrine Research Center, Tabriz University of Medical Sciences, Tabriz, Iran
Email: mehdizadeha@tbzmed.ac.ir

Received: 24/May/2021, Accepted: 26/September/2021

Abstract

Primordial germ cells develop into oocytes and sperm cells. These cells are useful resources in reproductive biology and regenerative medicine. The mesenchymal stem cells (MSCs) have been examined for in vitro production of primordial germ cell-like cells (PGLCs). This study aimed to summarize the existing protocols for MSCs differentiation into PGLCs. In limited identified studies, various models of MSCs, including those derived from adipose tissue, bone marrow, and Wharton's jelly, have been successfully differentiated into PGLCs. Although the protocols of specification induction are basically very similar, they have been adjusted to the mesenchymal cell type and the species of origin. The availability of MSCs has made it possible to customize conditions for their differentiation into PGLCs in several models, including humans. Refining germ cell-related signaling pathways during induced differentiation of MSCs will help to define extension to the protocols for PGLCs production.

Keywords: Adult Stem Cells, Cytological Techniques, Gametogenesis, Germ Cells, Retinol

Cell Journal(yakhteh), Vol 24, No 8, August 2022, Pages: 434-441

Citation: Fayezi Sh, Fayyazpour P, Norouzi Z, Mehdizadeh A. Strategies for mammalian mesenchymal stem cells differentiation into primordial germ cell-like cells: a review. Cell J. 2022; 24(8): 434-441. doi: 10.22074/cellj.2022.8087.

This open-access article has been published under the terms of the Creative Commons Attribution Non-Commercial 3.0 (CC BY-NC 3.0).

Introduction

Successful fertility in mammals is dependent on various biological processes, including oocyte maturity, ovulation, embryo formation, and implantation (1). In majority of multicellular organisms, germ cells are the origin of new organism, which transfer the genetic and epigenetic information to the next generation. Furthermore, these cells are the main source of totipotency to create a new organism (2). Two important phases of gamete development are i. Primordial germ cell (PGC) formation during early embryogenesis and active migration to gonadal ridge and ii. Receiving distinct environmental signals for controlled cell meiosis division, in oogenesis and spermatogenesis processes (3). Considering the unique capabilities of PGCs in the production of gametes, these cells would be precious resources in reproductive biology and regenerative medicine. Thus, laboratory production of primordial germ cell-like cells (PGCLCs) has been a growing trend for years.

Stem cells can build specialized cells of human body, and exert self-renewal and differentiative capacity (4). In general, stem cells are categorized as “embryonic” and “adult”. Pluripotent embryonic stem cells (ESCs) can generate all cell lineages of human tissues through differentiation into more specialized multipotent stem cells with ectodermal, mesodermal, or endodermal origin.

ESCs were first isolated from mouse embryo in 1981 (5). The pluripotent characteristics of ESCs have given

treatment hope in patients suffering from different diseases including infertility (6). However, the use of ESCs has been associated with tumorigenesis and ethical concerns, and researchers have tried to replace these cells with adult stem cells (7, 8).

Adult stem cells, also known as “somatic” stem cells, are found both in developing and adult tissues (9). Mesenchymal stem cells (MSCs) are multipotent stromal cells which are highly found in adipose tissue, umbilical cord blood and bone marrow; however, they can also be identified in other tissues and regions requiring wound healing (10). MSCs can be differentiated into different cell types with mesodermal and non-mesodermal origin such as adipocytes, osteoblasts, and chondrocytes (11). The easy harvesting of some MSCs types, including umbilical or adipose tissue derived MSCs, immunosuppressive properties, fewer ethical concerns, as well as simple and cost-effective culture and differentiation methods have made them a suitable alternative for ESCs and induced pluripotent stem cells (iPSCs) (12).

Remarkably, PGCLCs can be differentiated not only from ESCs, but also reprogrammed pluripotent stem cells (PSCs) generated either through somatic cell nuclear transfer or induced pluripotency (13). Differentiation induction in transdifferentiated cells is a newer strategy for *in vitro* production of PGCLCs. iPSCs are obtained by reprogramming mature somatic cells that have been used successfully to produce PGCLCs (14). In

transdifferentiation process, somatic stem cells are reprogrammed into cells of other germ layers and tissues, which is characterized by losing germ layer properties. The process of transdifferentiation to PGCLCs has been successfully induced in several somatic stem cell types such as skin-derived stem cells (15). The application of reprogramming and transdifferentiation prospectively circumvents the strict ethical limitations associated with obtaining PSCs from human embryos. In addition, genetically modified gametes can be obtained eventually using gene editing. However, somatic cells have rather different pattern of mutations (16) and epigenetic status (17) than that of germ cells. These differences can only be identified and characterized by strict monitoring at the genetic level, which have not yet been well developed.

Induction of PSCs into PGCLCs has been examined in two-dimensional culture (18) and embryoid bodies (19). Despite inherent differences, in both mouse and human PSC types, bone morphogenetic proteins (BMPs) have been identified as essential inducers of PGC specification. Using cytokines such as retinoic acid, co-culture with somatic cells and conditioned media, successful experiments have been performed. Further, in other studies by manipulation of transcriptional regulators expression deleted in azoospermia-like (*Dazl*) family genes (20) or using small molecules such as kinase inhibitors, successful PGCLC meiosis induction have been achieved in human iPSCs (21).

Wnt signaling plays an important role in gastrulation process especially in mesoderm and endoderm differentiation. It has also been suggested that Wnt signaling inhibition stabilizes the undifferentiated state of PSCs. Moreover, during induction of human iPSCs in defined conditions through Wnt signaling, an initial differentiation stage to mesoderm-like cells has been identified (14). These cells express genes such as Eomesodermin promoting commitment to PGCLCs of iPSCs through *Sox17* upregulation (22). Such a phenomenon has also been shown in PSCs (23). Subsequently, using BMP4, mesoderm-like cells were differentiated into PGCLC (24). In this process, B lymphocyte-induced maturation protein 1 (Blimp1) suppresses the "neuronal differentiation" program and its expression is as a key feature of the PGC specification (14). Shirzeily et al. (25) in their study also demonstrated the differentiation ability of mouse adipose tissue and bone marrow-derived MSCs into primordial germ cells by expressing *Mvh*, *Dazl*, *Stra8*, and *Scp3* specific markers.

Based on the findings, it is hypothesized that the mesoderm-like cells might be efficient precursors to form germ cell line with fewer ethical considerations than ESCs and iPSCs (26).

This review aims to overview the utilized MSC types and differentiation protocols for *in vitro* germ cell production with a focus on human and certain other mammalian models. Initially, the background of PGC development in the mouse model will be reviewed. Then, the existing

studies on the production of PGCLCs from MSCs will be discussed by cell origin. Finally, the relevant information on all-trans-retinoic acid (RA) and BMP4 participation, as common factors used in the PGC specification, will be outlined.

The search for published records was carried out in the PubMed, EMBASE (Elsevier) and Google Scholar in January and August 2021 without limiting the search by date of publication and geographical region. The search terms were "mesenchymal stem cell", "mesenchymal stromal cells", "Wharton Jelly cells", "mesenchymal progenitor cells", "germ cells", "oogonial stem cells", "germline stem cells", "primordial germ cells", and "primordial germ cell-like cells". In addition, the operators "AND" and "OR" were applied for "primordial germ cells" or "primordial germ cell-like cells" and the other terms.

Authors independently screened the records by reading the title and abstract. Only peer reviewed full-length records covering the mammalian MSCs differentiation into primordial germ cell-like cells were included by experimental models.

In initial search, we retrieved 159 potentially relevant records, from which 50 were duplicates. Of the papers screened by reading the title and abstract, 77 studies were included (Fig.1).

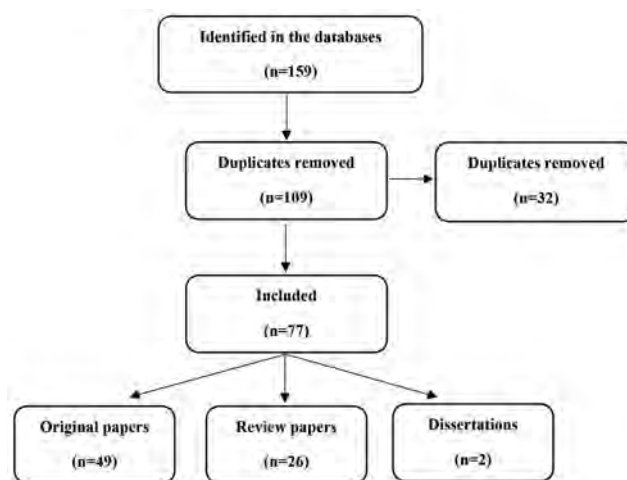


Fig.1: Flow chart of the review records selection.

Overview of mice primordial germ cell generation

Wnt3A from trophoblasts together with BMP4 and BMP8b from amniotic adjacent mesenchyme inducing PGC specification. PGCs are the first population of germ cells which are established during the development (Fig.2) and are the immediate precursors of both oocytes and spermatogonia. In mice, PGCs are initially identified as an approximately 40-cell cluster in the incipient allantois

based on day 7.25 (E7.25) of embryonic life. These cells then migrate to the developing hindgut endoderm and mesentery at E7.75 and E9.5, and colonize the genital ridges at E10.5, respectively (2).

An important event during the proliferative phase of PGCs is epigenetic reprogramming (27), especially a genome-wide DNA demethylation (28). *Blimp1* and *Prdm14* promote PGC specification via repressing somatic genes. PGCs retain remarkable pluripotential capabilities as shown by the ability to generate teratomas and pluripotent cell lines. Despite partial differences, both mouse and human PGCs express a group of 'naïve' and 'general' pluripotency factors. A transcription program involving the expression of the RNA-binding protein *Dazl* subsides PGCs pluripotential capabilities and prime them toward germline commitment (29).

In female XX embryos, PGCs will continue the

proliferation until E13.5 to reach a 25000 cell population. Afterwards, they enter to the prophase I of meiotic division and will be arrested in diplotene stage of meiosis prophase I. In contrast, XY PGCs enter the mitotic arrest upon entry into the genital ridges, and stay silent in the G0/G1 phase of the cell cycle for the remaining embryonic period. Around day 5 postpartum many of these cells resume proliferation, whereby some of them will be recruited as spermatogonial stem cells (30).

Strategies for germ cell differentiation from mesenchymal stem cells

As summarized in Table 1, several studies have been reported that MSCs originally show germ cells characteristics, and in the presence of certain chemicals, they can also be differentiated into PGCLCs, potentially applicable as a therapeutic approach for infertility (31-33).

Table 1: Studies using mesenchymal stem cells to produce germ cell-like cells

Cell source	Cytokines		Additional strategy	Differentiation time (day)	Final cell type	Reference
	RA (μ M)	BMP4 (ng/ml)				
BM-MSC						
Rat	1	-	-	21	PGCLC	(11)
Mouse	-	20	-	4	PGCLC	(32)
Mouse	-	1-25	-	4	PGCLC	(33)
Mouse	1	-	-	2	PGCLC	(25)
Ram	-	100	TGF- β 1 treatment	21	Male GCLC	(34)
WJ-MSC						
Human	1	-	Co-culture with placental cells	14	PGCLC	(35)
Human	1	10	-	21	PGCLC	(36)
Human	10	-	-	14	PGCLC	(37)
Human	-	12.5	Overexpressed CD61	7	Male GCLC	(38)
Human	-	-	Follicular fluid, cumulus cells conditioned medium	21	PGCLC	(39)
Human	2	-	-	14	PGCLC	(40)
Ad-MSC						
Mouse	1	-	-	2	PGCLC	(25)
Human	10	-	-	21	PGCLC	(41)
Human	1	-	-	7-21	Male GCLC	(42)
Human	10	-	Co-culture with Sertoli cells	21	Male GCLC	(43)
Human	-	25	Overexpressed miR-106b	4	PGCLC	(44)
Canine	-	-	Overexpressed CD61	2 and 10	PGCLC	(45)
FF-MSC						
Human	-	-	BMP15 treatment	21	Female GCLC	(46)

Ad; Adipose tissue, BM; Bone marrow, FF; Follicular fluid, GCLC; Germ cell-like cell, PGCLC; Primordial germ cell-like cell, WJ; Wharton's jelly, and MSC; Mesenchymal stem cell.

Bone marrow-derived mesenchymal stem cells

BMP4 is one of the most frequently used factor for stem cell differentiation (47). Using BMP4, several protocols have been established to differentiate MSCs, including PGCLCs from bone marrow-derived (BM)-MSCs. Leading studies have used feeder layer, respectively and fetal bovine serum to support cell proliferation. For example, the mouse myoblast cell line C2C12 feeder layer in the presence of an interleukin 6 class cytokine was used to support proliferation (32). The cells obtained from rat, mouse, and human have been examined and various BMP4 concentrations have been employed from 1 to 100 ng/ml. In one study, RA was used as the PGCLCs differentiation inducer (11).

In the study by Ghasemzadeh-Hasankolaei et al. (34), although transforming growth factor (TGF)- β 1 was more effective than BMP4, BMP4 could significantly boost the male germ cell markers. In addition to inducing differentiation, BMP4 had a positive effect on cell proliferation and survival (33). In three studies, the induction period was shorter than 5 days (25, 31, 33), while, in two studies the induction period was 21 days (11, 34). In two studies, mouse vasa homologue (Mvh) marker was employed to determine the extent of differentiation into germ cells (32, 33). This marker is expressed in germ cells up to the post-meiotic stage in both males and females (48).

In only two studies, isolated MSCs were characterized before induction of differentiation (11, 33). For this purpose, CD90⁺, CD105⁺, CD34⁻ and CD45⁻ molecular pattern was used to isolate and detect the cells. After inducing differentiation, several germ cell markers including c-Kit, Dazl, Stella, and Fragilis (also known as interferon induced transmembrane protein 3) were assessed. Fragilis is highly expressed in mouse PGCs at E6.5-7.25 together with Stella (Fig.2). In two studies, serum concentrations of 20% (32) and 10% (11) were used to support cell growth and proliferation. In the study of Shirazi et al. (32), comparison of migrating cells with migrated cells revealed a pattern of differentiation markers similar to PGCLCs. In one study the differentiation capabilities of BM-MSCs and ADSCs were compared. While both cell populations had the potential to become PGCLCs, BM-MSCs indicating a greater potential (25).

Wharton's jelly-derived mesenchymal stem cells

Since BM-MSCs isolation is an invasive and complicated process, the use of umbilical cord or Wharton's jelly (WJ)-MSCs is considered more convenient. The isolation of these cells from umbilical cord or placenta of a newborn is non-complicated, and non-invasive with a lower risk of contamination and ethical concerns (35). In addition to multipotent properties of these cells, which are between adult cells and ESCs, they seem to have a high potential to be differentiated into germ cells (49).

The strategies used to differentiate PGCLCs from WJ-

MSCs are more diverse than BM-MSCs. Co-culture and genetic manipulation methods have been employed as supporting or adjuvant factors with RA and BMP4 treatments.

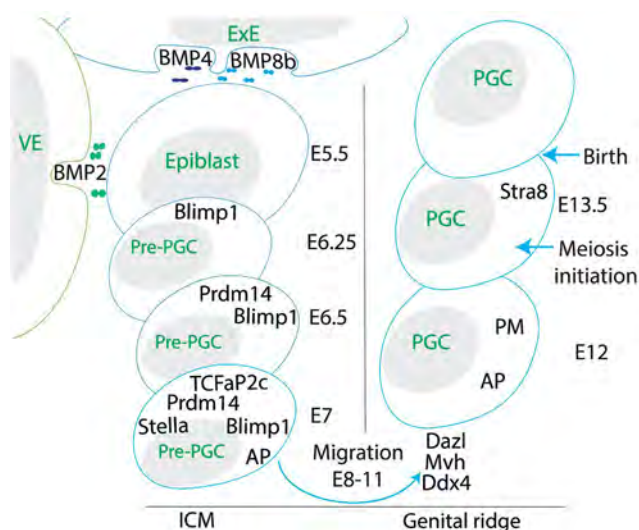


Fig.2: Female mice primordial germ cell (PGC) generation. The extraembryonic endoderm (ExE) layer, which is in contact with epiblast, secretes BMP4. Signals generated by ExE and visceral endoderm (VE) play important roles in inducing differentiation to PGCs. B lymphocyte-induced maturation protein 1 (Blimp1) is the first expressed marker of PGCs precursor at embryonic day (E) 6.25. BMP4 and BMP8b secreted by ExE and BMP2 secreted by proximal VE induce differentiation to Blimp1⁺PGC precursors in the posterior proximal epiblast at E6.25. Initial PGCs at E6.5 and E7 express the transcription factors Prdm14 and Stella, respectively. By the fate determination of the germ cells, they begin to proliferate and migrate to the base of the yolk sac and show strong alkaline phosphatase (AP) activity. Then, they start migrating from inner cell mass (ICM) to the genital ridge. These cells express the pluripotency gene markers (PM) *Oct4*, *Nanog*, and *Sox2*, which are important for PGC growth and germination. Deleted in azoospermia-like (*Dazl*), mouse vasa homologue (*Mvh*) and ATP-dependent RNA helicase *Ddx4* expression lead to germ cell commitment and indicate formation of post-migrating gonocytes. PGCs express the signaled by retinoic acid 8 (*Stra8*) from E13.5 which initiates the transition between mitosis and meiosis in oogenesis (26).

Compared with RA induction, the placental cell co-culture method further increased the early germ cell markers, *Oct4*, and ATP-dependent RNA helicase *Ddx4*. However, no significant differences were observed for specific cell markers such as growth differentiation factor 9 (*GDF9*) and zona pellucida glycoprotein 3 (*Zp-3*). *GDF9* is a growth factor from the TGF- β family. This factor is expressed in large amounts in eggs that plays an important role in folliculogenesis plus ovulation (50). *Zp-3* as a receptor mediates the initial binding of sperm to the egg (51).

Based on these results, it seems that in MSCs differentiation induction into PGCLCs, BMP4 is not a substitutive factor, but a complementary or amplifying factor of RA. In support of this hypothesis, initial treatment

of human WJ-MSC with BMP4 and RA outperformed BMP4 alone. In addition, co-culture with placental cells and RA also showed fewer germ cell-specific markers than BMP4 and RA combination (36).

Human follicular fluid and cumulus cells-conditioned medium could induce expression of oocyte specific genes and proteins (39). These factors also induced morphological changes matching oocyte-like cell differentiation. The observed effect has been related to potent growth factors of cumulus cells secretome such as epidermal growth factor. The potential of cells derived from follicular fluid to differentiate into oocyte-like cells further demonstrate the possibility of developing germ cells from adult stem cells (46).

In optimizing the development of PGCLCs, genetic manipulation is a potential strategy. Through overexpression and suppression of selected genes, the differentiation pathway can be oriented in the relevant direction. This approach can also facilitate *in vitro* induction of differentiation into PGCLCs. For this purpose, the genes involved in embryonic development are prioritized. In a study, obtaining male PGCLCs, CD61 or Integrin beta-3 was overexpressed in human placental MSCs. This manipulation alone increased the PGCLC markers such as c-Kit, sex determining region Y-Box 2 (*Sox2*), and *SSEA1*. Treatment of manipulated cells with BMP4 enhanced male-PGCLC differentiation, which was characterized by an increase in the signaling through retinoic acid 8 (*Stra8*) marker (38).

Adipose-derived stem cells

It has recently been shown that MSCs derived from adipose tissue can be differentiated into PGCLCs with BMP4 treatment or transfection by miR-106b (44). BMP4 has not been used in any of the other five studies on adipose-derived stem cells (ADSCs). Nevertheless, RA has been used alone or in combination with co-culture. Genetic manipulation of ADSCs has also been described as a successful means to induce PGC specification.

The Sertoli cell co-culture (43), testicular cell-conditioned medium (42), and testosterone (43) were used to induce male PGCLCs with RA. In addition to direct differentiation induction, treatment with RA and testosterone indirectly enhanced the differentiation of ADSCs into male PGCLC by promoting the viability and secretory activity of sertoli feeder cells. Similar to human WJ-MSCs (48), increased CD61 expression in Canine ADSCs alone significantly elevated PGC specification and stem cell markers compared to control cells (42). Examination of TGF- β signaling showed that CD61 expression significantly enhanced the level of Smad2 phosphorylation, without affecting the level of phosphorylated Smad2/3 and Smad3.

Retinoic acid and bone morphogenetic proteins pathways

All-trans-retinoic acid

Retinol is obtained as retinyl ester from plants β -carotene.

RA is one of the main retinol metabolites with potent biological capabilities related to proliferation and differentiation (52). On the cell surface, RA is taken up by retinol binding protein encoded by steroidogenic acute regulatory protein (StAR) 6 (53). Lecithin:retinol acyl transferase is also required for retinol uptaking and esterification (Fig.3A). Inside the cell, the transferase and dehydrogenase enzymes convert retinol to retinyl ester, retinaldehyde, and then RA. RA binds to cellular RA binding protein 2 that is transferred into the nucleus (54). In the presence of RA, the retinoid-X receptor (RXR)/RA receptor (RAR) heterodimer complex interacts with DNA and activates the transcription of RA “primary response” genes (55).

Transcription activation is one of the primary steps of RA-associated differentiation process occurring during several minutes to hours after RA addition to the culture media. A number of “immediate early” genes or “primary response” genes are the direct targets of RA (Fig.3B) (56).

RA-mediated gene expression regulation often involves polycomb group (PcG) proteins (Fig.3C). PcG proteins can form a complex of gene-silencing proteins, which play a central role in embryogenesis, patterning, and differentiation (57). Following RA in addition to stem cell culture medium, a fast dissociation of PcG proteins occurred, leading to the induction of differentiation-related genes expression, including *Stella*, *Fragilis*, and *Stra8* (58). Thus, retinoids provide an essential early signal to induce a certain cascade for totipotent and lineage restricted stem cell differentiation (55).

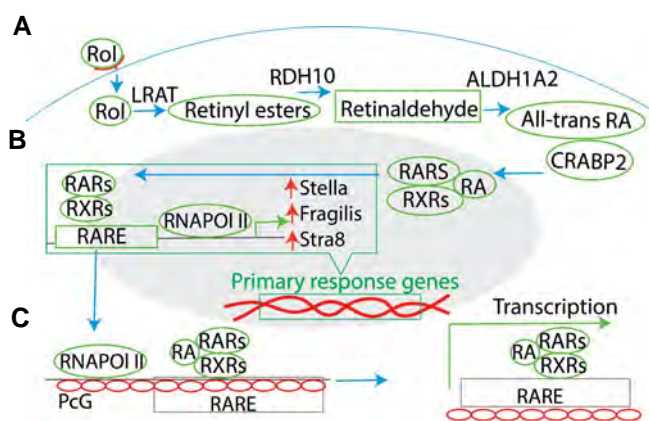


Fig.3: Retinoic acid signaling pathway in the regulation of germ-cell related gene expression. **A.** On the cell surface, retinol (Rol) by binding to retinol binding protein enters the target stem cell and is converted to all-trans retinoic acid (RA) following the lecithin:retinol acyl transferase (LRAT), retinol dehydrogenase 10 (RDH10) and aldehyde dehydrogenase 1a2 (ALDH1A2) reactions. Then, RA is transferred to the nucleus by binding to cellular retinoic acid binding protein 2 (CRABP2). Once in the nucleus, RA is initially bound to retinoic acid receptors (RARs) and the RA-RARs complex by binding to retinoid X receptors (RXRs) will interact with RA primary response genes (53). **B.** RA primary response genes have some enhancers known as RA response element (RARE) which RARs/RXRs complex binds to, leading to RNAPII activation and increased PGCs-related genes, including *Stella*, *Fragilis*, and *Stra8*, expression (55). **C.** PcG proteins form a gene-silencing complex for gene expression regulation. RA causes the dissociation of these proteins and activates the differentiation-related genes expression (57, 59).

bone morphogenetic proteins

PGCLC production from MSCs has been studied in both human and mouse models. Studies on the mouse and rat models have predominantly applied BM-MSCs. Despite promising early results on the differentiation of mouse BM-MSCs into PGCLCs, no follow-up data has been published on human BM-MSCs. MSCs of WJ and adipose tissue origin used in the human model studies (Table 1). However, the current knowledge on the mechanism of MSCs differentiation into PGCLCs is not persuasive enough. As the isolation of MSCs in humans is far easier than the obtaining ESCs, establishing suitable conditions for them to differentiate into PGCLCs will progress more rapidly. The recent studies that have efficiently differentiated MSCs are good models for future mechanistic studies, though failure to control the key variables remains a major limitation. Figure 4 illustrates the BMPs signaling pathway in the regulation of germ-cell related gene expression.

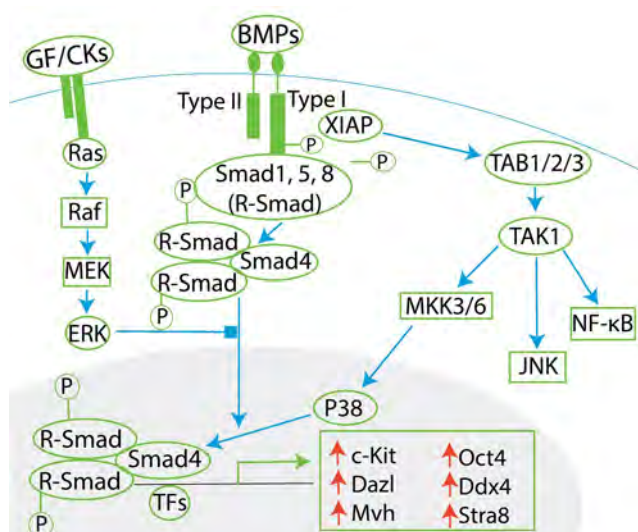


Fig.4: BMPs signaling pathway in the regulation of germ-cell related gene expression. BMPs act via type I and type II receptors. These receptors interaction results in receptor I-mediated phosphorylation of Smad1, Smad5, and Smad8 (R-Smad). Two phosphorylated R-Smads in combination with Smad4 form a heterotrimeric complex which is transmitted into the nucleus and regulates the PGCs differentiation-related target genes (such as *c-Kit*, *Dazl*, *Mvh*, *Oct4*, *Ddx4* and *Stra8*) expression together with the other transcription factors (TFs). X-linked inhibitor of apoptosis (XIAP) also links the BMP receptor signals to TGF β 1 activated tyrosine kinase 1 (TAK1). Then, TAK1 activates Map kinase kinase isoforms 3/6 (MKK3/6), JNK and NF- κ B. Mitogen-activated protein kinase (MAPK) activated by growth factors (GFs) or cytokines (CKs) through Ras/Raf/MEK can inhibit the Smad nuclear translocation and consequently inhibit the BMP signaling pathway (60).

In vitro differentiation of MSC using RA and BMP4 has provided a customizable approach for improving conditions (Fig.5).

The available methods in this area have a number of limitations. Defining standard functional assays in this area will enable us to improve the conditions for

producing PGCLCs. Evidence suggests that the mouse PSC is not very similar to the human PSC in terms of its pluripotency nature, making the PGCLC properties obtained from these two species different. For example, in very similar differentiation induction protocols, human PGCLCs, unlike mice PGCLCs, are negative for *Ddx4* and *Dazl* genes, analogous to early stage PGCs (14, 61). Refining germ cell-related signaling pathways will enhance preferential differentiation of somatic MSCs into PGCLCs.

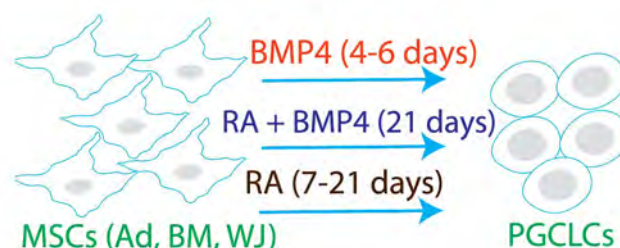


Fig.5: Induction of germ cell-like cells (PGCLCs) from mesenchymal stem cells (MSCs). The cells can be differentiated into PGCLCs from adipose tissue (Ad), bone marrow (BM), and Wharton jelly (WJ) cultured in the presence of BMP4. Alternatively, or in combination with BMP4, retinoic acid (RA) can also be used as an inducer.

Discovering gene expression signatures using RNA sequencing methods will allow determining the functional potential of PGCLCs without the need for further differentiation. In determining such characteristics, the intrinsic differences between cell types from different species must be taken into account. The difference in the initial pluripotency state is attributed to the limited response of rat ESCs compared to mice ESCs to PGCLCs differentiation stimuli. Indeed, induced expression of the PGC transcriptional repressor *Blimp1* by genetic manipulation increased differentiation towards cells expressing PGCLC markers (62). Moreover, human PGCs, unlike mice PGCs, do not express the pluripotency factor *Sox2*, while requiring *Sox17* for PGC specification (24). Thus, depending on the studied species, additional strategies may be needed to obtain more mature PGCLCs, such as co-culture with somatic gonadal cells.

A reasonable similarity between ESC-induced PGCLCs and *in vivo* PGCs has previously been reported (63). However, no study has yet compared the transcript of PGCLCs obtained from MSCs with *in vivo* PGCs or PGCLCs from ESCs, reprogrammed cells, or transdifferentiated cells. The use of a CRISPR/Cas9 screening platform to identify the factors required for PGC development in a new study (64) is a good example of a mechanistic study of the PGC specification.

The development of safe and efficient protocols in this field will provide useful resources for the PGCLCs in fertility science. Certainly, a fully defined condition cannot be provided with somatic cell co-culture strategy

or serum supplementation. Nevertheless, using co-culture techniques, signaling and environmental cues related to PGC specification can be investigated. With these techniques, the effect of different types of somatic cells can be tested comparatively. In this way, more effective cells are identified during screening, after which the potent player can be identified. In that framework, the indirect effect of nutrients on cell development through somatic cells can be determined (65). Further, the bioactive components might be identified by serum or follicular fluid pre-fractionation (66, 67). For instance, follicular fluid has shown preserving effects on the stemness characteristics of human granulosa cells (68). In the approach of employing MSCs to produce PGCLCs, there is a great opportunity for manipulation before differentiation. So far, two studies (48, 52) have shown direct MSCs towards PGCLCs through genetic manipulation. With this strategy, the activity of related signaling pathways has been studied. Gene therapy can be performed once optimal PGCLCs are achieved. Thus, as with cases of reprogramming and transdifferentiation, genetically modified PGCLCs can be obtained from MSCs in genetic diseases.

At present, *in vivo* PGCLC grafting is mainly used to obtain gametes, as no suitable *in vitro* condition has yet been established for this purpose. For instance, Hayashi and Surani (63) successfully used somatic cells from mice embryonic ovaries to direct oogenesis from PGCLC, but the efficiency of oocytes derived from PGCLC to produce zygotes was only 53%. Providing appropriate conditions for the proliferation and maintenance of PGCLCs is a challenge in this regard. Many factors such as cell species, age, and sex affect MSC's ability to eventually differentiate into gametes. Initial identification and purification of MSCs using exclusive and robust markers is an essential requirement for achieving optimal and defined conditions. Another important factor is the optimal duration of differentiation induction. Accordingly, it is necessary to determine the dynamics of markers in an integrated way. In addition, the appropriate stage of differentiation needs to be determined according to the ability of proliferation and subsequent differentiation into gamete lineages.

Conclusion

The availability of MSCs has made it possible to customize conditions for their differentiation into PGCLCs in several models, including humans. Umbilical cord, adipose tissue, and bone marrow are prospective sources of MSCs for germ cell line regeneration. Refining germ cell-related signaling pathways during induced differentiation of MSCs will help define extension to the protocols for PGCLCs production.

Acknowledgments

This study was supported by Endocrine Research Center (grant No. 59420) and Faculty of Advanced Medical Sciences at Tabriz University of Medical Sciences, Iran. Authors declare no conflict of interest in this study.

Authors' Contributions

Sh.F.; Contributed to the conception, design, and

drafting. P.F., Z.N.; Contributed to the literature review. A.M.; Was responsible for overall supervision. All authors read and approved the final manuscript.

References

- Kahnamouyi S, Nouri M, Farzadi L, Darabi M, Hosseini V, Mehdi-zadeh A. The role of mitogen-activated protein kinase-extracellular receptor kinase pathway in female fertility outcomes: a focus on pituitary gonadotropins regulation. *Ther Adv Endocrinol Metab*. 2018; 9(7): 209-215.
- Chen D, Sun N, Hou L, Kim R, Faith J, Aslanyan M, et al. Human primordial germ cells are specified from lineage-primed progenitors. *Cell Rep*. 2019; 29(13): 4568-4582.
- Larose H, Shami AN, Abbott H, Manske G, Lei L, Hammoud SS. Gametogenesis: a journey from inception to conception. *Curr Top Dev Biol*. 2019; 132: 257-310.
- Suman S, Domingues A, Ratajczak J, Ratajczak MZ. Potential clinical applications of stem cells in regenerative medicine. *Adv Exp Med Biol*. 2019; 1201: 1-22.
- Eguizabal C, Aran B, Chuva de Sousa Lopes SM, Geens M, Heindryckx B, Panula S, et al. Two decades of embryonic stem cells: a historical overview. *Hum Reprod Open*. 2019; 2019(1): hoy024.
- Zhao YX, Chen SR, Su PP, Huang FH, Shi YC, Shi QY, et al. Using mesenchymal stem cells to treat female infertility: an update on female reproductive diseases. *Stem Cells Int*. 2019; 2019: 9071720.
- Wuputra K, Ku CC, Wu DC, Lin YC, Saito S, Yokoyama KK. Prevention of tumor risk associated with the reprogramming of human pluripotent stem cells. *J Exp Clin Cancer Res*. 2020; 39: 1-24.
- Volarevic V, Markovic BS, Gazdic M, Volarevic A, Jovicic N, Arsenijevic N, et al. Ethical and safety issues of stem cell-based therapy. *Int J Med Sci*. 2018; 15(1): 36.
- Zakrzewski W, Dobrzyński M, Szymonowicz M, Rybak Z. Stem cells: past, present, and future. *Stem Cell Res Ther*. 2019; 10(1): 1-22.
- Mohr A, Zwacka R. The future of mesenchymal stem cell-based therapeutic approaches for cancer—From cells to ghosts. *Cancer Lett*. 2018; 414: 239-249.
- Kumar K, Das K, Madhusoodan A, Kumar A, Singh P, Mondal T, et al. Rat bone marrow derived mesenchymal stem cells differentiate to germ cell like cells. Available from: <https://www.biorxiv.org/content/10.1101/418962v1.full> (24 May 2021).
- Lee SH. The advantages and limitations of mesenchymal stem cells in clinical application for treating human diseases. *Osteoporos Sarcopenia*. 2018; 4(4): 150.
- Easley CA, Latov DR, Simerly CR, Schatten G. Adult somatic cells to the rescue: nuclear reprogramming and the dispensability of gonadal germ cells. *Fertil Steril*. 2014; 101(1): 14-19.
- Sasaki K, Yokobayashi S, Nakamura T, Okamoto I, Yabuta Y, Kurimoto K, et al. Robust *in vitro* induction of human germ cell fate from pluripotent stem cells. *Cell Stem Cell*. 2015; 17(2): 178-194.
- Sun R, Sun YC, Ge W, Tan H, Cheng SF, Yin S, et al. The crucial role of Activin A on the formation of primordial germ cell-like cells from skin-derived stem cells *in vitro*. *Cell Cycle*. 2015; 14(19): 3016-3029.
- Garcia-Nieto PE, Morrison AJ, Fraser HB. The somatic mutation landscape of the human body. *Genome Biol*. 2019; 20(1): 1-20.
- Rahbari R, Wuster A, Lindsay SJ, Hardwick RJ, Alexandrov LB, Turki SA, et al. Timing, rates and spectra of human germline mutation. *Nat Genet*. 2016; 48(2): 126-133.
- Gell JJ, Liu W, Sosa E, Chialastri A, Hancock G, Tao Y, et al. An extended culture system that supports human primordial germ cell-like cell survival and initiation of DNA methylation erasure. *Stem Cell Rep*. 2020; 14(3): 433-446.
- Mitsunaga S, Shioda K, Isselbacher KJ, Hanna JH, Shioda T. Generation of human primordial germ cell-like cells at the surface of embryoid bodies from primed-pluripotency induced pluripotent stem cells. *J Vis Exp*. 2019; (143).
- Gulimiheranmu M, Wang X, Zhou J. Advances in female germ cell induction from pluripotent stem cells. *Stem Cells Int*. 2021; 8849230.
- Fang F, Li Z, Zhao Q, Ye Z, Gu X, Pan F, et al. Induced pluripotent stem cells derived from two idiopathic azoospermia patients display compromised differentiation potential for primordial germ cell fate. *Front Cell Dev Biol*. 2020; 8: 432.
- Kojima Y, Sasaki K, Yokobayashi S, Sakai Y, Nakamura T, Yabuta Y, et al. Evolutionarily distinctive transcriptional and signaling pro-

- grams drive human germ cell lineage specification from pluripotent stem cells. *Cell Stem Cell*. 2017; 21(4): 517-532.
23. Pierson Smela M, Sybirna A, Wong FCK, Surani MA. Testing the role of SOX15 in human primordial germ cell fate. *Wellcome Open Res*. 2019; 4: 122.
 24. Yokobayashi S, Okita K, Nakagawa M, Nakamura T, Yabuta Y, Yamamoto T, et al. Clonal variation of human induced pluripotent stem cells for induction into the germ cell fate. *Biol Reprod*. 2017; 96(6): 1154-1166.
 25. Shirzeily MH, Pasbakhsh P, Amidi F, Mehrannia K, Sobhani A. Comparison of differentiation potential of male mouse adipose tissue and bone marrow derived-mesenchymal stem cells into germ cells. *Int J Reprod Biomed*. 2013; 11(12): 965.
 26. Saitou M, Miyauchi H. Gametogenesis from pluripotent stem cells. *Cell Stem Cell*. 2016; 18(6): 721-735.
 27. Rassoulzadegan M, Cuzin F. Epigenetic heredity: RNA-mediated modes of phenotypic variation. *Ann NY Acad Sci*. 2015; 1341: 172-175.
 28. Zeng Y, Chen T. DNA methylation reprogramming during mammalian development. *Genes*. 2019; 10(4): 257.
 29. Nicholls PK, Schorle H, Naqvi S, Hu YC, Fan Y, Carmell MA, et al. Mammalian germ cells are determined after PGC colonization of the nascent gonad. *Proc Natl Acad Sci USA*. 2019; 116(51): 25677-25687.
 30. Wang JH, Li Y, Deng SL, Liu YX, Lian ZX, Yu K. Recent research advances in mitosis during mammalian gametogenesis. *Cells*. 2019; 8(6): 567.
 31. Nayernia K, Lee JH, Drusenheimer N, Nolte J, Wulf G, Dressel R, et al. Derivation of male germ cells from bone marrow stem cells. *Lab Invest*. 2006; 86(7): 654-663.
 32. Shirazi R, Zarnani AH, Soleimani M, Abdolvahabi MA, Nayernia K, Kashani IR. BMP4 can generate primordial germ cells from bone-marrow-derived pluripotent stem cells. *Cell Biol Int*. 2012; 36(12): 1185-1193.
 33. Mazaheri Z, Movahedin M, Rahbarizadeh F, Amanpour S. Different doses of bone morphogenetic protein 4 promote the expression of early germ cell-specific gene in bone marrow mesenchymal stem cells. *In Vitro Cell Dev Biol Anim*. 2011; 47(8): 521-525.
 34. Ghasemzadeh-Hasankolaei M, Sedighi-Gilani M, Eslaminejad M. Induction of ram bone marrow mesenchymal stem cells into germ cell lineage using transforming growth factor- β superfamily growth factors. *Reprod Domest Anim*. 2014; 49(4): 588-598.
 35. Asgari HR, Akbari M, Abbasi M, Ai J, Korouji M, Aliakbari F, et al. Human Wharton's jelly-derived mesenchymal stem cells express oocyte developmental genes during co-culture with placental cells. *Iran J Basic Med Sci*. 2015; 18(1): 22.
 36. Amidi F, Hoseini MA, Nia KN, Habibi M, Kajbafzadeh AM, Mazaheri Z, et al. Male germ-like cell differentiation potential of human umbilical cord Wharton's jelly-derived mesenchymal stem cells in co-culture with human placenta cells in presence of BMP4 and retinoic acid. *Iran J Basic Med Sci*. 2015; 18(4): 325.
 37. Dissanayake D, Patel H, Wijesinghe P. Differentiation of human male germ cells from Wharton's jelly-derived mesenchymal stem cells. *Clin Exp Reprod Med*. 2018; 45(2): 75-81.
 38. Li B, Liu W, Zhuang M, Li N, Wu S, Pan S, et al. Overexpression of CD61 promotes hUC-MSC differentiation into male germ-like cells. *Cell Prolif*. 2016; 49(1): 36-47.
 39. Zolfaghar M, Mirzaeian L, Beiki B, Najji T, Moini A, Eftekhari-Yazdi P, et al. Wharton's jelly derived mesenchymal stem cells differentiate into oocyte like cells in vitro by follicular fluid and cumulus cells conditioned medium. *Heliyon*. 2020; 6(10): e04992.
 40. Alifi F, Asgari HR. Alteration in expression of primordial germ cell (PGC) markers during induction of human amniotic mesenchymal stem cells (hAMSCs). *J Reprod Infertil*. 2020; 21(1): 59.
 41. Liu H, Chen M, Liu L, Ren S, Cheng P, Zhang H. Induction of human adipose-derived mesenchymal stem cells into germ lineage using retinoic acid. *Cell Reprogram*. 2018; 20(2): 127-134.
 42. Bräunig P, Glanzner W, Rissi V, Gonçalves P. The differentiation potential of adipose tissue-derived mesenchymal stem cells into cell lineage related to male germ cells. *Arq Bras Med Vet Zootec*. 2018; 70(1): 160-168.
 43. Luo Y, Xie L, Mohsin A, Ahmed W, Xu C, Peng Y, et al. Efficient generation of male germ-like cells derived during co-culturing of adipose-derived mesenchymal stem cells with Sertoli cells under retinoic acid and testosterone induction. *Stem Cell Res Ther*. 2019; 10(1): 91.
 44. Mahboudi S, Parivar K, Mazaheri Z, Irani S. Mir-106b cluster regulates primordial germ cells differentiation from human mesenchymal stem cells. *Cell J*. 2021; 23(3): 294.
 45. Fang J, Wei Y, Lv C, Peng S, Zhao S, Hua J. CD61 promotes the differentiation of canine ADMSCs into PGC-like cells through modulation of TGF- β signaling. *Sci Rep*. 2017; 7(1): 1-9.
 46. Taheri M, Saki G, Nikbakht R, Eftekhari AR. Bone morphogenetic protein 15 induces differentiation of mesenchymal stem cells derived from human follicular fluid to oocyte-like cell. *Cell Biol Int*. 2021; 45(1): 127-139.
 47. Li Q, Zhang S, Sui Y, Fu X, Li Y, Wei S. Sequential stimulation with different concentrations of BMP4 promotes the differentiation of human embryonic stem cells into dental epithelium with potential for tooth formation. *Stem Cell Res Ther*. 2019; 10(1): 1-8.
 48. Toyooka Y, Tsunekawa N, Takahashi Y, Matsui Y, Satoh M, Noce T. Expression and intracellular localization of mouse Vasa-homologue protein during germ cell development. *Mech Dev*. 2000; 93(1-2): 139-149.
 49. Hass R, Kasper C, Böhm S, Jacobs R. Different populations and sources of human mesenchymal stem cells (MSC): a comparison of adult and neonatal tissue-derived MSC. *Cell Commun Signal*. 2011; 9(1): 12.
 50. Otsuka F, McTavish KJ, Shimasaki S. Integral role of GDF-9 and BMP-15 in ovarian function. *Mol Reprod Dev*. 2011; 78(1): 9-21.
 51. Han L, Monné M, Okumura H, Schwend T, Cherry AL, Flot D, et al. Insights into egg coat assembly and egg-sperm interaction from the X-ray structure of full-length ZP3. *Cell*. 2010; 143(3): 404-415.
 52. Mongan NP, Gudas LJ. Diverse actions of retinoid receptors in cancer prevention and treatment. *Differentiation*. 2007; 75(9): 853-870.
 53. Kawaguchi R, Yu J, Honda J, Hu J, Whitelegge J, Ping P, et al. A membrane receptor for retinol binding protein mediates cellular uptake of vitamin A. *Science*. 2007; 315(5813): 820-825.
 54. Schug TT, Berry DC, Shaw NS, Travis SN, Noy N. Opposing effects of retinoic acid on cell growth result from alternate activation of two different nuclear receptors. *Cell*. 2007; 129(4): 723-733.
 55. Gudas LJ, Wagner JA. Retinoids regulate stem cell differentiation. *J Cell Physiol*. 2011; 226(2): 322-330.
 56. Li G, Margueron R, Hu G, Stokes D, Wang Y-H, Reinberg D. Highly compacted chromatin formed in vitro reflects the dynamics of transcription activation in vivo. *Mol Cell*. 2010; 38(1): 41-53.
 57. Simon JA, Kingston RE. Mechanisms of polycomb gene silencing: knowns and unknowns. *Nat Rev Mol Cell Biol*. 2009; 10(10): 697-708.
 58. Kashyap V, Gudas LJ. Epigenetic regulatory mechanisms distinguish retinoic acid-mediated transcriptional responses in stem cells and fibroblasts. *J Biol Chem*. 2010; 285(19): 14534-14548.
 59. Amat R, Gudas LJ. RAR γ is required for correct deposition and removal of Suz12 and H2A. Z in embryonic stem cells. *J Cell Physiol*. 2011; 226(2): 293-298.
 60. Derynck R, Zhang YE. Smad-dependent and Smad-independent pathways in TGF- β family signalling. *Nature*. 2003; 425(6958): 577-584.
 61. Irie N, Weinberger L, Tang WW, Kobayashi T, Viukov S, Manor YS, et al. SOX17 is a critical specifier of human primordial germ cell fate. *Cell*. 2015; 160(1-2): 253-268.
 62. Taylor RM. Investigation into germ cell fate determination of rat embryonic stem cells. Presented for the Ph.D., Edinburgh. University of Edinburgh. 2020.
 63. Hayashi K, Surani MA. Self-renewing epiblast stem cells exhibit continual delineation of germ cells with epigenetic reprogramming in vitro. *Development*. 2009; 136(21): 3549-3556.
 64. Oliveira GPMSda. The identification of novel factors required for the development of primordial germ cells. Presented for the Ph.D., Cambridge. University of Cambridge. 2020.
 65. Fayezi S, Ghaffari Novin M, Darabi M, Norouzian M, Nouri M, Farzadi L. Primary culture of human cumulus cells requires stearyl-coenzyme A desaturase 1 activity for steroidogenesis and enhancing oocyte in vitro maturation. *Reprod Sci*. 2018; 25(6): 844-853.
 66. Mardomi A, Nouri M, Farzadi L, Zarghami N, Mehdizadeh A, Yousefi M, et al. Human charcoal-stripped serum supplementation enhances both the stearyl-coenzyme A desaturase 1 activity of cumulus cells and the. *Hum Fertil (Camb)*. 2019; 22(3): 212-218.
 67. Eyvaznejad E, Nouri M, Ghasemzadeh A, Mehdizadeh A, Shahnaizi V, Asghari S, et al. Steroid-depleted polycystic ovarian syndrome serum promotes in vitro oocyte maturation and embryo development. *Gynecol Endocrinol*. 2018; 34(8): 698-703.
 68. Yousefi S, Soleimanirad J, Hamdi K, Farzadi L, Ghasemzadeh A, Kazemi M, et al. Distinct effect of fetal bovine serum versus follicular fluid on multipotentiality of human granulosa cells in in vitro condition. *Biologicals*. 2018; 52: 44-48.

The Effect of miR-106b-5p Expression in The Production of iPS-Like Cells from Mice SSCs during The Formation of Teratoma and The Three Embryonic Layers

Amir Hossein Hasani Fard, M.Sc.^{1#}, Fatemeh Kamalipour, M.Sc.^{1#}, Zohreh Mazaheri, Ph.D.², Seyed Jalil Hosseini, Ph.D.^{1*}

1. Men's Health and Reproductive Health Research Center, Shahid Beheshti University of Medical Sciences, Tehran, Iran
2. Department of Anatomical Sciences, Faculty of Medical Sciences, Tarbiat Modares University, Tehran, Iran

*Corresponding Address: P.O.Box: 19899/34148, Men's Health and Reproductive Health Research Center, Shahid Beheshti University of Medical Sciences, Tehran, Iran
Email: jhosseinee@gmail.com

#These authors contributed equally to this work.

Received: 24/July/2021, Accepted: 04/December/2021

Abstract

Objective: According to the mounting data, microRNAs (miRNAs) may play a key role in reprogramming. miR-106b is considered as an enhancer in reprogramming efficiency. Based on induced pluripotent stem cells (iPSCs), cell treatments have a huge amount of potential. One of the main concerns about using iPSCs in therapeutic settings is the possibility of tumor formation. It is hypothesized that a procedure that can reprogram cells with less genetic manipulation reduces the possibility of tumorigenicity.

Materials and Methods: In this experimental study, miR-106b-5p transduced by pLV-miRNA vector into mice isolated spermatogonial stem cells (SSCs) to achieve iPS-like cells. Then the transduced cells were cultured in specific conditions to study the formation of three germ layers. The tumorigenicity of these iPS-like cells was investigated by transplantation into male BALB/C mice.

Results: We show that SSCs can be successfully reprogrammed into induced iPS-like cells by pLV-miRNA vector to transduce the hsa-mir-106b-5p into SSCs and generating osteogenic, neural and hepatoblast lineage cells *in vitro* as a result of pluripotency. Although these iPS-like cells are pluripotent, they cannot form palpable tumors *in vivo*.

Conclusion: These results demonstrate that infection of hsa-mir-106b-5p into SSCs can reprogram them into iPSCs and advanced germ cell lineages without tumorigenicity. Also, a novel approach for studying the generation of iPSCs and the application of iPS or iPS-like cells in regenerative medicine is presented.

Keywords: Induced Pluripotent Stem Cells, Mir-106b, Spermatogonial Progenitor Cell, Transplantation, Tumorigenicity

Cell Journal(yakhteh), Vol 24, No 8, August 2022, Pages: 442-448

Citation: Hasani Fard AH, Kamalipour F, Mazaheri Z, Hosseini SJ. The effect of miR-106b-5p expression in the production of iPS-Like cells from mice SSCs during the formation of teratoma and the three embryonic layers. Cell J. 2022; 24(8): 442-448. doi: 10.22074/cellj.2022.8147.

This open-access article has been published under the terms of the Creative Commons Attribution Non-Commercial 3.0 (CC BY-NC 3.0).

Introduction

Yamanaka and colleagues were the first ones who produced adult fibroblasts into induced pluripotent stem cells (iPSCs) in a laboratory setting in 2006 providing the basis for substantial advancements in cell reprogramming technology (1, 2). Cell reprogramming has been used in developmental and stem cell biology and regenerative medicine fields for the last decade to investigate the potential of iPSCs in generating targeted cell types (3). In general, iPSCs may be produced *in vitro* from a variety of somatic cell types. Fibroblasts of mesodermal origins, endodermal hepatocytes, and ectoderm keratinocytes have been the most common cells used for this purpose till now (4-6). Spermatogonia stem cells (SSCs) are a type of testicular stem cell that has the ability to self-renew and differentiate into sperm cells. Current knowledge on biotechnology suggests that SSCs can be more efficient and safe in cell pluripotency studies over embryonic stem cell or adult somatic cell-based technologies. SSCs isolation from an individual's testicular tissue eliminates ethical and immunological concerns in cell treatments. As reported in previous studies, generating iPSCs from

adult fibroblasts is required retroviral transduction of pluripotent stem cell genes such Oct4, Sox2, klf4, c-Myc (OSKM), results in retroviral infection and teratomas. In contrast, SSCs can be reprogrammed to iPSCs in a specific culture medium without the addition of oncogenes or the use of retroviruses. However, tumorigenicity has been reported in this method (7, 8). According to new research, SSCs may be self-reprogrammed in a feeder-free reprogramming technique. Furthermore, SSCs can express the octamer-binding transcription factor4 (Oct4), a key factor in sustaining pluripotency in stem cells (9).

MicroRNAs (miRNAs) are a type of small non-coding RNA that are functional in the self-renewal, pluripotency, and differentiation of human embryonic stem cells (hESCs). MiRNAs play a crucial role in animal development by targeting mRNAs and regulating genes post-transcriptionally (10). Some miRNAs, including miR-106 increased reprogramming efficiency. miR-106b was reportedly one of the miRNAs with the highest expression of OSKM. These factors are known as the main factors that can be used for reprogramming (11). miR-106b belongs to the polycistronic miR-106b25

cluster and is found inside an intron of the *MCM7* gene; It can significantly improve iPSC efficiency and boost the reprogramming process by targeting *Tgfb2* and *p21* (12, 13).

According to reports from several laboratories, Yamanaka-induced pluripotency cells have the capacity to generate teratomas (14, 15). Probably, this specification is related to extensive genetic manipulation and the use of multiple viral vectors. Tumorigenicity has led to the limitation of the application of iPSCs in medicine, so a technique that can reprogram cells with less genetic manipulation reduces the possibility of tumorigenicity. According to the capacity of SSCs in converting to pluripotent cells and features of miRNAs mentioned above, we investigated the ability of reprogrammed SSCs into iPS-like cells by pLV-miRNA vector to transduce the hsa-mir-106b-5p into SSCs and generating three germ layers (ectoderm, endoderm, and mesoderm). Furthermore, we studied the capability of these iPS-like cells in tumorigenicity by measuring the size and pathology of tumors caused by the subcutaneous injection of cells into mice.

Material and Methods

Animals

Male BALB/C mice 8-10 weeks old and weighing 18-24 g, were treated with cyclosporine in a dose of 10 mg/kg per day by gavage. Transplanted mice received cyclosporine until two weeks after transplantation. Mice were maintained under sterile conditions on a 12-hour light-dark cycle at a constant temperature. Food and drink were freely available. All experiments were approved by the Ethics Committee of Shahid Beheshti University of Medical Sciences and following the Declaration of Helsinki (IR.SBMU.REC.1398.072).

Isolation and culture of SSCs

For the isolation of SSCs, testis of BALB/C mice suppressed by cyclosporine were collected and also isolation was performed by enzymatic digestion as described in our previous study. Spermatogonia cells were cultured for one week. According to the previous protocols explained in our earlier study, an antibody directed against promyelocytic leukemia zinc finger (PLZF) was used to

identify the SSCs. Cells were identified with primary and secondary antibodies that were labeled with fluorescent reagents (16).

The pLV-miRNA vector production in bacteria

The pLV-miRNA vector, which carried the hsa-mir-106b lentivirus and comprised green fluorescent protein (GFP) in infected *E. coli* BL21, was utilized to generate iPS-like cells (mir-p081, Biosettia, San Diego, CA, USA). The *E. coli* BL21 colony was cultured in 5 ml of Lysogeny broth (LB) medium (Sigma-Aldrich, USA) for 16 hours in a 37°C shaker incubator at 180 rpm. To determine the presence of vector in the bacteria, it was cultured for 24 hours in LB agar medium containing 100 µg/ml ampicillin. Vector purification from *E. coli* BL21 colonies was deployed by GF-1 Plasmid DNA Extraction Kit (Vivantis, Malaysia) instructions.

The quantitative reverse transcriptase polymerase chain reaction (qRT-PCR) technique was applied to ensure the accuracy of the extracted pLV-miRNA vector. The 16s-RNA as a bacterial reference gene and mir-106b primers are listed in Table 1. The sequences of forward and reverse primers were designed by using GeneRunner software. The cDNA was synthesized according to the manufacturer's instructions (Fermentas, USA). PCR products were electrophoresed on 1% agarose gel along with 1 kb DNA Ladder Marker and examined.

Transduction of the hsa-mir-106b-5p vector to SSC colonies

To vector transduction, SSCs are inserted into the cells of a cell culture well. Then, in a microtube, 500 µl of culture media and 7.5 µl of lipofectamine 3000 (Invitrogen, USA) are combined. In a separate microtube, 500 µl of media is combined with 0.5 µg of plasmid and 7.5 µl of lipofectamine 3000. The contents of the two microtubes were combined and incubated at room temperature for 10 to 15 minutes. Finally, 250 µl of the prepared sample was pipetted into each plate housing, and the cells were incubated for three days at 37°C. It is important to validate the increase in miRNA after transduction of the virus carrying the hsa-miR-106b-5p gene into the cells. A fluorescent microscope was used to confirm viral transduction since the plasmid contains a GFP tracer reagent (Olympus BX51).

Table 1: The sequences of primers used for evaluation of the extracted pLV-miRNA vector

Primer	Primer sequence (5'–3')
16s-RNA	F: ACTCCTACGGGAGGCAGCAG R: ATTACCGCGGCTGCTGG
Stem loop	GTTGGCTCTGGTGCAGGGTCCGAGGTATTCGCACCAGAGCCAANNNNN
miR106b	F: ACUGCAGUGCCAGCACTT R: GGCAAAGTGCTTACAGTGC

Examination of iPSC-like cell differentiation into all three germ layers *in vitro* phase

Differentiation into three germ layers was performed in two groups of cells: hsa-mir-106b-5p induction and without-hsa-mir-106b-5p induction as control group (treated with the empty vector). Both experimental groups were placed in a hanging drop culture, a concentration of 5×10^4 cells/ml suspension was prepared to soak in 20 μ l drops to produce the embryoid body (EB). Procedure includes holding cells in a droplet of culture medium and turning the microplate upside down to produce 3D spheroids. Surface tension forces and gravity are two factors that keep cells suspended (17). At the end of the procedure in each experimental group, the differentiation of iPSC-like cells was observed in 5 randomly chosen fields under a fluorescence microscope.

Differentiation into the ectodermal derivative

Cells were transferred into a 12-cell gelatinized microplate containing α -minimum essential medium (α -MEM, Sigma-Aldrich, USA) with 3% fetal bovine serum (FBS, Gibco, UK). Toward induction of neural phenotype in the EBs in two weeks, the 5×10^{-7} molar concentration of retinoic acid (Sigma-Aldrich, USA) was administered. Two weeks later, a beta-tubulin marker (Santa Cruz, USA) was used to examine the differentiation of adult neural cells (18).

Differentiation into the mesodermal derivative

Cells were grown in a six-cell plate when the entire culture surface was covered with cells, and their media changed with a bone differentiation medium to generate osteogenic lineage cells as a mesodermal lineage in transduced cells. This medium included Dulbecco's Modified Eagle Medium (DMEM, Gibco, UK) with 10% bovine serum (Gibco, UK), 10 mM beta glycerol phosphate (Sigma-Aldrich, USA), 10 nM dexamethasone (Sigma-Aldrich, USA), and 50 g/ml ascorbic 3-phosphate (Sigma-Aldrich, USA). The cells were then put on mesenchymal cells by using a sampler. For 21 days, cells were cultured in a humidified 37°C incubator with 5% CO₂. Finally, immunocytochemistry was performed to validate the differentiation of cells using the alkaline phosphatase marker (Santa Cruz, USA) (19).

Differentiation into the endodermal derivative

Cells were cultured for 28 days in DMEM medium (Gibco, UK) containing 20 μ l ascorbic acid (Sigma-Aldrich, USA) 20 μ l, 10 ng/ml hepatocyte growth factor (HGF, Merck, Germany), 10 ng/ml oncostatin M (OSM, Sino Biological, China), 10% FBS (Gibco, UK). Immunocytochemistry was used to establish the presence of the albumin marker (Santa

Cruz, USA) that enabled the cells to differentiate into hepatocytes (20).

Tumorigenicity of cells

Cells were transplanted into 20 immunodeficient male BALB/C mice (4-6 weeks). Transplantation was applied in four groups (n=5): SSCs (negative control), iPSCs as a positive control were obtained by using the method described by Baharvand and colleagues (21). They were provided by Stem Cells Technology Research Center. hsa-mir-106b-5p control (SSCs with empty vector), and hsa-mir-106b-5p (SSCs infected with hsa-mir-106b-5p). 5×10^6 μ l of culture medium was transplanted by subcutaneous injections into the loose skin over the mice back, and assessed tumor formation after eight weeks. Generation of tumors were measured by a caliper. The tumors were then isolated and stained for pathological examination using the hematoxylin and eosin technique.

Results

Confirmation of the nature of SSCs

Cell culture experiments were performed with male BALB/c mice testis. SSCs were isolated from seminiferous tubules of the testis and cultivated in DMEM conditions. In the testis, PLZF is a spermatogonia-specific transcription factor that is detected to identify SSCs (22). Immunocytochemistry analysis demonstrated high purity and proliferation of SSCs by the expression of the PLZF marker (Fig. 1A).

Expression of miR106b in transfected bacteria

The presence of the mir106b was determined by the qRT-PCR method. Results indicated a significant expression in mir106b in the transfected *E. coli* group compared to the non-transfected *E. coli* group.

Confirmation of transduced cells

Transduction of hsa-mir-106b-5p into SSCs confirmed by tracing the GFP protein reagent with a fluorescence microscope (Fig. 1B).

Differentiation of iPSC-like cells into all three germ layers

Differentiation into the ectoderm derivative

The biomarker class III beta-tubulin is known for expresses in neural lineage cells (23). Therefore, a beta-tubulin marker was used to identify neurons in cultured cells. Immunocytochemistry analyzes revealed that the hsa-mir-106b-5p induction cell group differentiated into neurons, but there was no differentiation to neural cells in the without- hsa-mir-106b-5p induction cell group (Fig. 2).

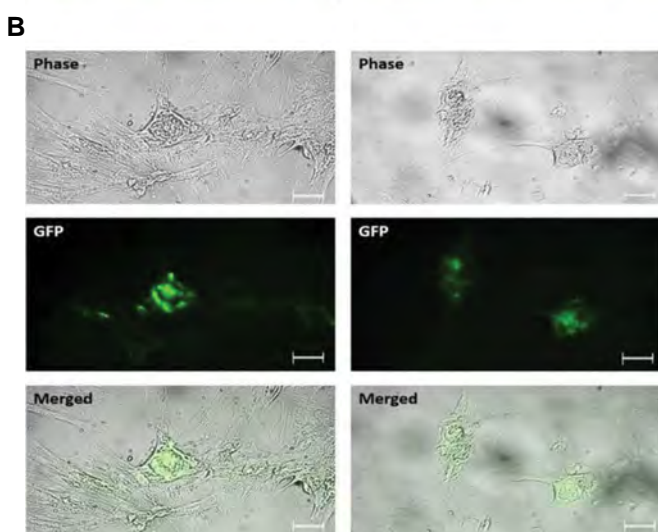
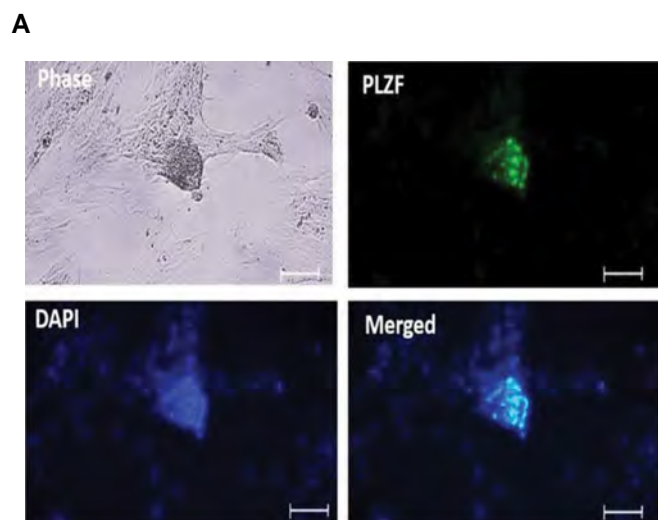


Fig.1: Confirmation of SSC nature as well as transfect. **A.** Immunocytochemical characterization of promyelocytic leukemia zinc finger (PLZF) in cultured spermatogonia stem cells (SSCs). Immunocytochemistry analysis of PLZF expression in the SSC (scale bar: 50 μ m). **B.** Tracing the GFP protein reagent with a fluorescence microscope to confirm transduction. The phase contrast, fluorescent, and merged photomicrographs demonstrate the transduction of hsa-mir-106b-5p into SSCs (scale bar: 40 μ m).

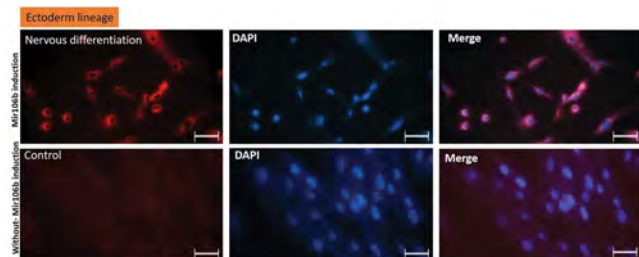


Fig.2: Fluorescent immunocytochemistry of beta-tubulin marker to detect ectodermal derivatives. hsa-mir-106b-5p induction group: differentiated nervous cells exhibited. Without-hsa-mir-106b-5p induction group: no differentiation detected (scale bar: 20 μ m).

Differentiation into the mesoderm derivative

As shown by immunocytochemistry analyzes of alkaline phosphatase (ALP) in Figure 3, iPS-like cells

with induction of hsa-mir-106b-5p were differentiated to osteogenic lineage cells. ALP is a frequently used marker for observing cell lineages of the embryonic mesoderm such as osteogenic lineage (24). However, osteocyte differentiated cells were not detected in the group without hsa-mir-106b-5p induction.

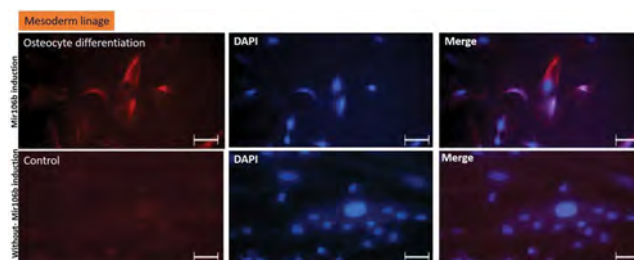


Fig.3: Fluorescent immunocytochemistry of alkaline phosphatase marker to detect mesodermal derivatives. hsa-mir-106b-5p induction group: differentiated osteocyte cells exhibited. Without-hsa-mir-106b-5p induction group: no differentiation detected (scale bar: 20 μ m).

Differentiation into the endoderm derivative

Adult functional hepatocytes secrete albumin into the culture medium which is used as a marker to identify endoderm lineage cells (25). Immunocytochemistry analyzes in Figure 4 showed that at the completion of the procedure, in the hsa-mir-106b-5p induction cell group, hepatocytes produced intracellular albumin but were incapable to released albumin into the extracellular environment. As a result, the cells were hepatocyte-like and developed into hepatocyte lines. However, the differentiated cells were not functional.

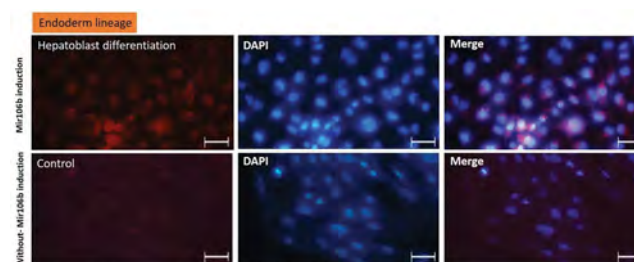


Fig.4: Fluorescent immunocytochemistry of Albumin marker to detect Endodermal derivatives. hsa-mir-106b-5p induction group: Albumin marker expressed in the hepatocyte-like cells but not detected in the secretion of the cells. Without-hsa-mir-106b-5p induction group: no differentiation detected (scale bar: 20 μ m).

Tumor growth in mice

Four independent experiments were performed, each using a different colony of have transduced SSCs and none-transduced cells. In three experimental groups [the SSCs negative control], has-mir-106b-5p control (empty vector), and hsa-mir-106b-5p (SSCs infected with hsa-mir-106b-5p) no palpable tumors were observed at the end of the experiment after two months. In contrast, the

iPSCs (positive control) formed palpable tumors at the site of injection in the mice back. Histological examination of tissue sections revealed tumorigenicity that accrued by iPSCs injection and the tumors grew $0.5 \times 1 \times 1$ cm at week eight, when the animals were sacrificed (Fig.5).

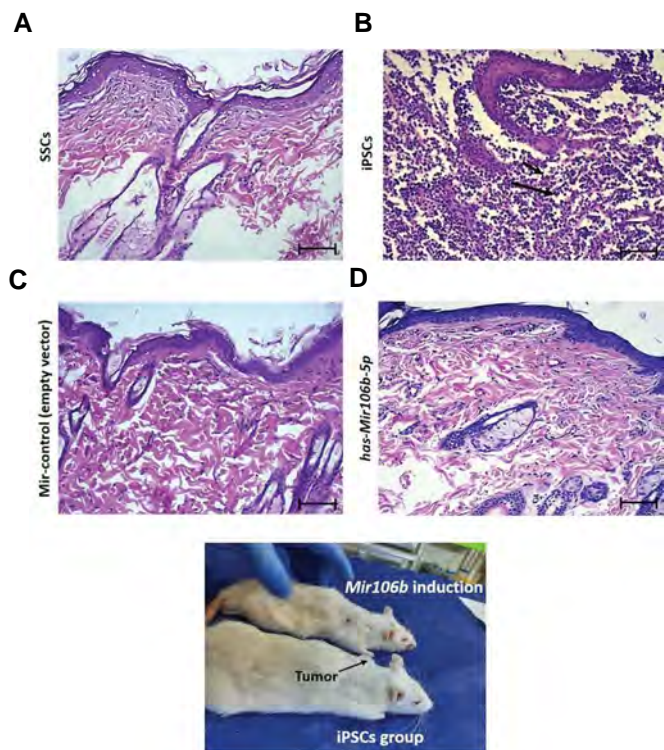


Fig.5: Histology of tumor formation in immunodeficient BALB/C mice following transplantation. **A.** In SSC group no teratomas were formed. **B.** Tumor formation (black arrows) in mice after transplantation of iPSCs. **C.** In Mir-control, and **D.** Mir106b-5p groups no teratomas were formed. (Hematoxylin & Eosin staining, scale bar: 100 μ m). SSC; Spermatogonial Stem Cell and iPSCs; Induced pluripotent stem cells.

Discussion

Studies have shown that induced pluripotency SSCs can differentiate *in vitro* into the three germ layers including endoderm, mesoderm, and ectoderm. SSCs can conveniently be induced into pluripotent stem cells in a specified culture medium (26, 27). Shinohara and colleagues reported in 2004 that they had generated embryonic stem-like cells (ES-like) from mouse testis SSCs that were phenotypically resembling to ES cells (28). Reprogramming competence of SSCs qualified them into the proper cells for iPSCs in rodents and human research (29). These iPS cells produce teratomas after transplantation which is the most significant obstacle of using these cells in medicine. Our findings demonstrate that induction of pluripotency in SSCs can be achieved by inducing hsa-mir106b-5p. These iPS-like cells could establish embryonic lineages. Also, these cells did not show tumorigenicity, which is their privilege compared to other reprogrammed cells.

Tumor creation in iPSCs is related to the activation of

some oncogenes such as c-Myc. Nakagawa et al. (30) reported that removing c-Myc from the reprogramming process resulted in the development of pluripotent cells but eliminated teratoma formation. We have observed SSCs can be successfully reprogrammed into iPS-like cells using procedures without multiple retroviral transductions. It can be concluded that hsa-mir-106b-5p does not target c-Myc gene, and we generated pluripotent cells without tumorigenic properties. Previously, it was reported that the miR-106b-5p cluster significantly increased during reprogramming stages, inhibiting this cluster decreases reprogramming efficiency, so it is a reprogramming activity regulator (12). In addition, studies showed that certain miRNA families, such as miR-17, miR-106, miR-520, miR-372, miR-195, and miR-200, are upregulated in human pluripotent stem cells (hPSCs) as compared to adult differentiated cell types. Moreover, miRNA clusters can promote reprogramming into iPSCs. The miR-106b-25 cluster is proven to be early active in the reprogramming of mouse embryonic fibroblasts (31-34). Lin and colleagues induced mir-302 into human hair follicle cells by an inducible vector; this procedure resulted in some human embryonic specific gene expression, such as NANOG, OCT3/4, SOX2 so these somatic cells were successfully reprogrammed to iPSCs (35). Nguyen and colleagues revealed that co-expression of miR-524-5p with OSKM factors in human somatic cells leads to generate iPSCs. According to their study, miR-524-5p initiates reprogramming by targeting ZEB2 and SMAD4 genes, which are epithelial-to-mesenchymal transition-related genes (36). Based on the functional role of mir-106b in cell reprogramming, the dosage of hsa-mir-106b, a naturally present miRNA in spermatogonia stem cells was enhanced in this technique by infecting the pLV-miRNA vector into isolated SSCs to generate iPSCs (37). Here, these iPS-like cells showed pluripotent characteristics and successfully differentiated into osteogenic cells (mesoderm derivative), neuronal cells (ectoderm derivative) and hepatocyte lineage (endoderm derivative) as a result of reprogramming. Isolated SSCs from adult mice have been shown to be capable of reprogramming and differentiating into all three embryonic germ layers under three defined culture conditions, as well as generating teratomas in immunodeficient mice (38). Another study by Lim and colleagues reported *in vitro* expression of three germline markers in the EB-like structures in iPSCs of human SSCs (39). These findings authenticate that induction of pluripotency in SSCs can lead them to produce embryonic layers. Although pluripotency of iPS cells is a remarkable result in cell-based therapies, the tumorigenicity of this type of cells is still a concern for clinical applications (40). Based on findings in this study, transduction of hsa-mir106b-5p to SSCs by one vector and limited genetic manipulation led to reprogramming of SSCs into pluripotent cells without the capability of tumor formation. Through this method, there can be a new prospect at the generation of iPSCs and the application of iPS or iPS-like cells in regenerative medicine. This method can be an acceptable alternative

for techniques that are involved with substantial genetic manipulation. Besides, vectors as a viral basis element are not allowed to use considerably in the human body, so we can take advantage of them in a minimum of manipulation to produce pluripotent cells without tumorigenicity.

Conclusion

The results of this study showed that using this new method in infecting hsa-mir-106b-5p into SSCs, leads to reprogramming them and turning them into pluripotent cells. iPSC-like cells differentiated successfully into germ layers as a result of pluripotency. On the other hand, iPSC-like cells do not cause tumors, which is a significant characteristic of iPSCs in medical applications. This reprogramming method provides a simplified and convenient way to convert SSCs into pluripotent cells with less ethical and immunological concerns in cell treatments.

Acknowledgements

The Men's Health and Reproductive Health Research Center at Shahid Beheshti University of Medical Sciences funded this research. We thank the Histogenotech firm and its employees for their input and experience, substantially aided the research. Data openly available in a public repository that issues datasets with DOIs. The authors declare that they have no competing interests.

Authors' Contributions

A.H.H.F., Z.M., S.J.H.; Proposed and performed experimental works, and data collection. F.K.; Performed bioinformatics work. F.K., A.H.H.F.; Contributed to article writing and manuscript approving. All authors read and approved the final manuscript.

References

- Liu G, David BT, Trawczynski M, Fessler RG. Advances in pluripotent stem cells history, mechanisms, technologies, and applications. *Stem Cell Rev Rep*. 2020; 16(1): 3-32.
- Takahashi K, Yamanaka S. Induction of pluripotent stem cells from mouse embryonic and adult fibroblast cultures by defined factors. *Cell*. 2006; 126(4): 663-676.
- Pires CF, Rosa FF, Kurochkin I, Pereira CF. Understanding and modulating immunity with cell reprogramming. *Front Immunol*. 2019; 10: 2809.
- Corbett JL, Duncan SA. iPSC-derived hepatocytes as a platform for disease modeling and drug discovery. *Front Med*. 2019; 6: 265.
- Lim SJ, Ho SC, Mok PL, Tan KL, Ong AH, Gan SC. Induced pluripotent stem cells from human hair follicle keratinocytes as a potential source for in vitro hair follicle cloning. *PeerJ*. 2016; 4: e2695.
- Miller JD, Schlaeger TM. Generation of induced pluripotent stem cell lines from human fibroblasts via retroviral gene transfer. *Methods Mol Biol*. 2011; 767: 55-65.
- Aponte PM. Spermatogonial stem cells: Current biotechnological advances in reproduction and regenerative medicine. *World J Stem Cells*. 2015; 7(4): 669.
- Dym M, Kokkinaki M, He Z. Spermatogonial stem cells: mouse and human comparisons. *Birth Defects Research (Part C)*. 2009; 87(1): 27-34.
- Lee SW, Wu G, Choi NY, Lee HJ, Bang JS, Lee Y, et al. Self-reprogramming of spermatogonial stem cells into pluripotent stem cells without microenvironment of feeder cells. *Mol Cells*. 2018; 41(7): 631.
- Wienholds E, Plasterk R H. MicroRNA function in animal development. *FEBS Lett*. 2005; 579 (26): 5911-5922.
- Doelman MJH, Feyen DAM, de Veij Mestdagh CF, Sluijter JPG. Cardiac regeneration and microRNAs: regulators of pluripotency, reprogramming, and cardiovascular lineage commitment. In: Madonna R, editor. *Stem Cells and cardiac regeneration*. 1st ed. Cham: Springer; 2016; 79-109.
- Li Z, Yang CS, Nakashima K, Rana TM. Small RNA-mediated regulation of iPSC cell generation. *EMBO J*. 2011; 30(5): 823-834.
- Mehlich D, Garbicz F, Włodarski PK. The emerging roles of the polycistronic miR-106b-25 cluster in cancer—a comprehensive review. *Biomed Pharmacother*. 2018; 107: 1183-1195.
- Gutierrez-Aranda I, Ramos-Mejia V, Bueno C, Munoz-Lopez M, Real PJ, Mácia A, et al. Human induced pluripotent stem cells develop teratoma more efficiently and faster than human embryonic stem cells regardless the site of injection. *Stem Cells*. 2010; 28(9): 1568-1570.
- Knoepfler PS. Deconstructing stem cell tumorigenicity: a roadmap to safe regenerative medicine. *Stem Cells*. 2009; 27(5): 1050-1056.
- Hasani Fard AH, Mohseni Kouchesfehiani H, Jalali H. Investigation of cholestasis-related changes in characteristics of spermatogonial stem cells in testis tissue of male Wistar rats. *Andrologia*. 2020; 52(9): e13660.
- Velasco V, Shariati SA, Esfandyarpour R. Microtechnology-based methods for organoid models. *Microsyst Nanoeng*. 2020; 6(1): 1-13.
- Bakhshalizadeh S, Esmaeili F, Houshmand F, Ebrahimi Hafshejani M, Ghasemi S. Neuronal differentiation of GFP expressing P19 embryonal carcinoma cells by deprenyl, an antiparkinson drug. *J Shahrekord Univ Med Sci*. 2014; 16.
- Mazaheri Z, Movahedin M, Rahbarizadeh F, Amanpour S. Different doses of bone morphogenetic protein 4 promote the expression of early germ cell-specific gene in bone marrow mesenchymal stem cells. *In Vitro Cell Dev Biol Anim*. 2011; 47(8): 521-525.
- Fekri Aval S, Zarghami N, Mohammadi SA, Nouri M. Isolation of mesenchymal stem cells from human adipose tissue and comparison of miRNA-16 and miRNA-125b expression before and after differentiation into adipocytes and liver cells. Presented for the Ph.D., Tabriz. Tabriz University of Medical Sciences. 2017.
- Ahmadi A, Moghadasali R, Ezzatizadeh V, Taghizadeh Z, Nassiri SM, Asghari-Vostikolaee MH, et al. Transplantation of mouse induced pluripotent stem cell-derived podocytes in a mouse model of membranous nephropathy attenuates proteinuria. *Sci Rep*. 2019; 9(1): 1-13.
- Costoya JA, Hobbs RM, Barna M, Cattoretti G, Manova K, Sukhwani M, et al. Essential role of Plzf in maintenance of spermatogonial stem cells. *Nat Genet*. 2004; 36(6): 653-659.
- Locher H, de Rooij KE, de Groot JC, van Doorn R, Gruis NA, Löwik CW, et al. Class III β -tubulin, a novel biomarker in the human melanocyte lineage. *Differentiation*. 2013; 85(4-5): 173-181.
- Lansley SM, Searles RG, Hoi A, Thomas C, Moneta H, Herrick SE, et al. Mesothelial cell differentiation into osteoblast and adipocyte-like cells. *J Cell Mol Med*. 2011; 15(10): 2095-2105.
- Freyer N, Knöspel F, Strahl N, Amini L, Schrade P, Bachmann S, et al. Hepatic differentiation of human induced pluripotent stem cells in a perfused three-dimensional multicompartment bioreactor. *Biores Open Access*. 2016; 5(1): 235-248.
- Pellicano R, Caviglia GP, Ribaldone DG, Altruda F, Fagoonee S. Induced pluripotent stem cells from spermatogonial stem cells: potential applications. In: Birbrair A, editor. *Cell sources for iPSCs*. 1st ed. London: Academic Press; 2021; 15-35.
- Yang M, Deng B, Geng L, Li L, Wu X. Pluripotency factor NANOG promotes germ cell maintenance in vitro without triggering dedifferentiation of spermatogonial stem cells. *Theriogenology*. 2020; 148: 68-75.
- Kanatsu-Shinohara M, Inoue K, Lee J, Yoshimoto M, Ogonuki N, Miki H, et al. Generation of pluripotent stem cells from neonatal mouse testis. *Cell*. 2004; 119(7): 1001-1012.
- Chen Z, Hong F, Wang Z, Hao D, Yang H. Spermatogonial stem cells are a promising and pluripotent cell source for regenerative medicine. *Am J Transl Res*. 2020; 12(11): 7048.
- Nakagawa M, Koyanagi M, Tanabe K, Takahashi K, Ichisaka T, Aoi T, et al. Generation of induced pluripotent stem cells without Myc from mouse and human fibroblasts. *Nat Biotechnol*. 2008; 26(1): 101-106.
- Anokye-Danso F, Snitow M, Morrissey EE. How microRNAs facilitate reprogramming to pluripotency. *J Cell Sci*. 2012; 125(18): 4179-4787.
- Greve T S, Judson RL, Blelloch R. microRNA control of mouse and human pluripotent stem cell behavior. *Annu Rev Cell Dev Biol*.

- 2013; 29: 213-239.
33. Leonardo TR, Schultheisz HL, Loring JF, Laurent LC. The functions of microRNAs in pluripotency and reprogramming. *Nat Cell Biol.* 2012; 14(11): 1114-1121.
 34. Lüningschrör P, Hauser S, Kaltschmidt B, Kaltschmidt C. MicroRNAs in pluripotency, reprogramming and cell fate induction. *Biochim Biophys Acta Mol Cell Res.* 2013; 1833(8): 1894-1903.
 35. Lin SL, Chang DC, Lin CH, Ying SY, Leu D, Wu DT. Regulation of somatic cell reprogramming through inducible mir-302 expression. *Nucleic Acids Res.* 2011; 39(3): 1054-1065.
 36. Nguyen PNN, Choo KB, Huang CJ, Sugii S, Cheong SK, Kamarul T. miR-524-5p of the primate-specific C19MC miRNA cluster targets TP53IPN1-and EMT-associated genes to regulate cellular reprogramming. *Stem Cell Res Ther.* 2017; 8(1): 1-15.
 37. Tong MH, Mitchell DA, McGowan SD, Evanoff R, Griswold MD. Two miRNA clusters, Mir-17-92 (Mirc1) and Mir-106b-25 (Mirc3), are involved in the regulation of spermatogonial differentiation in mice. *Biol Reprod.* 2012; 86(3): 72.
 38. Guan K, Nayernia K, Maier LS, Wagner S, Dressel R, Lee JH, et al. Pluripotency of spermatogonial stem cells from adult mouse testis. *Nature.* 2006; 440(7088): 1199-1203.
 39. Lim JJ, Kim HJ, Kim KS, Hong JY, Lee DR. In vitro culture-induced pluripotency of human spermatogonial stem cells. *Biomed Res Int.* 2013; 2013.
 40. Lee AS, Tang C, Rao MS, Weissman IL, Wu JC. Tumorigenicity as a clinical hurdle for pluripotent stem cell therapies. *Nat Med.* 2013; 19(8): 998-1004.
-

Differentiation of Alginate-Encapsulated Wharton Jelly-Derived Mesenchymal Stem Cells into Insulin Producing Cells

Zahra Poursafavi, M.Sc.¹, Saeid Abroun, Ph.D.^{2*}, Saeid Kaviani, Ph.D.², Nasim Hayati Roodbari, Ph.D.¹

1. Biology Department, Science and Research Branch, Islamic Azad University, Tehran, Iran
2. Department of Hematology, Faculty of Medical Sciences, Tarbiat Modarres University, Tehran, Iran

*Corresponding Address: Department of Hematology, Faculty of Medical Sciences, Tarbiat Modarres University, Tehran, Iran
Email: abroun@modares.ac.ir

Received: 22/May/2021, Accepted: 16/October/2021

Abstract

Objective: Insulin insufficiency due to the reduced pancreatic beta cell number is the hallmark of diabetes, resulting in an intense focus on the development of beta-cell replacement options. One approach to overcome the problem is to search for alternative sources to induce insulin-producing cells (IPCs), the advent of mesenchymal stem cells (MSCs) holds great promise for producing ample IPCs. Encapsulate the MSCs with alginate improved anti-inflammatory effects of MSC treatment. This study aimed to evaluate the differentiation of wharton jelly-derived MSCs into insulin producing cells using alginate encapsulation.

Materials and Methods: In this experimental study, we established an efficient IPCs differentiation strategy of human MSCs derived from the umbilical cord's Wharton jelly with lentiviral transduction of Pancreas/duodenum homeobox protein 1 (*PDX1*) in a 21-day period using alginate encapsulation by poly-L-lysine (PLL) and poly-L-ornithine (PLO) outer layer. During differentiation, the expression level of *PDX1* and secretion of insulin proteins were increased.

Results: Results showed that during time, the cell viability remained high at 87% at day 7. After 21 days, the differentiated beta-like cells in microcapsules were morphologically similar to primary beta cells. Evaluation of the expression of *PDX1* and *INS* by quantitative reverse transcriptase-polymerase chain reaction (qRT-PCR) on days 7, 14 and 21 of differentiation exhibited the highest expression on day 14. At the protein level, the expression of these two pancreatic markers was observed after *PDX1* transduction. Results showed that the intracellular and extracellular insulin levels in the cells receiving *PDX1* is higher than the control group. The current data showed that encapsulation with alginate by PLL and PLO outer layer permitted to increase the microcapsules' beta cell differentiation.

Conclusion: Encapsulate the transduced-MSCs with alginate can be applied in an *in vivo* model in order to do the further analysis.

Keywords: Alginate, Diabetes, Insulin, Mesenchymal Stem Cells

Cell Journal(yakhteh), Vol 24, No 8, August 2022, Pages: 449-457

Citation: Poursafavi Z, Abroun S, Kaviani S, Hayati Roodbari N. Differentiation of alginate-encapsulated wharton jelly-derived mesenchymal stem cells into insulin producing cells. Cell J. 2022; 24(8): 449-457. doi: 10.22074/cellj.2022.8081.

This open-access article has been published under the terms of the Creative Commons Attribution Non-Commercial 3.0 (CC BY-NC 3.0).

Introduction

Diabetes is one of the metabolic disorders which are caused by impaired insulin secretion, insulin dysfunction, or both. Numerous pathogenic processes contribute to the progression of diabetes, which has a wide range from progressive autoimmune destruction of pancreatic cells toward ultimately insulin deficiency and insulin resistance. Until 2017, 387 millions of people worldwide suffer from diabetes, and that number is expected to reach in to 500 millions by 2030 (1). These statistics have led the international diabetes federation (IDF) in to describe this disease as one of the most serious human health challenges in the 21st century (2).

So far, no certain cure option for diabetes currently exists. At present, taking oral medications and insulin injections are common treatments. Transplantation of islets isolated from the donor pancreas could also be a therapy for diabetes. However, this treatment also has some restrictions, including limited islets required for transplantation, side effects of long-term immunosuppressive drugs, and short-term survival

after transplantation. Recently, the application of stem cells that differentiate into pancreatic beta cells has drawn great attention as one of the treatment options for diabetes (3). Some studies suggested that embryonic stem cells, induced pluripotent stem cells (iPCs), bone marrow-mesenchymal stem cells (BM-MSCs) and adipose tissue-MSCs can differentiate into IPCs both *in vitro* and *in vivo* (4). Stem cells with the ability to differentiate into insulin-producing cells (IPCs) are becoming the most promising therapy for diabetes mellitus that reduce the major limitations of availability and allogeneic rejection of beta cell transplantations (5, 6).

Previous studies have reported that IPCs were derived from embryonic stem cells in mice and humans (7, 8). MSCs have potentials for differentiating into various tissues, immunomodulatory effects and the invasiveness of the procedure. Therefore MSCs can overcome the obstacles seen with embryonic stem cells (9).

MSCs are the most important candidates for cell

therapy which are obtained from different sources including BM, adipose tissue, blood, amniotic fluid and umbilical cord of newborns. Recently umbilical cord derived MSCs from Wharton jelly have drawn many attentions because of their differentiation, migration and protective properties compare to other kinds of stem cells. Hu et al. (10) evaluated the application of umbilical cord's Wharton jelly-derived MSCs (WJ-MSCs) for type 1 diabetic patients and obtained promising results. Another study established that transplantation of placenta-derived MSCs for patients with type 2 diabetes was safe, easy, and potentially effective (11).

Alginate hydrogels have demonstrated high applicability as a structure for cell immobilization. Alginate is recognized in properties such as its ability to make hydrogels at physiological conditions, gentle dissolution of gels for cell retrieval, transparency for microscopic evaluation, gel pore network that allows diffusion of nutrients and wastes in addition to its reduced risk of graft failure (12). Encapsulation is a method used to protect implanted cells from immune system attack and it may enhance the survival rate and differentiation of implanted cells by the increased of cytokines secreted by encapsulated cells to the microenvironment (6, 13). Microencapsulation is widely used for encapsulation of cells or bioactive molecules, gene therapy and drug delivery. Hydrogels are the most widely used materials for cell microencapsulation because of their high porosity that leads to high permeability of oxygen, nutrients, and metabolites (14). Alginate widely used for cell encapsulation provides protection of the encapsulated cells against the host's immune system (15). Previous studies demonstrated that MSC encapsulated in alginate could survive locally after implantation *in vivo* (16).

The transplantation of pancreatic islets in immune protective capsules holds the promise as a functional cure for type 1 diabetes (17), about 40 years after the first proof of principal study (18). Gene therapy, as an advanced technology to treat diseases cannot be treated with conventional medicine and can be applied to a wide range of diseases that includes many methods of gene transfer (19). Gene therapy had been approved for diseases such as cystic fibrosis, diabetes, autoimmune diseases, heart diseases Alzheimer's disease, Parkinson's disease, various cancers (20). Gene therapy by viral vector and non-viral transduction may be useful techniques to treat diabetes (21). Insulin generation in MSCs through genetic engineering is a promising therapeutic for patients with diabetes (22). In previous study it was indicated that PDX1-transduced hBM-MSCs differentiate into IPCs (21). This study aimed to evaluate the differentiation of wharton jelly-derived MSCs into insulin producing cells using alginate encapsulation.

Material and Methods

Isolation of MSCs from Wharton jelly

In this experimental study, umbilical cords were collected from healthy full-term deliveries after receiving consent from parents. The collection and using of human biological specimens were approved by the Ethics Committee of the Islamic Azad University-Science and Research Branch (IR. IAU.SRB.REC.1398.214). The Umbilical cords were transferred in serum-free Dulbecco's Modified Eagle Medium/F12 (DMEM/F-12, Hyclone, Logan, UT, USA) and transferred to the laboratory immediately. After washing, the Umbilical cords samples-were cut into 2-3 cm sections, the umbilical vessels removed, and Wharton jelly was collected and minced into pieces. The pieces were plated in tissue culture flasks containing an enzymatic solution of collagenase and hyaluronidase, in DMEM/F-12 medium supplemented with 10% fetal bovine serum (FBS, Gibco, USA) and incubated at 37°C in a humidified 5% CO₂ incubator for 45 minutes to 2 hours. This allows Wharton jelly loosening and separation from the Umbilical cords without complete digestion. After the incubation period, the Umbilical cords pieces are transferred to a new Petri dish or culture flask containing fresh DMEM to remove any remaining enzymes (23).

Flow cytometry analysis

Human MSCs single-cell suspensions were harvested using a 0.05% trypsin/ Ethylenediaminetetraacetic acid (EDTA) solution; after FBS neutralization incubated in blocking buffer [1% FBS in Dulbecco's phosphate-buffered saline (DPBS)] for 30 minutes. Next, 1×10^6 cells were separately incubated for 1 hour at 4°C with an optimal dilution of conjugated antibodies that included anti-CD73-FITC (ab28061), anti-CD45-FITC (ab27287), anti-CD90-FITC (ab11155), anti-CD34-PE (ab157304), and anti-CD105-PE (ab91138), all from Abcam (Cambridge, UK). Flow cytometry experiments were performed with a BD FACSCalibur Flow Cytometer (BD Biosciences) and data analyzed by the Flowing software.

Multilineage differentiation

To confirm the multipotency of WJ-MSCs, osteogenic and adipogenic differentiation were verified with alizarin red and oil red O staining respectively. To induce osteogenesis, WJ-MSCs treated with osteogenic differentiation medium, alpha minimum essential medium (Life Technologies, USA) supplemented with 10% FBS (Gibco, USA), 10 mmol/L β -glycerophosphate (Sigma-Aldrich, USA), 0.1 mmol/L dexamethasone (Sigma-Aldrich, USA) and 50 mmol/L ascorbic acid (Sigma-Aldrich, USA) for 21 day. For adipogenesis, the cells were treated with adipogenic differentiation medium

in alpha minimum essential medium supplemented with 10% FBS, 1 mmol/L dexamethasone (Sigma-Aldrich, USA), 10 mg/mL insulin (Sigma-Aldrich, USA), 0.5 mmol/L isobutyl-methylxanthine (Sigma-Aldrich, USA) and 100 mmol/L indomethacin (Sigma-Aldrich, USA) for 21 day.

Transduction of WJ-MSCs

To transduce *PDX1* using lentivirus system, approximately 1×10^6 MSCs were seeded in 48-well plates. The Lentivector Packaging kit (Invitrogen, USA, K4975-00) including the pPackH1 Packaging Plasmid (mixture of pPACKH1-GAG, pPACKH1-REV, and pVSV-G plasmids, 0.5 $\mu\text{g}/\mu\text{l}$) and the transfer vector Plenti-Pdx1-PURO (0.5 $\mu\text{g}/\mu\text{l}$) containing an enhanced *PDX1*, was used to transduce *PDX1* into WJ-MSCs. Virion particles were produced in 293T cells (Invitrogen, Carlsbad, CA, USA) by transfection using the TransIT-2020 Transfection Reagent (Mirus, Madison, WI, USA). The 293T cells were seeded in 75-cm² flasks at an initial density of 1.3×10^5 cells/cm² with 10 ml of DMEM containing 10% FBS, 50 U/ml penicillin, and 50 $\mu\text{g}/\text{ml}$ streptomycin. At 24 hours post-transfection, the media was replaced with fresh DMEM with 2% FBS. The medium was changed every 24 hours for 3 days. The media was removed, pooled, and filtered (pore size: 0.45 μm ; Merck Millipore, Rockland, MA, USA), and centrifuged at $50,000 \times g$ for 90 minutes. The resulting pellets were resuspended in serum-free DMEM. The virus titer was determined by transducing 293T cells with the viral preparation and examining *PDX1* expression using polymerase chain reaction (PCR) analysis. The virus titers used in experiments were $1\text{-}2 \times 10^7$ transducing units/ml.

After virus exposure, transduced MSCs were cultured in serum-containing medium for 5-8 days, and medium was changed every 48 hours. The transduction efficacy was assessed 5 days after transduction. Cells were rinsed with phosphate buffer solution (PBS Gibco BRL, Grand Island, NY, USA) and incubated with 0.5% trypsin/0.2% EDTA (Sigma-Aldrich, USA) for 10 minutes to dissociate the cells. The viability of dispersed cells was evaluated by trypan blue exclusion.

Investigation of differentiation of WJ-MSCs into insulin-producing cells

Quantitative reverse transcriptase-polymerase chain reaction

The expression of pancreatic-specific genes *PDX1* and *INS* was analyzed by quantitative reverse transcriptase-polymerase chain reaction (qRT-PCR) in differentiated cells on days 7, 14, and 21. MSCs that were not cultured in the differentiating medium containing high glucose DMEM supplemented with 0.5 mmol/L β -mercaptoethanol (Invitrogen, USA, 1% non-essential amino acids (Gibco, UK), 20 ng/ml β -fibroblast growth factor (bFGF, Sigma-

Aldrich, USA), 20 ng/ml (EGF, Sigma-Aldrich, USA), 2% B27 (Gibco, UK), 2 mmol/L L-glutamine (Hyclone, USA), 10 ng/ml β -cellulin (Sigma-Aldrich, USA), 10 ng/ml activin A (Sigma-Aldrich, USA), 2% B27 and 10 mmol/L nicotinamide (Sigma-Aldrich, USA) (7) were used as negative control, and PANC-1 cell line (pancreatic epithelial cells) was used as a positive control (24).

Total cellular RNA was extracted by the TRIzol reagent[®] (Sigma-Aldrich, T9424) and used for cDNA synthesis with the Revert Aid First Strand cDNA Synthesis Kit (Fermentas, Germany, K1632) according to the manufacturer's instructions. Quantitative RT-PCR was carried out with the SYBR Green Master Mix (Takara Bio, Inc., RR081Q) with a real-time RT-PCR system (Corbett Life Science, Rotor-Gene 6000, Australia). The expression levels of the target genes were calculated using the $2^{-\Delta\text{Ct}}$ method with glyceraldehyde 3-phosphate dehydrogenase (*GAPDH*) as the internal control for normalization. Primer sequences for target genes are listed in Table 1.

Western blotting

For western blot analysis at the end of treatment, on day 21, the cells were lysed in commercial lysis buffer (Qproteome Mammalian Protein Prep Kit, QIAGEN) according to the manufacturer's protocol. The solubilized protein fractions of each sample (50 μg) from three biological replicates were separated on a 12% sodium dodecyl sulfate polyacrylamide gel electrophoresis (SDS-PAGE) and transferred onto a PVDF membrane (Amersham Biosciences, USA) by semi-dry blotting (Bio-Rad, USA) using transfer buffer (10 mM NaCHO₃, 3 mM Na₂CO₃, 20% methanol). Membranes were blocked with Tris-buffered saline with Tween[®] 20 (TBST, 20 mM tris-HCl, pH=7.6, 150 mM NaCl, and 0.1% Tween-20) that contained 5% BSA and then incubated overnight with the primary antibody at 4°C. After three times washing with TBST, the membranes were incubated with horseradish peroxidase (HRP)-conjugated secondary antibody at room temperature for 1 hour. Signals were detected with ECL substrate using Hyperfilm. Protein band intensity was normalized to the level of beta-actin. Each experiment was repeated at least three times.

Encapsulation of WJ-MSCs

The encapsulation of WJ-MSCs was performed as reported by Kanafi et al. (25), with slight modifications. An alginate solution (2% w/v) was prepared by dissolving 2 g of low viscosity alginic acid sodium salt (Low viscosity 100-300 cP, Sigma-Aldrich, USA) in 100 ml of deionized water. The alginate solution was mixed by overnight vortexing. To prepare cell-encapsulated beads, WJ-MSCs at passage 4 were harvested and a cell density of 5×10^5 was mixed in 1 ml of alginate solution. The alginate solution was transferred to a 5 ml syringe (22 Gauge) and then extruded dropwise into an ice-cold 100 mM calcium

chloride (CaCl₂, Sigma-Aldrich, USA) solution. The droplets were left 10 minutes in the CaCl₂ solution for polymerization. Cell-encapsulated microcapsules were then transferred to 35 mm tissue culture dishes containing 1.5 ml DMEM medium supplemented with FBS. The WJ-MSC beads were incubated at 37°C in 5% CO₂ incubator for 72 hours and then used for further experiments.

Decapsulation

Three days after encapsulation, microcapsules containing WJ-MSCs were washed by PBS twice, and 10 ml of decapsulation solution (EDTA, 50 mM and HEPES, 10 mM in PBS, Sigma-Aldrich, USA) was added, then the beads were incubated at 37°C for 10 minutes. The cells were pelleted by centrifugation at 3000 rpm for 10 minutes. This cell pellet was used for RNA isolation or protein extraction.

Cell viability assessment

Assessment of WJ-MSCs viability was performed using the MTT assay. The cells at a density of 2×10^5 /well were inoculated into a 96-well plate. The WJ-MSCs were divided into transduce and transduced groups. The plates were placed in an incubator at 5% CO₂ at 37°C overnight. WJ-MSCs were transduced with Plenti-Pdx1-PURO lentivirus (5×10^9 TU/ml) at 200 MOI based on the results of transfection efficiency, and WJ-MSCs in the untransfected group received an equivalent dose of PBS. Cells in one of the four plates were incubated with the MTT solution at 7, 14, and 21 days after transfection. After 4 hours, the medium was removed, and 150 µl of dimethylsulfoxide (DMSO) added to each well. Absorbance was measured at 570 nm using an ELISA reader (Biochrom Anthos 2020, UK).

Insulin assay and response to glucose

Insulin level in the medium was measured by human insulin ELISA kit (Millipore, Billerica, MA, USA) according to the manufacturer's instructions. Total protein in the medium was measured by the BCA assay using fresh culture medium as a blank. To determine the cell response to glucose at different concentrations, the insulin levels were evaluated with different glucose concentrations (0, 5.5, 15 and 25 mM). 1×10^6 cells were initially incubated for 3 hours in glucose-free Krebs-Ringer bicarbonate buffer (KRB). This was followed by incubation for 1 hour in 3.0 mL of KRB containing 0, 5.5, 15, or 25 mM glucose concentrations. The supernatant was collected at the end of each incubation period. The collected samples were using the ELISA assay (26). We evaluated the insulin level in positive control group to confirm the insulin ELISA kit.

Statistical analysis

All experiments were conducted in at least three independent repeats and performed in the same passage. Statistical analysis was performed using GraphPad Prism 5.02 (GraphPad Software, Inc, USA). Comparisons between groups were performed by one-way analysis of variance (ANOVA) followed by the Tukey post-hoc test. The independent t test analysis was carried out to identify statistical differences between the two observations. The difference between data was considered to be significant at $P < 0.05$.

Results

Derivation and characterization of WJ-MSCs

MSCs derived from human umbilical cord's Wharton Jelly, human WJ-MSCs had fibroblastic-like phenotype (Fig.1A), the cells were small and fusiform at the first passage. After third passage, the cells seem fully expanded with many cytoplasmic processes. To confirm the mesenchymal identity, the expression of MSC-specific markers was examined. Results from flow cytometry showed that the expression (%) of these markers including CD105, CD90 and CD73 in WJ-MSCs were 97.4, 96.70 and 95.3, respectively. While hematopoietic specific markers such as CD34 and CD45 did not have significant expression in these cell populations. These results confirm that the isolated cells from human umbilical cord's Wharton jelly are MSCs (Fig.1B). WJ-MSCs are determined as multipotent stem cells that are able to differentiate into specific lineages like osteoblastic and adipocytic. Thus, the osteogenic differentiation assay was performed to examine the differentiation ability of isolated MSCs into these two lineages. Intracellular lipid droplets staining using oil red- O showed the adipogenesis of WJ-MSCs. While in the undifferentiated WJ-MSCs, these observations were absent. Alizarin staining demonstrated the formation of calcium oxalates on the differentiated MSCs, which was not detected in the undifferentiated cells. These findings confirmed the characterization of cells as WJ-MSCs and indicate that the MSCs have potential to differentiate into these lineages (Fig.1C).

Differentiation of MSCs derived from Wharton jelly into IPCs

To investigate whether transduction of WJ-MSCs with *PDX1* leads to their differentiation into IPCs *in vitro*, we used the lentiviral vector to transfer the *PDX1* gene into MSCs (Fig.2A). For this, WJ-MSCs were cultured in 6-well plates at 1×10^6 cells/well (at passage number 3), when the confluency were reached 70-80%, transduction was performed (Fig.2B). After selecting the transduced cells using puromycin (at a concentration of 2 mg/ml),

these cells were cultured in serum-free newly culture medium for 21 days (Fig.2C). To evaluate the transduction efficiency of target cells, we evaluated the expression of beta cell-specific genes *PDX1* and *INS* by qRT-PCR on days 7, 14 and 21 of culture (Fig.3A-C). We found that the expression levels of *PDX1* and insulin genes in the PDX1-transduced group were higher than the negative control groups. Whereas, the difference between PDX1-transduced group and positive

control groups (pancreatic cell) was not significant. On day 7, *PDX1* and *INS* showed the lowest expression, and on day 14, exhibited the highest expression. We also examined the expression of these genes at the protein level by Western blotting; the expression of these proteins was examined 21 days after *PDX1* transduction of WJ-MSCs. The results showed that PDX1 protein level was increased in transduced group (Fig.3D).

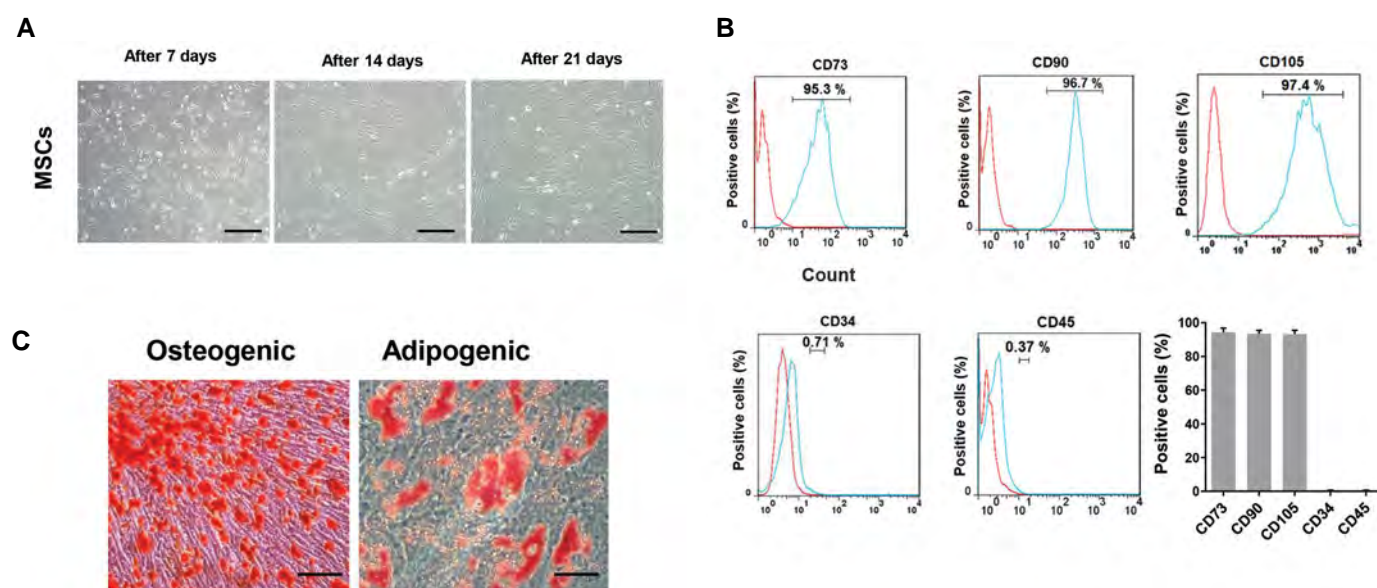


Fig.1: Isolation of MSCs from Wharton jelly, culture, and identification. **A.** Culture of WJ-MSCs during 21 days (scale bar: 100 μ m). **B.** Evaluation of CD markers by flow cytometry. The WJ-MSCs expressed CD105, CD90, and CD73 but they expressed CD34 and CD45 at very low level. Each cell treatment was assayed on three technical replicates on three different samples of WJ-MSCs. **C.** Alizarin red staining after 21 day of culture in osteogenic medium indicated the osteogenic differentiation potential of WJ-MSCs (scale bar: 50 μ m). Oil red staining after 21 day of culture in adipogenic medium showed the adipogenic differentiation potential of WJ-MSCs. Data for each day represent mean cells number and error bars show standard error of the mean (SEM) of triplicate experiment (n=3). MSC; Mesenchymal stem cells and CD; Cluster of differentiation.

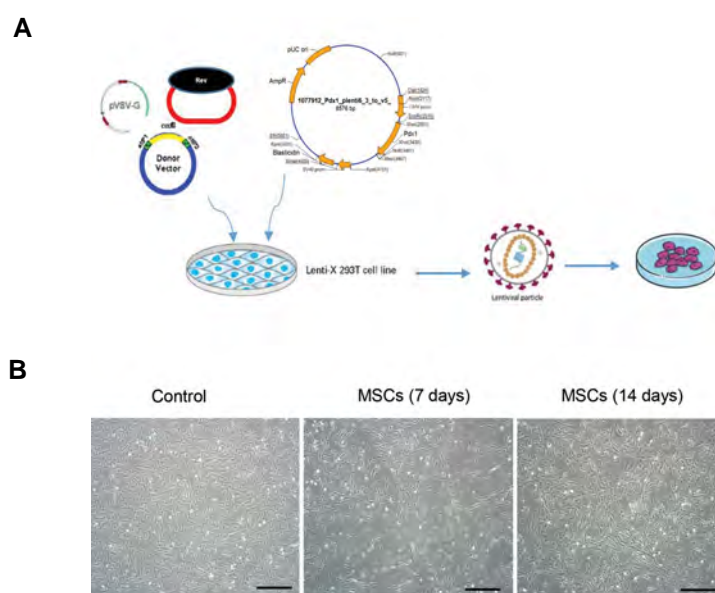


Fig.2: Differentiation of WJ-MSCs into IPCs. **A.** Schematic summary of transduction *pdx1*-planti in cultured WJ-MSCs. **B.** Morphology of WJ-MSCs were transduced with the PDX1 gene using the Lentiviral vector system (scale bar: 200 μ m). WJ-MSCs; Wharton jelly-derived mesenchymal stem cells and IPCs; Induce insulin-producing cells.

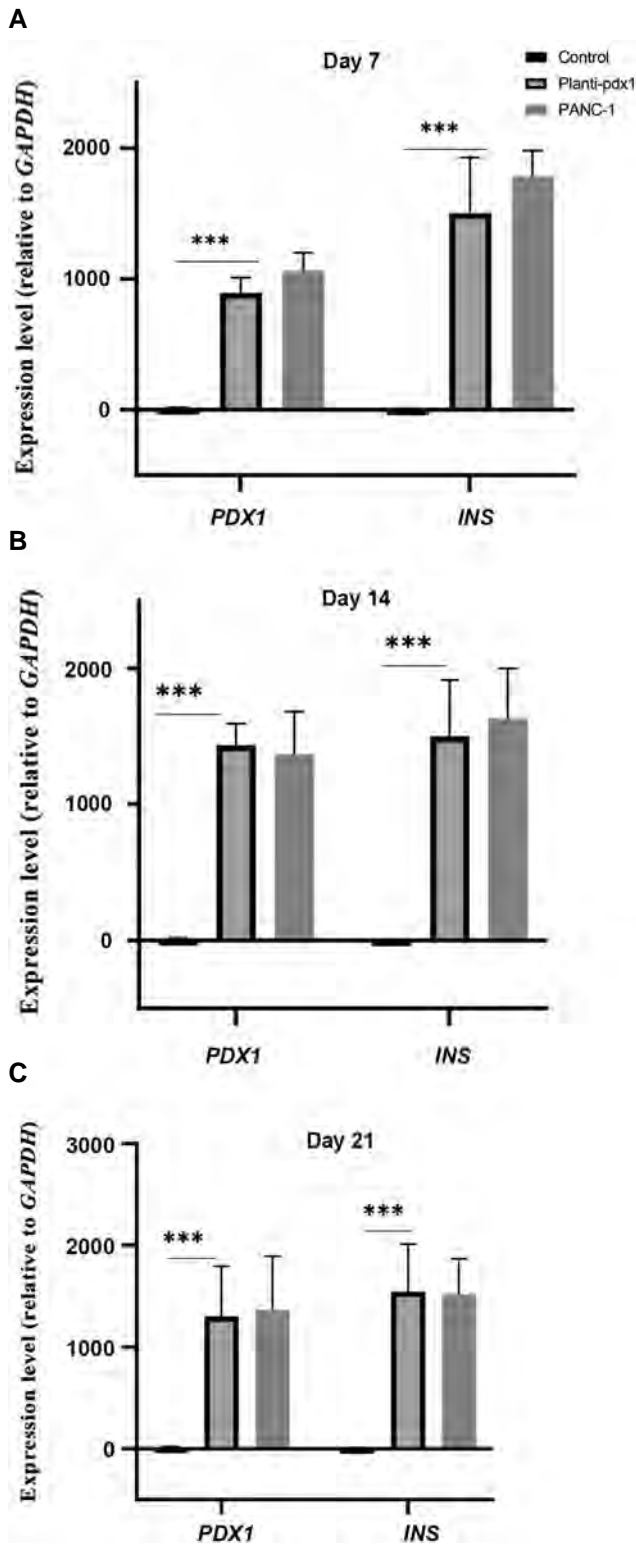


Fig.3: Investigation of differentiation of WJ-MSCs into IPCs. **A., B., C.** Expression of pancreatic-specific genes *PDX1* and *INS* was analyzed by qRT-PCR in differentiated cells on days 7, 14 and 21. MSCs that were not cultured in the differentiating medium were used as negative control, and PANC-1 cell line was used as positive control. Glyceraldehyde 3-phosphate dehydrogenase (*GAPDH*) was considered as the housekeeping control. Each experiment was conducted with in triplicate (n=3). **D.** Western blot analysis for *PDX1* and its phosphorylated form (p*PDX1*) in MSC-Pdx1. Values represent mean and error bars show standard error of the mean (SEM) of triplicate experiment (n=3). ***, P<0.001, WJ-MSCs; Wharton jelly-derived mesenchymal stem cells, IPCs; Induce insulin-producing cells, and qRT-PCR; Quantitative reverse transcriptase–polymerase chain reaction.

Viability, and intra- and extracellular insulin levels in encapsulated PDX1-transduced MSCs

In order to evaluate the effect of cell encapsulation by alginate hydrogel, the cell viability was evaluated by MTT assay on days 7, 14 and 21 after encapsulation (Fig.4A, B). The results showed 98% viability in the group that the cells were decapsulated immediately after encapsulation. After 7 days of cell encapsulation, cell viability remained high at about 87%. However, this rate was decreased to 79% following 14 days due to repeated passages. The viability of transduced-MSCs significantly increased following encapsulation by alginate on day 21. At the following examinations, to evaluate the functionality of encapsulated differentiated cells carrying *PDX1*, intra- and extracellular insulin levels were measured on day 14 using ELISA assay. Results showed that the intracellular and extracellular insulin levels in the MSCs receiving *PDX1* is higher than the control group at concentration of 5.5, 15 and 25 ng/mg insulin protein (Fig.5A, B).

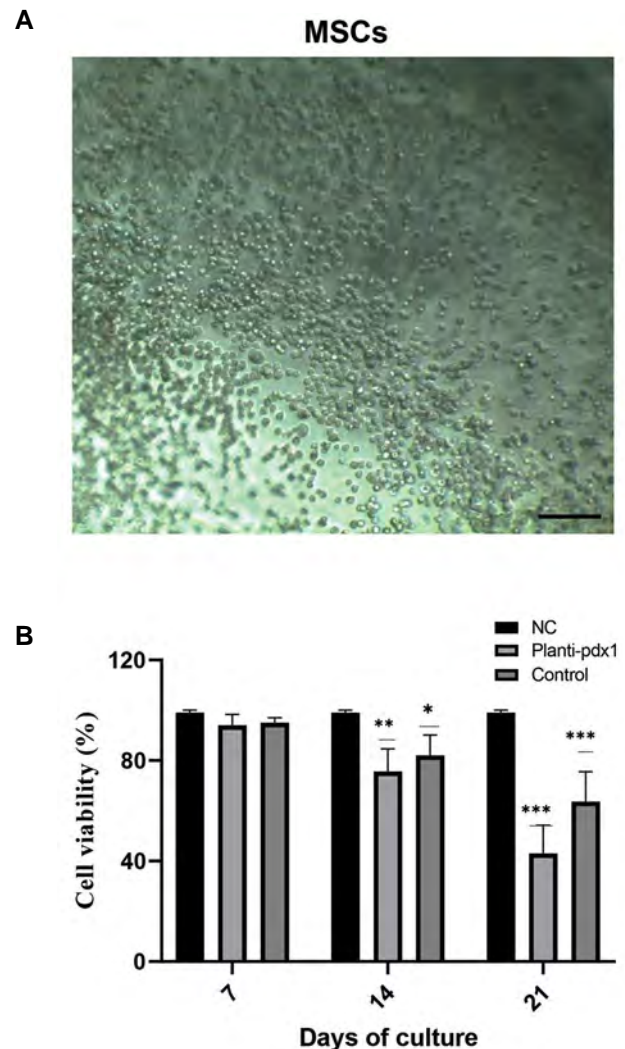


Fig.4: Encapsulated MSCs in alginate hydrogels. **A.** The microscopic image of the capsules containing MSCs showed the uniform distribution of the cells within hydrogel. The average diameter of the capsules is 650 μ m (scale bars: 50 μ m). **B.** Percentage of viable cells evaluated by MTT assay, after 7, 14 and 21 days (n=3). MSCs; Mesenchymal stem cells, NC; Negative control, *, P<0.05, **, P<0.01, and ***, P<0.001.

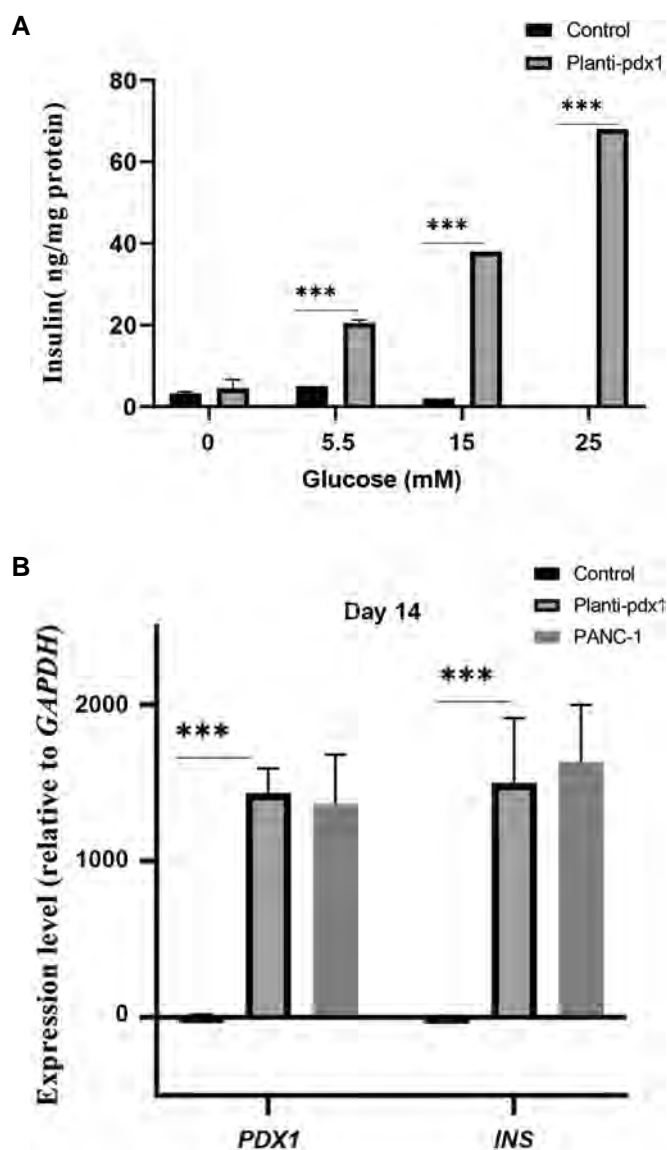


Fig.5: Insulin assay and response to glucose. **A.** The expression of level insulin protein in the differentiated cells compared to the undifferentiated cells. Conversion factor for insulin: $1 \mu\text{g}=23 \text{ mU/L}$, $1 \text{ mU}=0.6 \text{ pmol/L}$. **B.** Concentrations of intracellular insulin protein content in differentiated cells compared to undifferentiated cells. Conversion factor for insulin: $1 \mu\text{g}=23 \text{ mU/L}$, $1 \text{ mU}=0.6 \text{ pmol/L}$ ($n=3$). Control group; Cells without encapsulation and transduction. ***; Significant.

Discussion

The prevalence of diabetes is steadily increasing worldwide, making it one of the most challenging health issues of the 21st century (2). Therefore, it is necessary to search new effective treatment strategies aimed at recovering lost IPCs and inhibiting autoimmune destruction of endocrine progenitor cells (27). Also, results of a meta-analysis by El-Badawy and El-Badri showed that MSCs could be beneficial in patients with type 1 and type 2 diabetes (28). Differentiation of BM-MSCs and adipose tissue-MSCs into IPCs provides a new and promising strategy to reconstitute pancreatic endocrine function (26). In line with previous studies, our results showed, WJ-MSCs were differentiated into IPCs. Therefore, WJ-MSCs are a promising source for applying in diabetes due

to their availability, low cost, and immune-modulatory properties. To produce IPCs from WJ-MSC origin, two methods of indirect and direct differentiation are used (29, 30). Indirect differentiation is performed using chemicals (e.g., nicotinamide and growth factors) and direct differentiation is based on genetic manipulation (31). We showed that transfer of *PDX1* gene with lentiviral vector caused the differentiation of WJ-MSCs into IPCs, and confirming obtained results, an increase in the expression of pancreatic-specific genes such as *PDX1* and insulin was observed. The results of our study were comparable to the findings of Rahmati et al. (32), in which the transfer of *PDX1* gene to mouse MSCs with lentiviral method led to the differentiation of these cells to IPCs. In a study by Soltanian et al. (33), assembling three-dimensional (3D) pancreatic organoids (containing human embryonic stem cell-derived *PDX1*-positive pancreatic progenitors, MSCs, and endothelial cells) implanted into the peritoneal cavity of immunodeficient mice where it remained for 90 days. Their results indicated that 3D organoids developed more vascularization and a higher number of insulin-positive cells and improvement of human C-peptide secretions. Lima et al. (34) through overexpression of three beta cell-specific genes *PDX1*, Neurogenin-3 (*NEUROG3*), and V-maf musculoaponeurotic fibrosarcoma oncogene homolog A (*MAFA*) by adenoviral vectors, trans-differentiated pancreatic exocrine cells into beta-like cells both morphologically and functionally. In this study, we indicated that *PDX1*-transduced MSCs group differentiate into IPCs.

Besides, for a durable treatment of insulin-dependent diabetes mellitus, it is crucial to establish a functional system that, in addition to supporting the insulin secretion in response to different levels of glucose, protecting from immune system. The viability and function of differentiated WJ-MSCs is the most important issue in the use of these cells in diabetes therapy. In this study, alginate hydrogel was used for encapsulation of the cells to avoid a declined survival. One important characteristic of alginate is its very limited inherent cell adhesion and cellular interaction, that is an advantage for cell encapsulation applications (12). The technique to cell immobilization, particularly pancreatic islet cells, in calcium alginate matrices was developed by Lim and Sun (18). By coating the alginate gel bead with polycations like PLL, PLO, or chitosan, the strength of the surface coating as well as the capsule porosity can be controlled (12). In this study, for production of alginate droplets (microcapsules), the viscous solution of alginate was mixed with the cells and then these were stabilized by treatment with polycationic polymers. A combination of PLL and PLO was applied as polycation in order to improve the strength of outer surface of microcapsules. The essential requirements for cell culture i.e. porosity, stability and permeability were reached by alginate in MSCs differentiation into IPCs (35). Consistent results by some studies were reported that pancreatic islet, ESC- and iPSC-derived IPCs encapsulated using alginate could maintain the viability both *in vivo* and *in vitro* (36).

The differentiated WJ-MSCs which were encapsulated by alginate, showed an increased cell viability, however this value was decreased to 79% after 14 days. Thickening of the outer layer by polycationic polymers may also cause the insufficient nutrient and oxygen consumption, which results in a significant reduction in cell viability on day 21. However, despite declined cell viability, insulin secretion levels did not decrease on days 7, 14 and 21. The high number of viable cells in viscous alginate capsules can also lead to high insulin secretion. Encapsulation MSCs with alginate enhance the survival rate and differentiation of transduced MSCs (37).

Similar results have been obtained from other studies. In a recent study, alginate solution improved survival and maintenance of cell functionality in encapsulation of BRIN-BD11 beta cell line, and also the expression of *INS* was increased by 66% (38). Recently, Kuncorojakti et al. (3) evaluated the encapsulation of human dental pulp-derived stem cells (hDPSCs)-derived IPCs by alginate and pluronic F127-coated alginate. Obtained results showed that alginate and alginate combined with pluronic F127 preserved hDPSCs viability and allowed glucose and insulin diffusion in and out. In hDPSC-derived IPCs maintained viability for at least 14 days and sustained pancreatic endoderm marker (NGN3), NKX6.1, MAF-A, ISL-1, GLUT2 as pancreatic islet markers, and intracellular pro-*INS* and *INS* expressions for a 14-days period. In another study, differentiation of WJ-MSCs into IPCs using a lentiviral system containing the GFP reporter gene and its transmission to diabetic NOD mice showed an elevated level of serum insulin and an improved glucose tolerance. Mice treated with WJ-MSCs-GFP had significantly lower blood sugar and higher survival rates than control mice (39). Results from a recent study by De Mesmaeker et al. (40) showed that encapsulation of porcine islet cells by alginate hydrogel in microsphere form enabled long-term glycaemic control in immune-compromised mouse model of diabetes. This intracapsular functional beta cell mass formation involved beta cell replication, significant increasing number, and maturation toward human adult beta cells.

Conclusion

Our results showed that the differentiation of WJ-MSCs into Insulin Producing Cells is increased in PDX1-transduced MSCs group. The *INS* level in encapsulated PDX1-transduced MSCs with alginate was increased compared to the control group. Therefore due to the ability of WJ-MSC in amelioration fibrosis, modulation inflammation and enhancement vascular growth, MSCs could offer a promising treatment option for patients with endocrine disorders.

Acknowledgements

This work was financial supported by Royan Institute. We thank the collaboration and the valuable help of Maryam Hajikaram for Transduction experiment, Masoumeh Zare for language assistance and graphical picturing. There is

no conflict of interest in this study.

Authors' Contributions

Z.P.; Participated in study design, data collection and evaluation, drafting and statistical analysis. S.K., N.H.R.; Were involved in data analysis and interpretation. S.A.; Was involved in conducting the experiments, manuscript proof, administrative and financial support. All authors read and approved the final manuscript.

References

- Association AD. Diagnosis and classification of diabetes mellitus. *Diabetes care*. 2010; 33 Suppl 1: S62-S69.
- Shaw JE, Sicree RA, Zimmet PZ. Global estimates of the prevalence of diabetes for 2010 and 2030. *Diabetes Res Clin Pract*. 2010; 87(1): 4-14.
- Kuncorojakti S, Rodprasert W, Yodmuang S, Osathanon T, Pavasant P, Srisuwatanasagul S, et al. Alginate/Pluronic F127-based encapsulation supports viability and functionality of human dental pulp stem cell-derived insulin-producing cells. *J Biol Eng*. 2020; 14(1): 1-15.
- Pokrywczynska M, Krzyzanowska S, Jundzill A, Adamowicz J, Drewa T. Differentiation of stem cells into insulin-producing cells: current status and challenges. *Arch Immunol Ther Exp (Warsz)*. 2013; 61(2): 149-158.
- Yu S, Li C, Hou Xg, Hou Wk, Dong JJ, Lei S, et al. Differentiation of bone marrow-derived mesenchymal stem cells from diabetic patients into insulin-producing cells in vitro. *Chin Med J*. 2007; 120(9): 771-776.
- Yakhkeshi S, Rahimi S, Sharafi M, Hassani SN, Taleahmad S, Shahverdi A, et al. In vitro improvement of quail primordial germ cell expansion through activation of TGF-beta signaling pathway. *J Cell Biochem*. 2018; 119(6): 4309-4319.
- Schiesser JV, Wells JM. Generation of β cells from human pluripotent stem cells: are we there yet? *Ann N Y Acad Sci*. 2014; 1311: 124-137.
- Chmielowiec J, Borowiak M. In vitro differentiation and expansion of human pluripotent stem cell-derived pancreatic progenitors. *Rev Diabet Stud*. 2014; 11(1): 19-34.
- Moshtagh PR, Emami SH, Sharifi AM. Differentiation of human adipose-derived mesenchymal stem cell into insulin-producing cells: an in vitro study. *J Physiol Biochem*. 2013; 69(3): 451-458.
- Hu J, Yu X, Wang Z, Wang F, Wang L, Gao H, et al. Long term effects of the implantation of Wharton's jelly-derived mesenchymal stem cells from the umbilical cord for newly-onset type 1 diabetes mellitus. *Endocr J*. 2013; 60(3): 347-357.
- Jiang R, Han Z, Zhuo G, Qu X, Li X, Wang X, et al. Transplantation of placenta-derived mesenchymal stem cells in type 2 diabetes: a pilot study. *Front Med*. 2011; 5(1): 94-100.
- Andersen T, Auk-Emblem P, Dornish M. 3D cell culture in alginate hydrogels. *Microarrays*. 2015; 4(2): 133-161.
- Kin K, Yasuhara T, Kameda M, Tomita Y, Umakoshi M, Kuwahara K, et al. Cell encapsulation enhances antidepressant effect of the mesenchymal stem cells and counteracts depressive-like behavior of treatment-resistant depressed rats. *Mol Psychiatry*. 2020; 25(6): 1202-1214.
- Sarker B, Rompf J, Silva R, Lang N, Detsch R, Kaschta J, et al. Alginate-based hydrogels with improved adhesive properties for cell encapsulation. *Int J Biol Macromol*. 2015; 78: 72-78.
- Sun J, Tan H. Alginate-based biomaterials for regenerative medicine applications. *Materials*. 2013; 6(4): 1285-1309.
- Choi S, Kim JH, Ha J, Jeong BI, Jung YC, Lee GS, et al. Intra-articular injection of alginate-microencapsulated adipose tissue-derived mesenchymal stem cells for the treatment of osteoarthritis in rabbits. *Stem Cells Int*. 2018; 2018.
- Strand BL, Coron AE, Skjak-Braek G. Current and future perspectives on alginate encapsulated pancreatic islet. *Stem Cells Transl Med*. 2017; 6(4): 1053-1058.
- Lim F, Sun AM. Microencapsulated islets as bioartificial endocrine pancreas. *Science*. 1980; 210(4472): 908-910.
- Kumar SR, Markusic DM, Biswas M, High KA, Herzog RW. Clinical development of gene therapy: results and lessons from recent successes. *Mol Ther Methods Clin Dev*. 2016; 3: 16034.
- Tsokos GC, Nepom GT. Gene therapy in the treatment of autoim-

- immune diseases. *J Clin Invest*. 2000; 106(2): 181-183.
21. Allahverdi A, Abroun S, Jafarian A, Soleimani M, Taghikhani M, Eskandari F. Differentiation of human mesenchymal stem cells into insulin producing cells by using a lentiviral vector carrying PDX1. *Cell J*. 2015; 17(2): 231.
 22. Gerace D, Martiniello-Wilks R, Simpson A. Diabetes reversal via gene transfer: building on successes in animal models. *Res Rep Endocr Disord*. 2015; 5: 15-29
 23. Varaa N, Azandeh S, Khodabandeh Z, Gharravi AM. Wharton's jelly mesenchymal stem cell: Various protocols for isolation and differentiation of hepatocyte-like cells; narrative review. *Iran J Med Sci*. 2019; 44(6): 437-448.
 24. Noguchi H, Xu G, Matsumoto S, Kaneto H, Kobayashi N, Bonner-Weir S, et al. Induction of pancreatic stem/progenitor cells into insulin-producing cells by adenoviral-mediated gene transfer technology. *Cell Transplant*. 2006; 15(10): 929-938.
 25. Kanafi MM, Ramesh A, Gupta PK, Bhonde RR. Dental pulp stem cells immobilized in alginate microspheres for applications in bone tissue engineering. *Int Endod J*. 2014; 47(7): 687-697.
 26. Gabr MM, Zakaria MM, Refaie AF, Abdel-Rahman EA, Reda AM, Ali SS, et al. From human mesenchymal stem cells to insulin-producing cells: comparison between bone marrow-and adipose tissue-derived cells. *Biomed Res Int*. 2017; 2017.
 27. Fiorina P, Voltarelli J, Zavazava N. Immunological applications of stem cells in type 1 diabetes. *Endocr Rev*. 2011; 32(6): 725-754.
 28. El-Badawy A, El-Badri N. Clinical efficacy of stem cell therapy for diabetes mellitus: a meta-analysis. *PLoS One*. 2016; 11(4): e0151938.
 29. Czubak P, Bojarska-Junak A, Tabarkiewicz J, Putowski L. A modified method of insulin producing cells' generation from bone marrow-derived mesenchymal stem cells. *J Diabetes Res*. 2014; 2014: 628591.
 30. Ranjbaran H, Abediankenari S, Amiri MM. Enhanced differentiation of wharton's jelly-derived mesenchymal stem cells in insulin-producing cells by the extract of nigella sativa seeds. *Iran Red Crescent Med J*. 2018; 20(3).
 31. Sharma A, Rani R. Do we really need to differentiate mesenchymal stem cells into insulin-producing cells for attenuation of the autoimmune responses in type 1 diabetes: immunoprophylactic effects of precursors to insulin-producing cells. *Stem Cell Res Ther*. 2017; 8(1): 167.
 32. Rahmati S, Alijani N, Kadivar M. In vitro generation of glucose-responsive insulin producing cells using lentiviral based pdx-1 gene transduction of mouse (C57BL/6) mesenchymal stem cells. *Biochem Biophys Res Commun*. 2013; 437(3): 413-419.
 33. Soltanian A, Ghezelayagh Z, Mazidi Z, Halvaei M, Mardpour S, Ashtiani MK, et al. Generation of functional human pancreatic organoids by transplants of embryonic stem cell derivatives in a 3D-printed tissue trapper. *J Cell Physiol*. 2019; 234(6): 9564-9576.
 34. Lima MJ, Muir KR, Docherty HM, McGowan NW, Forbes S, Heremans Y, et al. Generation of functional beta-like cells from human exocrine pancreas. *PLoS One*. 2016; 11(5): e0156204.
 35. Barati G, Nadri S, Hajian R, Rahmani A, Mostafavi H, Mortazavi Y, et al. Differentiation of microfluidic-encapsulated trabecular meshwork mesenchymal stem cells into insulin producing cells and their impact on diabetic rats. *J Cell Physiol*. 2019; 234(5): 6801-6809.
 36. Alagpulinsa DA, Cao JJ, Driscoll RK, Sîrbulescu RF, Penson MF, Sremac M, et al. Alginate-microencapsulation of human stem cell-derived β cells with CXCL 12 prolongs their survival and function in immunocompetent mice without systemic immunosuppression. *Am J Transplant*. 2019; 19(7): 1930-1940.
 37. Khatab S, Leijts MJ, van Buul G, Haecck J, Kops N, Nieboer M, et al. MSC encapsulation in alginate microcapsules prolongs survival after intra-articular injection, a longitudinal in vivo cell and bead integrity tracking study. *Cell Biol Toxicol*. 2020; 36(6): 553-570.
 38. Duruksu G, Polat S, Kayış L, Gürcan NE, Gacar G, Yazir Y. Improvement of the insulin secretion from beta cells encapsulated in alginate/poly-L-histidine/alginate microbeads by platelet-rich plasma. *Turk J Biol*. 2018; 42(4): 297-306.
 39. Tsai PJ, Wang HS, Lin GJ, Chou SC, Chu TH, Chuan WT, et al. Undifferentiated Wharton's jelly mesenchymal stem cell transplantation induces insulin-producing cell differentiation and suppression of T-cell-mediated autoimmunity in nonobese diabetic mice. *Cell Transplant*. 2015; 24(8): 1555-1570.
 40. De Mesmaeker I, Robert T, Suenens KG, Stangé GM, Van Hulle F, Ling Z, et al. Increase functional β -cell mass in subcutaneous alginate capsules with porcine prenatal islet cells but loss with human adult islet cells. *Diabetes*. 2018; 67(12): 2640-2649.

Investigation of Signals and Transcription Factors for The Generation of Female Germ-Like Cells

Saman Ebrahimi, Ph.D.¹, Alireza Shams, Ph.D.^{2*}, Parvaneh Maghami, Ph.D.¹, Azadeh Hekmat, Ph.D.¹

1. Department of Biology, Science and Research Branch, Islamic Azad University, Tehran, Iran
2. Department of Anatomy, School of Medicine, Alborz University of Medical Sciences, Karaj, Iran

*Corresponding Address: P.O.Box: 3149969415, Department of Anatomy, School of Medicine, Alborz University of Medical Sciences, Karaj, Iran
Email: dr.shams@abzums.ac.ir

Received: 11/October/2021, Accepted: 27/February/2022

Abstract

Objective: Primordial germ cell (PGCs) lines are a source of a highly specialized type of cells, characteristically oocytes, during female germline development *in vivo*. The oocyte growth begins in the transition from the primary follicle. It is associated with dynamic changes in gene expression, but the gene-regulating signals and transcription factors that control oocyte growth remain unknown. We aim to investigate the differentiation potential of mouse bone marrow mesenchymal stem cells (mMSCs) into female germ-like cells by testing several signals and transcription factors.

Materials and Methods: In this experimental study, mMSCs were extracted from mice femur bone using the flushing technique. The cluster-differentiation (CD) of superficial mesenchymal markers was determined with flow cytometric analysis. We applied a set of transcription factors including retinoic acid (RA), titanium nanotubes (TNTs), and fibrin such as TNT-coated fibrin (F+TNT) formation and (RA+F+TNT) induction, and investigated the changes in gene, *MVH/DDX4*, expression and functional screening using an *in vitro* mouse oocyte development condition. Germ cell markers expression, (*MVH / DDX4*), was analyzed with Immunocytochemistry staining, quantitative transcription-polymerase chain reaction (RT-qPCR) analysis, and Western blots.

Results: The expression of CD was confirmed by flow cytometry. The phase determination of the TNTs and F+TNT were confirmed using x-ray diffraction (XRD) and scanning electron microscope (SEM), respectively. Remarkably, applying these transcription factors quickly induced pluripotent stem cells into oocyte-like cells that were sufficient to generate female germ-like cells, growth, and maturation from mMSCs differentiation. These transcription factors formed oocyte-like cells specification of stem cells, epigenetic reprogramming, or meiosis and indicate that oocyte meiosis initiation and oocyte growth are not separable from the previous epigenetic reprogramming in stem cells *in vitro*.

Conclusion: Results suggested several transcription factors may apply for arranging oocyte-like cell growth and supplies an alternative source of *in vitro* maturation (IVM).

Keywords: Cell Differentiation, Germ cells, Transcription Factors

Cell Journal (Yakhteh), Vol 24, No 8, August 2022, Pages: 458-464

Citation: Ebrahimi S, Shams A, Maghami P, Hekmat A. Investigation of signals and transcription factors for the generation of female germ-like cells. Cell J. 2022; 24(8): 458-464. doi: 10.22074/cellj.2022.8303.

This open-access article has been published under the terms of the Creative Commons Attribution Non-Commercial 3.0 (CC BY-NC 3.0).

Introduction

All infertile couples generate at least one meiotically incomplete oocyte, approximately 7 to 16% (1, 2). Oocyte maturation failure, a bad egg syndrome, is occasionally absolute means no mature oocytes are generated. The key clinical features associated with this syndrome include: i. Primary infertility, ii. Repetitive generation of mostly immature oocytes, iii. Inability of *in vitro* maturation (IVM) to stimulate maturation, and iv. Breakdown of fertilization despite intracytoplasmic sperm injection (ICSI) (3).

In oocyte differentiation, oocyte growth and meiosis are two key processes. Meiosis initiation is believed to be regulated mainly by retinol's production, storage, and metabolism and its metabolite retinoic acid (RA). RA signaling is performed by its target genes, such as *Stra8*, which is essential for the initiation and progression of meiosis. Intrinsic factors such as *MVH* provide diploid germ cells ready for meiosis initiation when extracellular signals are received (4).

Because of their characteristic properties, ability to

self-renewal, cloning, and differentiation into many different cell types as pluripotency, stem cells have been recommended in biomedical applications. Recently, much progress has been obtained in understanding stem cell biology and our ability to manipulate their proliferation and differentiation to get functional cells (5). Hübner et al. (6) show that mouse embryonic stem cells can develop into oogonia that enter meiosis; Bahmanpour et al. (7) improved the rate of *in vitro* oocyte differentiation by using bone morphogenetic protein 4 (BMP4) and RA along with ovarian somatic cell co-culture. Similarly, nanomaterials have recently been synthesized, which increases the efficiency of stem cell differentiation and their biomedicine applications, respectively (8, 9).

Growth and differentiation factors can adhere to nano-supplied surfaces and they can be effectively delivered into the culture medium. Therefore, functional scaffolds made of TNT can be used to grow, biocompatibility, differentiate stem cells, and regenerate damaged tissues (10). However, the small scale of nanomaterials alters their physicochemical properties, making their interactions

toxic to stem cells. Therefore, the determination of nanomaterial bio-interactions is essential to increase the success of medical treatments and enhance the safety of biomedical devices (11).

Fibrin, made from fibrinogen and thrombin, has been introduced as a suitable biological polymer in which tissue engineering applications and growth factors are delivered in cell cultures (12). Significant advantages of fibrin hydrogels include flexibility, low cytotoxicity, and high effectiveness on nanomaterials with homogeneous distribution (13). This characteristic leads to improved cell growth, viability, and differentiation in response to growth factors (14). According to the mentioned characteristics of fibrin, chemical, structural and mechanical, a 3D scaffold is suitable for later tissue engineering applications (15, 16).

Here, we applied a set of transcriptional factors, RA and RA+F+TNT formation, comprising the underlying gene regulatory expression and validated these findings with functional screening. Furthermore, we endeavored to reconstitute pluripotent stem cell differentiation and thereby we generated oocyte-like cells competent for oocyte meiosis initiation, oocyte growth, and subsequent fertilization *in vitro*.

Material and Methods

Nanoparticles synthesis

The TiO₂ nanoparticles were synthesized by the hydrothermal method described by Khoshnood et al. (17), then particles from 10 to 15 nm, which present micropores and mesopores on their surface, were obtained.

Isolation and culture

In this experimental study, the flushing technique was performed to isolate mouse bone marrow mesenchymal stem cells (mMSCs) from mice femur bone. The cell suspensions were transferred into 15 mL centrifugation tubes and were resuspended in DMEM medium (F12: REF:32500-035 Gibco, USA) supplemented with 10% FBS (Sigma-Aldrich, USA), 1% penicillin, and streptomycin (BI-1203 BIO IDEA Company, USA) mixture, and 1% Gluta MAX (Gibco, USA), and seeded in 25 cm² culture medium flask for maintaining at 37°C humidified incubator with 5% CO₂. At 80-90% confluency, cells were harvested with 0.05% Trypsin-EDTA solution (Gibco, USA) and replated in treatment groups (RA and RA+F+TNT formation). All protocols followed for the utilization of animals were approved by the Ethics Committee of Islamic Azad University, Science and Research Branch, Tehran, Iran, approval ID: IR.IAU.SRB.REC.1400.276.

Induction of stem cells into female germ-like cells

The cells obtained from the 3rd passage were used for signals and transcription factors to generate female germ-like cells. Then they were seeded at a density of 2×10⁴

per well in 24-well plates and treated with 10⁻⁵ M RA and 50 µg/ml TNT-coated fibrin (fibrinogen+thrombin 1:1) in the medium as mentioned above for 14 days. The Cells were observed for morphological changes during 14 days of induction, after which immunocytochemistry and quantitative transcription-polymerase chain reaction (RT-qPCR) were performed.

Morphology characterization of F+TNT formation

The phase characterization of TiO₂ nanoparticles was determined by X-ray diffraction pattern (XRD) (Model PW1730, PHILIPS, Cu LFF lamp λ=1.540598 Å, phase size=0.05°, phase time=1 second, voltage 40 kV, current 30 mA, And 40 mV). The 30λ TNT was then added by incubation at 50 µg/ml (18-20) of TNT-PBS-solution (21) on fibrin to measure their excess biological function and differential behavior. Figures analyzed with scanning electron microscope (SEM) and image j software (v. 1.52).

Flow cytometry analysis

For flow cytometric analysis of cluster-differentiation (CD) mesenchymal superficial markers, after four passages, 2×10⁴ cells were removed for a panel of mMSCs antibodies. The Cells were dispersed with 0.25%- trypsin-EDTA (Gibco, USA) and resuspended in PBS supplemented with 0.5% FBS. The cells were aliquoted into several parts and incubated at 4°C for 20 minutes in the dark with monoclonal antibodies (AB92574, AB114052, AB28364, and AB10558) against the hematopoietic cell markers CD31-PE and CD45-FITC (AB6785 and AB6717), and MSC markers CD90-PE, and CD105-FITC (AB6785 and AB6717). Negative control samples were incubated with mouse IgG1- FITC/PE (11-4724) isotype antibodies to help differentiate nonspecific background signals from specific antibody signals. The samples were analyzed on a Partec cytometer (German), and the resulting data were processed using FloMax software (22).

Immunocytochemistry

For Immunocytochemistry analysis of the specific germ cell marker, *MVH*, the cells were washed with PBS after 14 days of induction and were fixed in 4% paraformaldehyde for 20 minutes at 25°C. The cell membrane was permeabilized with 0.1% Triton X-100 solution in PBS for 20 minutes. Nonspecific binding-site blocking was performed with 5% goat serum for 45 minutes without washing, then incubation with anti-MVH (Mouse monoclonal anti-human, 1:100; Abcam, USA) antibody overnight at 4°C. Subsequently, the cells were washed with PBS and incubated with FITC-conjugated Goat Anti-Rabbit (1:100; Abcam, USA) or Goat Anti-Mouse (1:100; Abcam, USA) for 1 hour at 25°C. Finally, the Nuclei were counterstained with DAPI (Sigma, UK) for 5 minutes, and an Immunofluorescence image was taken using a fluorescent microscope (22).

Quantitative transcription-polymerase chain reaction

Using Tri-Pure reagent (Invitrogen, San Diego, CA, USA) whole RNA isolate per the manufacturer's instructions. The DNA contamination in the RNA sample was deleted by RNase-free DNase I (Thermo Scientific, USA) for 30 minutes at 37°C. The RNA concentration and purity were specified using the spectrophotometric (WPA spectrophotometer, Biochrom, UK) method. Using a Transcriptor First Strand cDNA Synthesis kit (Roche), the RNA was reversely transcribed by random Hexamer and 1000 ng of DNA-free RNA. TaqMan probe (Life Technologies, India) was applied to survey the expression of *MVH*, which normalized against 18 seconds expression as a housekeeping gene *β -actin*. The PCR reaction components were mixed to procure a final volume of 20 μ L. The following components were applied: 0.5 μ L (25 ng) cDNA, 1 μ L TaqMan assay reagent, 10 μ L TaqMan universal master mix, and 8.5 μ L distilled water. The PCR cycling was as follows: 10 minutes at 95°C, polymerase activation, 40 cycles at 95°C for 15 seconds, and 60°C for 1 minute using a Rotor-Gene Q instrument (Qiagen, Germany). The relative expression of the gene, using the $\Delta\Delta$ Ct method, was analyzed by normalizing the Ct values of the target against 18 seconds (22). Sequences of the *MVH* primers used for RT-qPCR are:

F: 5'GTGGAAGTGGTTCGAGGTGGT3'
R: 5'CTGGTGGAGGAGGGGTA3'

and primers sequences of housekeeping gene, *β -actin* are:

F: 5'TCAGAGCAAGAGAGGCATCC3'
R: 5'GGTCATCTTCTCACGGTTGG3'

Western blots

Fifty μ g of proteins extracted by RIPA lysis buffer was used for sodium dodecyl sulfate-polyacrylamide gel electrophoresis (SDS-PAGE) and transferred to nitrocellulose membranes. The membrane was stained with rabbit polyclonal antibody against MVH (AB13840, Abcam, UK, 1:100 dilutions), and goat anti-mouse secondary antibodies (ab6789, Lucerna-Chem, Switzerland). The antibody-antigen interaction in the membranes was observed using an enhanced-chemiluminescent detection kit (Santa Cruz Biotechnology Inc, Santa Cruz, CA, USA) (23).

Statistical analysis

All data were presented as mean \pm SD (standard deviation) and were analyzed using SPSS (v 23, IBM, USA). One-way ANOVA and Tukey tests followed by Bonferroni posttest were used to compare the groups. The significant differences ($P < 0.05$) were calculated among various treatment groups.

Results

Flow cytometry

We evaluated several stem cell-associated CD markers

using flow cytometry to determine the CD markers of cultured cells in passage 3. The results illustrate the differential characteristics of stem cells and rule out the hematopoietic origin of isolated cells. The Cells were mostly positive for mMSCs markers, CD90 and CD105, and at least reacted with hematopoietic markers, CD31 and CD45: 95% of the cells express CD90, 72.6% of the cells express CD105, 0.23% of the cells express CD31, and 1.42% of the cells express CD45 (Fig.1). Negative control samples were incubated with IgG1-FITC/PE isotype antibodies in mice. The data represented three independent experiments as mean \pm SD.

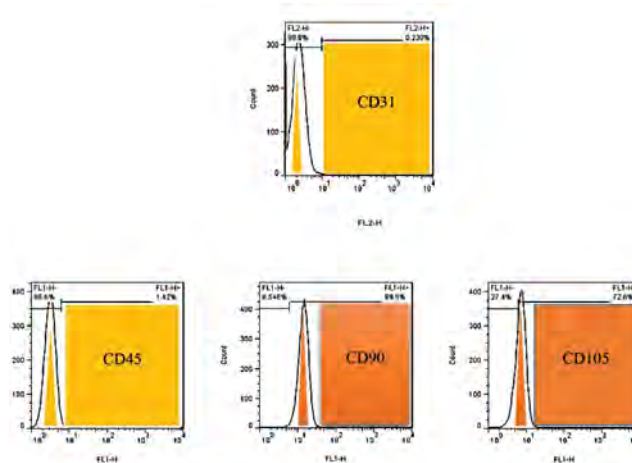


Fig.1: Flow cytometry results of CD expression in isolated mMSCs at third passage. The cells were mostly positive for the superficial mesenchymal markers: CD90=95.5%, CD105=72.6% and minimally expressed CD31=0.230% and CD45=1.42% (hematopoietic markers). The data were representative of three independent experiments, as mean \pm SD. Negative control samples were incubated with mouse IgG1-FITC/PE isotype antibodies to help differentiate nonspecific background signals from specific antibody signals.

Structural determination of TNTs and F+TNT formation

The XRD data for the sample synthesized at 120°C is consistent with the standard Anatase (USnano-America) pattern. Usually, diffraction peaks at 30°C indicate the presence of crystal defects or long-term non-sequence in TiO₂ nanoparticles. However, such a peak was not observed in our diffraction pattern which suggests the pure anatase phase of TiO₂ is formed by a quadrilateral anatase structure at 120°C. The absence of diffraction peaks at 27°C and 31°C indicates that this sample was free of rutile and TiO₂ brookite structures. The XRD pattern showed anatase phase TiO₂ nanoparticles only by diffraction at angles of 25, 37, 48, 54, 55, 63, 69, and 75°C (peak A, Fig.2A). The above results confirmed that the optimal calcination temperature for preparing pure anatase of TiO₂ nanocrystals by polymer gel was 120°C. The morphology of F+TNT formation was confirmed using SEM. It was observed that the surface area of TNT was increased compared with self-aggregation-TNT (Fig.2B).

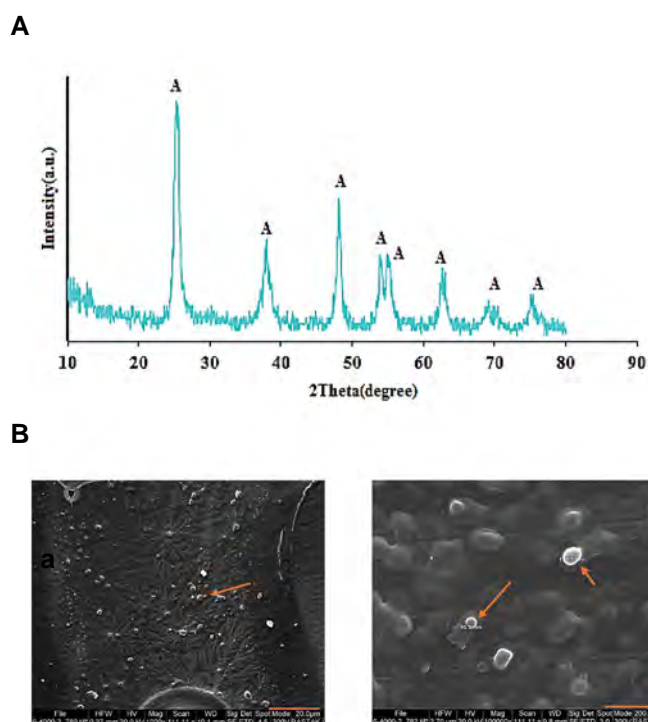


Fig.2: Structural determination of TNTs and F+TNT formation. **A.** X-ray diffraction patterns of TNT anatase phase in different angles (peak A). **B.** The SEM of F+TNT formation after 24 hours of incubation (scale bar of a: 20 µm, b: 200 nm). Orange arrows revealed the F+TNT transcription factor formation with (b) 90 to 115 nm approximate diameter. TNT; Titanium nanotube, F; Fibrin, and SEM; Scanning electron microscope.

Immunocytochemistry staining for specific oocyte-like cell marker, *MVH*, differentiation

The germ cell-related gene, *MVH*, was detected in all isolated cells using immunocytochemical analysis after 14 days. This experiment confirms that all mouse bone marrow cells have a differentiation potential into germ- and oocyte-like cells with signals and transcription factors. Under immuno-fluorescence microscopy, green fluorescent protein (*GFP*) expression was highly observed in mMSCs-derived female germ-like cells, treated with RA+F+TNT or RA compared to control cells. (Fig.3A, B).

RT-qPCR analysis of specific oocyte-like cell marker, *MVH*

RT-qPCR results show that all the cells expressed oocyte-like cell genes after 14 days of transcription factor inductions. However, the quality and quantity of expression differed among two germ cell marker groups, *MVH*. In this experiment, F+TNT transcription factors showed more significant potential to be differentiated into oocyte-like cells. A significantly higher relative gene expression level of F+TNT was observed compared with RA and control ($P < 0.05$). The results of this analysis show that co-administration of transcription factors has a higher potential for differentiation of mMSCs into female germ-like cells than individual transcription factor (Fig.4).

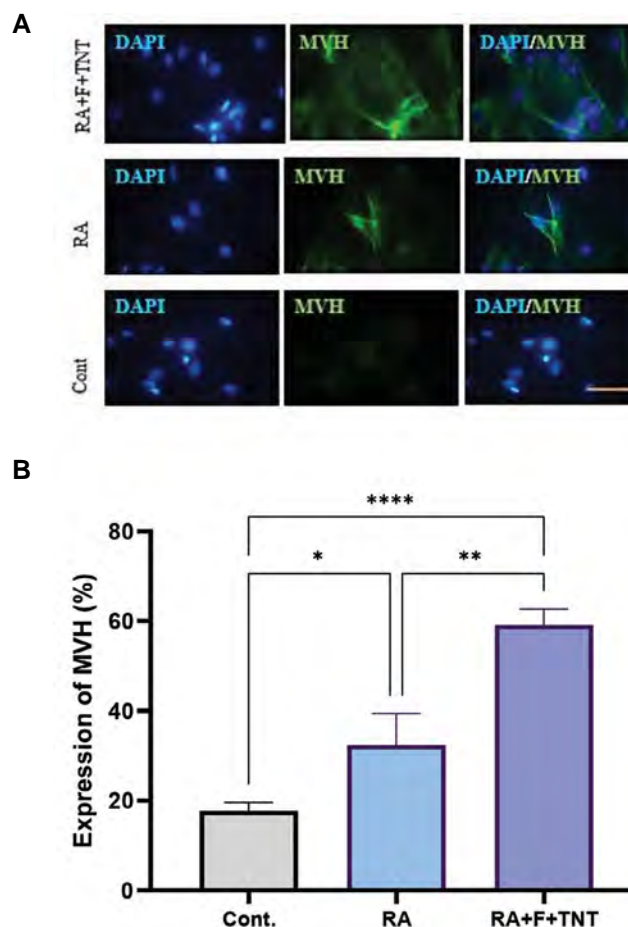


Fig.3: Expression of germ cell markers (*MVH* and *GFP*) in mMSCs-derived female germ-like cells. **A.** Immunocytochemistry staining of mMSCs for specific female germ cells marker, *MVH*, after 14 days of differentiation induction. The Nuclei were counter-stained with DAPI and *GFP* intensity was quantified (scale bar: 100 µm). **B.** Quantitative analysis of Immunocytochemistry images. *, $P < 0.0194$, **, $P < 0.0010$, ****, $P < 0.0001$, mMSCs; Mouse bone marrow mesenchymal stem cells, RA; Retinoic acid, F; Fibrin, Cont; Control, and TNT; Titanium nanotube.

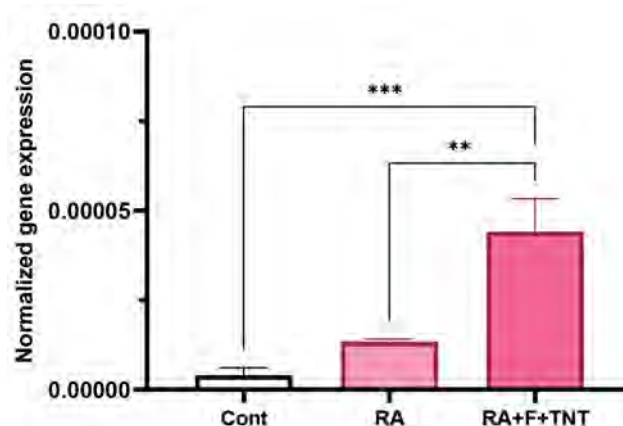


Fig.4: The RT-qPCR analysis of specific oocyte-like cell marker, *MVH*. RT-qPCR analysis of isolated mMSCs after signals and transcription factor induction under the influence of 10^{-5} M RA, 50 µg/ml TNT-coated fibrin formation for 14 days. The mMSCs treated by the RA+F+TNT compared with the RA and control cells showed significant potential to be differentiated into female germline cells due to the significantly higher relative gene expression level of *MVH* gene. **, $P < 0.0011$, ***, $P < 0.0003$, RT-qPCR; Quantitative transcription-polymerase chain reaction, mMSCs; Mouse bone marrow mesenchymal stem cells, RA; Retinoic acid, F; Fibrin, and TNT; Titanium nanotube.

Western blots of oocyte marker

Western blot analysis measured the expression of female germ cell-associated proteins (MVH) during oocyte-like cells formation from mMSCs after being cultured for 14 days. Furthermore, the level of MVH protein was higher in mMSCs treated with RA or RA+F+TNT compared to the level of MVH protein in the control cells (Fig.5).

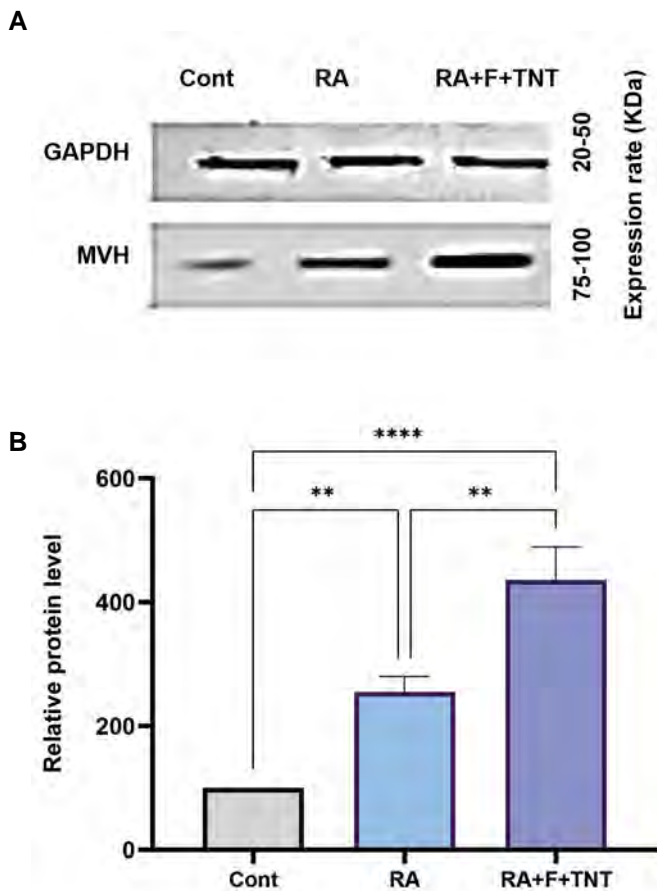


Fig.5: Western blot analysis of MVH expression in mice bone marrow-derived mMSCs. **A.** MVH protein levels were evaluated as specific differentiation markers to compare GAPDH reference protein using western blot analysis. **B.** Protein lysates from mMSCs were blotted and stained by MVH antibody. The level of MVH protein expression was higher in mMSCs treated with RA or RA+F+TNT compared to the level of MVH protein expression in the control cells. **, $P < 0.0034$, ****, $P < 0.0001$, indicated significant differences in the MVH expression between RA+F+TNT, RA, and the control, mMSCs; Mouse bone marrow mesenchymal stem cells, RA; Retinoic acid, F; Fibrin, and TNT; Titanium nanotube.

The mMSCs characterizations and signal epigenetic reprogramming for induced oocytes

The mMSCs from mice bone marrow were successfully cultured up to 4 passages, and the proliferation rate was confluency after 4-5 days following each passage. All cells had spindle-like morphology and, in some cases, possessed some long and short processes. During differentiation induction, the cells were treated with RA, RA+F+TNT formation for 14 days and observed every day to determine any differential morphological changes

under a phase-contrast microscope. In addition, size measurement and counting of oocytes were quantified using Image J software (v.1.52) (Fig.6).

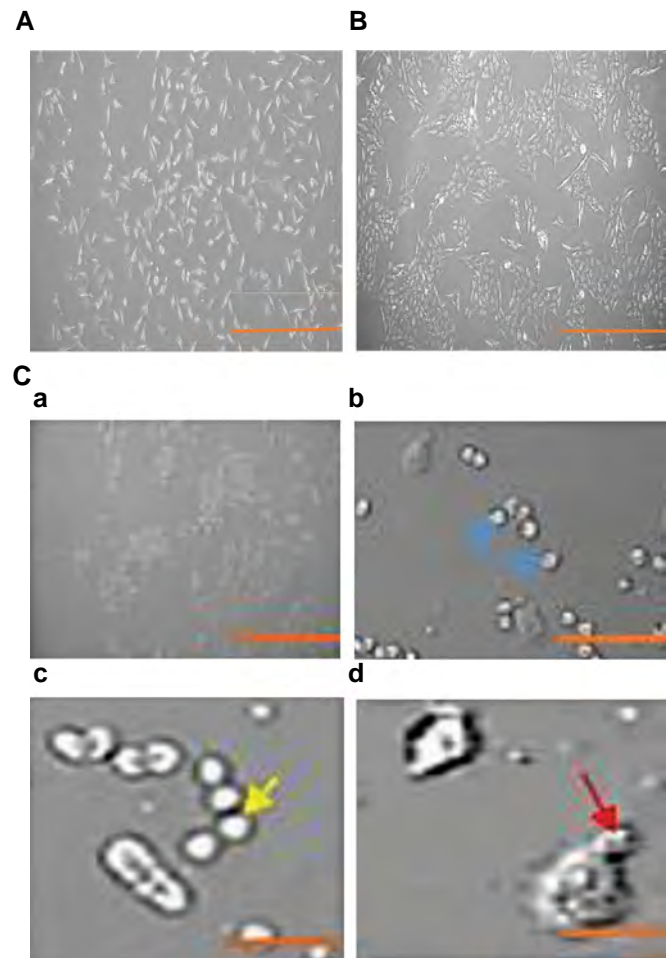


Fig.6: The isolated mMSCs and induced germ cells. **A.** Isolated mMSCs, passage 2, 24 hours after incubation (scale bar: 100 μ m). **B.** Spindle-shaped fibroblast-like of mMSCs, passage 3, in the 3rd passage (scale bar: 100 μ m). **C.** The mMSCs-derived oocyte-like cell size change and growth were observed after transcription factor inductions. The cell morphology was changed after F+TNT+RA treating. The first observation was the appearance of spindle-shaped mMSCs, which became large, circular, and long. The germ cells show a meiotic marker (MVH/DDX4). **a.** Oocyte-like cells generated from *in vitro* culturing (scale bar: 200 μ m), **b.** Primary oocyte with its nucleus arrested at prophase I of meiosis I, germinal vesical (GV), blue arrows (scale bar: 100 μ m), **c.** Primary oocyte-like cells undergoing meiosis I-nucleus and nucleolus have disappeared, germinal vesicle breakdown (GVBD), metaphase I (M I), yellow arrow, (scale bar: 50 μ m), and **d.** Secondary oocyte-like cells with the polar body (PB) resulting from meiosis I. Metaphase II (M II), red arrow (scale bar: 25 μ m).

Discussion

This study defines a set of transcription factors, which are promoted the differentiation of oocyte-like cells from mMSCs *in vitro*, which is expressed germ-like cell marker MVH/DDX4 at both mRNA and protein levels. This study will be a powerful protocol to elevate our understanding of the mechanisms underlying reprogramming in oocyte-like cell growth and of their potential application in IVM technologies.

Oocyte differentiation and development depend on continuous signaling interactions with somatic follicle cells *in vivo* (24). Signaling molecules; maturation-promoting factor (MPF), transcription, and translation of critical regulatory enzymes are the processes by which an oocyte acquires meiotic competence *in vivo*. The complex interaction between these factors and the determination of arrest versus progression is related to the delicate balance between the production and targeted degradation of signaling molecules, MPF (25-31). Finally, dysfunction on the molecular level, errors in MPF, and aberrations in chromosomal/spindle formation lead to meiotically oocyte maturation arrest. In the case of reports, changes in gonadotropin stimulation protocol, using IVM, and ICSI does not improve the treatment outcome for bad egg syndrome (3).

RA has been proven to act as a meiosis-inducing factor of meiosis in mouse gonads. RA induces *Stra8*, an RA-responsive gene in female primordial germ cell (PGCs), leading to meiosis in fetal female germ cells. Recently, reports have shown that RA can induce meiosis in PGCs before gonadal sex differentiation (32-37).

This study introduced several transcription factors, RA, RA+F+TNT, that can induce mMSCs into oocyte-like cells *in vitro*. Growth and differentiation factors can adhere to nanomaterial and fibrin, which enhance their effective delivery in culture medium and increase the developmental levels. The differentiated oocyte-like cells indicated that transcription factors are a prerequisite to activating the gene-excitatory expression driving oocyte growth *in vitro*. As such, our results complement recent studies which suggest that the principal role of epigenetic reprogramming is to activate the meiotic program. In addition, our observation showed that oocyte-like cell induction during oocyte growth is dependent on the epigenetic reprogramming in female germ-like cells. This finding provides new insight into the importance of epigenetic control and transcription factors in oocyte maturation. Furthermore, understanding possible roles of transcription factors in oocyte-like cell induction is necessary for new research. The culture conditions are a unique material that is invaluable for applications in assisted reproductive technology, such as IVM and ICSI.

Oocyte-like generation is challenging *in vitro*, and this involves both cytoplasmic and nuclear processes. This study showed the increased *MVH* expression at both mRNA and protein levels, as a result of using several transcription factors, RA, TNT, and fibrin, which indicates the effectiveness of these transcription factors in the production of female germ-like cells.

The mMSCs can be reprogrammed to an oocyte-like cell by transcription factors, RA, RA+F+TNT formation; little is known about factors that induce this reprogramming *in vivo* and *in vitro*. Furthermore, by understanding the mechanism of oocyte-like cell maturation *in vitro*, it is possible that IVM protocols could be promoted to obtain the signaling and transcription factors necessary for

oocyte maturation competence and performance *in vitro*.

Conclusion

Here, we demonstrate the induction of pluripotent stem cells from mouse bone mMSCs by introducing germ factors, *MVH*, under stem cell culture conditions and morphology determination of F+TNT induction. mMSCs exhibit the morphology and growth properties of germ-like cells and express germ cell marker genes following treatment with the above-mentioned transcription factors. These data demonstrate that oocyte-like cells can be directly generated from mMSCs by adding only a few defined factors.

Acknowledgments

We are thankful to Zohreh Mazaheri, a member of Basic Medical Sciences Research Center, Histogenotech Company, Tehran, Iran, and the laboratory assistants of the Histogenotech Company for sharing their valuable knowledge and experience in performing this study. The authors declare that there is no conflict of interests and funding support.

Authors' Contributions

S.E.; Conceived the presented idea. S.E., A.Sh., P.M., A.H.; Developed the proposal and performed the experiments. P.M., A.H.; Verified and monitored the analytical methods. S.E., A.Sh.; Investigated morphology characteristics of the TNTs and the TNTs-coated fibrin. A.Sh., P.M., A.H.; Supervised the findings of this work. All authors read and approved the final manuscript.

References

1. Bar-Ami S, Zlotkin E, Brandes JM, Itskovitz-Eldor J. Failure of meiotic competence in human oocytes. *Biol Reprod.* 1994; 50(5): 1100-1107.
2. Avrech OM, Goldman GA, Rufas O, Stein A, Amit S, Yoles I, et al. Treatment variables in relation to oocyte maturation: lessons from a clinical micromanipulation-assisted in vitro fertilization program. *J Assist Reprod Genet.* 1997; 14(6): 337-342.
3. Beall S, Brenner C, Segars J. Oocyte maturation failure: a syndrome of bad eggs. *Fertil Steril.* 2010; 94(7): 2507-2513.
4. Wang S, Wang X, Ma L, Lin X, Zhang D, Li Z, et al. Retinoic acid is sufficient for the in vitro induction of mouse spermatocytes. *Stem Cell Reports.* 2016; 7(1): 80-94.
5. Volarevic V, Bojic S, Nurkovic J, Volarevic A, Ljubic B, Arsenijevic N, et al. Stem cells as new agents for the treatment of infertility: current and future perspectives and challenges. *Biomed Res Int.* 2014; 2014: 507234.
6. Hübner K, Fuhrmann G, Christenson LK, Kehler J, Reinbold R, De La Fuente R, et al. Derivation of oocytes from mouse embryonic stem cells. *Science.* 2003; 300(5623): 1251-1256.
7. Bahmanpour S, Zarei Fard N, Talaei Khozani T, Hosseini A, Esmaeilpour T. Effect of BMP 4 preceded by retinoic acid and co-culturing ovarian somatic cells on differentiation of mouse embryonic stem cells into oocyte like cells. *Dev Growth Differ.* 2015; 57(5): 378-388.
8. Chimene D, Alge DL, Gaharwar AK. Two-dimensional nanomaterials for biomedical applications: emerging trends and future prospects. *Adv Mater.* 2015; 27(45): 7261-7284.
9. Solanki A, Kim JD, Lee KB. Nanotechnology for regenerative medicine: nanomaterials for stem cell imaging. *Nanomedicine (Lond).* 2008; 3(4): 567-578.
10. Hou Y, Cai K, Li J, Chen X, Lai M, Hu Y, et al. Effects of titanium nanoparticles on adhesion, migration, proliferation, and differen-

- tiation of mesenchymal stem cells. *Int J Nanomedicine*. 2013; 8: 3619-3630.
11. Kubo K, Tsukimura N, Iwasa F, Ueno T, Saruwatari L, Aita H, et al. Cellular behavior on TiO₂ nanonodular structures in a micro-to-nanoscale hierarchy model. *Biomaterials*. 2009; 30(29): 5319-5329.
 12. Duong H, Wu B, Tawil B. Modulation of 3D fibrin matrix stiffness by intrinsic fibrinogen–thrombin compositions and by extrinsic cellular activity. *Tissue Eng Part A*. 2009; 15(7): 1865-1876.
 13. Ziv-Polat O, Skaat H, Shahar A, Margel S. Novel magnetic fibrin hydrogel scaffolds containing thrombin and growth factors conjugated iron oxide nanoparticles for tissue engineering. *Int J Nanomedicine*. 2012; 7: 1259-1274.
 14. Rampichová M, Buzgo M, Míčková A, Vocetková K, Sovková V, Lukášová V, et al. Platelet-functionalized three-dimensional poly-ε-caprolactone fibrous scaffold prepared using centrifugal spinning for delivery of growth factors. *Int J Nanomedicine*. 2017; 12: 347-361.
 15. Janmey PA, Winer JP, Weisel JW. Fibrin gels and their clinical and bioengineering applications. *J R Soc Interface*. 2009; 6(30): 1-10.
 16. De Melo BAG, Jodat YA, Cruz EM, Benincasa JC, Shin SR, Porcionatto MA. Strategies to use fibrinogen as bioink for 3D bioprinting fibrin-based soft and hard tissues. *Acta Biomater*. 2020; 117: 60-76.
 17. Khoshnood N, Zamanian A, Massoudi A. Mussel-inspired surface modification of titania nanotubes as a novel drug delivery system. *Mater Sci Eng C Mater Biol Appl*. 2017; 77: 748-754.
 18. Lopez A. Respiratory system, thoracic cavity and pleura. *Pathologic basis of veterinary disease*. St. Louis, Mo: Mosby Elsevier; 2007; 463-558.
 19. García-Hevia L, Valiente R, Martín-Rodríguez R, Renero-Lecuna C, González J, Rodríguez-Fernández L, et al. Nano-ZnO leads to tubulin microtubule assembly and actin bundling, triggering cytoskeletal catastrophe and cell necrosis. *Nanoscale*. 2016; 8(21): 10963-10973.
 20. Anselmo AC, Zhang M, Kumar S, Vogus DR, Menegatti S, Helgeson ME, et al. Elasticity of nanoparticles influences their blood circulation, phagocytosis, endocytosis, and targeting. *ACS Nano*. 2015; 9(3): 3169-3177.
 21. Noori A, Ashrafi SJ, Vaez-Ghaemi R, Hatamian-Zaremi A, Webster TJ. A review of fibrin and fibrin composites for bone tissue engineering. *Int J Nanomedicine*. 2017; 12: 4937-4961.
 22. Asgari HR, Akbari M, Yazdekhasti H, Rajabi Z, Navid S, Aliakbari F, et al. Comparison of human amniotic, chorionic, and umbilical cord multipotent mesenchymal stem cells regarding their capacity for differentiation toward female germ cells. *Cell Reprogram*. 2017; 19(1): 44-53.
 23. Li P, Hu H, Yang S, Tian R, Zhang Z, Zhang W, et al. Differentiation of induced pluripotent stem cells into male germ cells in vitro through embryoid body formation and retinoic acid or testosterone induction. *Biomed Res Int*. 2013; 2013: 608728.
 24. Clarke HJ. Regulation of germ cell development by intercellular signaling in the mammalian ovarian follicle. *Wiley Interdiscip Rev Dev Biol*. 2018; 7(1): 10.
 25. Jamnongjit M, Hammes SR. Oocyte maturation: the coming of age of a germ cell. *Semin Reprod Med*. 2005; 23(3): 234-241.
 26. Dekel N. Cellular, biochemical and molecular mechanisms regulating oocyte maturation. *Mol Cell Endocrinol*. 2005; 234(1-2): 19-25.
 27. Nakanishi T, Kubota H, Ishibashi N, Kumagai S, Watanabe H, Yamashita M, et al. Possible role of mouse poly (A) polymerase mGLD-2 during oocyte maturation. *Dev Biol*. 2006; 289(1): 115-126.
 28. Rauh NR, Schmidt A, Bormann J, Nigg EA, Mayer TU. Calcium triggers exit from meiosis II by targeting the APC/C inhibitor XErp1 for degradation. *Nature*. 2005; 437(7061): 1048-1052.
 29. Eichenlaub-Ritter U, Peschke M. Expression in in-vivo and in-vitro growing and maturing oocytes: focus on regulation of expression at the translational level. *Hum Reprod Update*. 2002; 8(1): 21-41.
 30. Liang CG, Su YQ, Fan HY, Schatten H, Sun QY. Mechanisms regulating oocyte meiotic resumption: roles of mitogen-activated protein kinase. *Mol Endocrinol*. 2007; 21(9): 2037-2055.
 31. Huo LJ, Fan HY, Zhong ZS, Chen DY, Schatten H, Sun QY. Ubiquitin–proteasome pathway modulates mouse oocyte meiotic maturation and fertilization via regulation of MAPK cascade and cyclin B1 degradation. *Mech Dev*. 2004; 121(10): 1275-1287.
 32. Zhou Q, Li Y, Nie R, Friel P, Mitchell D, Evanoff RM, et al. Expression of stimulated by retinoic acid gene 8 (Stra8) and maturation of murine gonocytes and spermatogonia induced by retinoic acid in vitro. *Biol Reprod*. 2008; 78(3): 537-545.
 33. Zhou Q, Nie R, Li Y, Friel P, Mitchell D, Hess RA, et al. Expression of stimulated by retinoic acid gene 8 (Stra8) in spermatogenic cells induced by retinoic acid: an in vivo study in vitamin A-sufficient postnatal murine testes. *Biol Reprod*. 2008; 79(1): 35-42.
 34. Trautmann E, Guerquin MJ, Duquenne C, Lahaye JB, Habert R, Livera G. Retinoic acid prevents germ cell mitotic arrest in mouse fetal testes. *Cell Cycle*. 2008; 7(5): 656-664.
 35. Li H, Kim KH. Retinoic acid inhibits rat XY gonad development by blocking mesonephric cell migration and decreasing the number of gonocytes. *Biol Reprod*. 2004; 70(3): 687-693.
 36. Adams IR, McLaren A. Sexually dimorphic development of mouse primordial germ cells: switching from oogenesis to spermatogenesis. *Development*. 2002; 129(5): 1155-1164.
 37. Best D, Sahlender DA, Walther N, Peden AA, Adams IR. Sdmg1 is a conserved transmembrane protein associated with germ cell sex determination and germline-soma interactions in mice. *Development*. 2008; 135(8): 1415-1425.

Endothelin-1 Stimulates PAI-1 Protein Expression via Dual Transactivation Pathway Dependent ROCK and Phosphorylation of Smad2L

Hossein Babaahmadi-Rezaei, Ph.D.¹, Alireza Kheirollah, Ph.D.², Faezeh Seif, Ph.D.^{1,3*}

1. Hyperlipidemia Research Center, Department of Clinical Biochemistry, Faculty of Medicine, Ahvaz Jundishapur University of Medical Sciences, Ahvaz, Iran
2. Department of Biochemistry, Cellular and Molecular Research Center, Ahvaz Jundishapur University of Medical Sciences, Ahvaz, Iran
3. Department of Basic Sciences, Shoushtar Faculty of Medical Sciences, Shoushtar, Iran

*Corresponding Address: P.O.Box: 159, Hyperlipidemia Research Center, Department of Clinical Biochemistry, Faculty of Medicine, Ahvaz Jundishapur University of Medical Sciences, Ahvaz, Iran
Email: faezehseif@yahoo.com

Received: 18/July/2020, Accepted: 15/May/2021

Abstract

Objective: In addition to the carboxy region, Smad2 transcription factor can be phosphorylated in the linker region as well. Phosphorylation of Smad2 linker region (Smad2L) promotes the expression of plasminogen activator inhibitor type 1 (PAI-1) which leads to cardiovascular disorders such as atherosclerosis. The purpose of this study was to evaluate the role of dual transactivation of EGF and TGF- β receptors in phosphorylation of Smad2L and protein expression of PAI-1 induced by endothelin-1 (ET-1) in bovine aortic endothelial cells (BAECs). In addition, as an intermediary of G protein-coupled receptor (GPCR) signaling, the functions of ROCK and PLC were investigated in dual transactivation pathways.

Materials and Methods: The experimental study is an *in vitro* study performed on BAECs. Proteins were investigated by western blotting using protein-specific antibodies against phospho-Smad2 linker region residues (Ser245/250/255), phospho-Smad2 carboxy residues (465/467), ERK1/(Thr202/Thr204), and PAI-1.

Results: TGF (2 ng/ml), EGF (100 ng/ml) and ET-1 (100 nM) induced the phosphorylation of Smad2L. This response was blocked in the presence of AG1478 (EGFR antagonists), SB431542 (TGFR inhibitor), and Y27632 (Rho-associated protein kinase (ROCK) antagonist). Moreover, ET-1-increased protein expression of PAI-1 was decreased in the presence of bosentan (ET receptor inhibitor), AG1478, SB431542, and Y27632.

Conclusion: The results indicated that ET-1 increases the phosphorylation of Smad2L and protein expression of PAI-1 via induced the transactivation pathways of EGFR and TGFR. This study is the first attempt to scrutinize the significant role of ROCK in the protein expression of PAI-1.

Keywords: Atherosclerosis, ROCK, Smad2, Transactivation

Cell Journal (Yakhteh), Vol 24, No 8, August 2022, Pages: 465-472

Citation: Babaahmadi-Rezaei H, Kheirollah A, Seif F. Endothelin-1 stimulates PAI-1 protein expression via dual transactivation pathway dependent ROCK and phosphorylation of smad2L. Cell J. 2022; 24(8): 465-472. doi: 10.22074/cellj.2022.7720.

This open-access article has been published under the terms of the Creative Commons Attribution Non-Commercial 3.0 (CC BY-NC 3.0).

Introduction

Endothelin-1 (ET-1) is a strong vasoconstrictor peptide that is synthesized by endothelial cells, probably causing the promotion of endothelial dysfunction (1-4). The effect of ET-1 is exerted through G-protein-coupled receptors (GPCRs): ET_A and ET_B (5). GPCR family is the biggest group of cell surface receptors participating in a number of physiological or pathological circumstances (6). Therefore, understanding the different dimensions of GPCR signaling is essential for therapeutic purposes. GPCRs-driven signaling pathways include the classic pathway via direct binding of ligand to GPCR on the cell membrane leading to activation of heterotrimeric G proteins and multiple signaling pathways. In recent years, transactivation pathways of protein tyrosine kinase receptors (PTK) such as epidermal growth factor receptor (EGFR), as well as protein serine/threonine kinase receptors (PS/TK) like transforming growth factor receptor (TGFR) have been identified as part of the GPCR signaling (7-9). Recent studies have demonstrated that different GPCR agonists such as thrombin, ET-1, and

AngII can contribute to transactivation of EGFR and TGFR (10-12). According to our previous study, it has been determined that ET-1 results in TGFR transactivation endothelial cells (13).

TGF β receptors are a group of serine/threonine kinase receptors whose biological roles are performed by type I and type II receptor complexes (ALK5). TGF- β signaling is launched by interaction of a ligand to the T β RII/type I heterogenic complex leading to phosphorylation of the carboxy region of Smad proteins (14). Smad proteins are transcriptional factors that play a serious role in the TGF β -superfamily signals (15, 16). The Smads have three distinct regions: two conserved regions including N-terminal (MH1) and C-terminal (MH2) regions, and one non-conserved region -linker region- that links MH1 and MH2 regions. Besides the carboxy region, the linker region can be phosphorylated as well (16-18). In the Smad-dependent TGF- β signaling pathway, phosphorylation of C-terminal region occurs immediately by binding of TGF- β to the cell surface receptor. However,

in non-Smad signaling, phosphorylation of Smad2 linker region (Smad2L) occurs indirectly by an activated serine/threonine kinase such as ERK1/2, p38, or JNK. Recent studies have shown that in addition to TGF- β , GPCR agonists result in phosphorylation of Smad2L which can play a significant part in regulation of Smad's function (14). Phosphorylation of Smad2L increases the expression of proteoglycan synthesizing genes. It has been demonstrated that TGF- β /Smad pathway increases plasminogen activator inhibitor type 1 (PAI-1) expression in different cell types (19, 20). PAI-1 is a member of the superfamily of serine-protease inhibitors (serpin) that may cause vascular disorders such as endothelial dysfunction (21, 22). Studies have shown that growth factors such as TNF- α , TGF, GPCR agonists such as thrombin, and angiotensin II can lead to increased mRNA expression of PAI-1 (16, 21, 23). In 1996, it was shown for the first time that angiotensin II (Ang II) can induce transactivation pathways. Subsequently, some comprehensive researches have focused on understanding the underlying mechanism of transactivation pathway in different cell types. However, the details of this pathway and the signaling molecules that participate in transactivation pathways induced by ET-1 are not very clear in bovine aortic endothelial cells (BAECs). Therefore, in the current study and for the first time, not only the role of dual transactivation pathways induced by ET-1 were evaluated in phosphorylation of Smad2L and PAI-1 expressions in BAECs, but also the role of ROCK assessed in the ET-1 induced PAI-1 expression.

Materials and Methods

This experimental study was approved by the Ethics Committee of Ahvaz Jundishapur University of Medical Sciences (IRAJUMS.REC.1396.1.4). fetal bovine serum (FBS), penicillin-streptomycin solution, and low glucose (1 g/L) Dulbecco's modified Eagle's medium (DMEM) were obtained from Gibco (Invitrogen, Carlsbad, CA, USA). EGF, ET-1, Y27632, AG1478, SB431542, and neomycin were purchased from Sigma-Aldrich (St. Louis, MO, USA). Recombinant transforming growth factor- β , HRP anti-rabbit IgG-peroxidase antibody produced in goat, anti-phospho-Smad2L (ser245/250/255) rabbit polyclonal antibody, anti-phospho-Smad2C (ser465/467) rabbit polyclonal antibody, anti-phospho-ERK1/2(The202/204), PAI-1 antibody, and GAPDH were purchased from Cell Signaling Technology (Beverly, MA, USA).

Cell culture

Bovine aortic endothelial cells (BAEC) were gifted by Professor Peter J Little (School of Pharmacy, The University of Queensland, Australia). BAECs were cultured according to a previously-described procedure (13). In brief, the cells were cultivated in DMEM with 1 g/l glucose containing 10% FBS and 1% antibiotic; and when cells reached about 80 % confluence, they were pretreated with specific inhibitors in certain intervals. In the next step, ET-1 was added to the culture medium. BAECs were incubated with TGF β (2 ng/ml) for 1 hour

and with EGF (100 ng/ml) for 5 minutes, once alone and once in combination with each other (13, 24). To investigate the effects of ET-1 on phosphorylation of Smad2L, the BAECs were treated with ET-1 (100 nM), and then harvested at 5 and 15 minutes, 2, 4, and 8 hours intervals. In order to evaluate Smad2C phosphorylation, BAECs were treated with ET-1 (100 nM) and harvested at 1, 2, and 4 hours intervals (13). In order to evaluate ERK phosphorylation, BAECs were treated with ET-1 (100 nM) and were subsequently harvested at 5, 15 and 30 minutes, 1, 2, 4, and 8 hours intervals (25). The effects of SB431542 (10 μ M for 30 minutes) and AG1474 (10 μ M for 30 minutes) (24) inhibitors on pSmad2L were tested by pretreating the cells with them. Thereafter, ET-1 (100 nM) was added to the culture medium. The neomycin (100 μ M for 1 hour) (26) and Y27632 (10 μ M for 30 minutes) (13) inhibitors were tested on pSmad2L via pre-incubation of the cells prior to addition of ET-1 (100 nM) to the culture medium. To investigate the effects of ET-1 on protein expression of PAI-1, the BAECs were treated with ET-1 (100 nM) and then harvested at 30 minutes, 1, 2, 4, and 8 hours intervals (13). The effects of SB431542 (10 μ M for 30 minutes) (18) and AG1474 (10 μ M for 30 minutes) (24) inhibitors on protein expression of PAI-1 were tested by pretreating the cells with them prior to adding ET-1 (100 nM) to the culture medium. The neomycin (100 μ M for 1 hours) (26) and Y27632 (10 μ M for 30 minutes) (13) inhibitors were tested on protein expression of PAI-1 via preincubation of the cells prior to addition of ET-1 (100 nM) to the culture medium. The cells were harvested after 4 hours.

Western blot

Proteins were determined using the method of Seif et al. (4). Briefly, harvested cells were lysed in RIPA buffer. Then, the proteins were separated on 10% SDS-PAGE and transferred to a membrane (PVDF). After blocking steps, the membranes were incubated with primary antibodies. The membranes were washed and then exposed with a secondary anti-rabbit IgG antibody conjugated to horseradish peroxidase. The labeled antibodies were detected with chemiluminescence exposure.

Statistical analysis

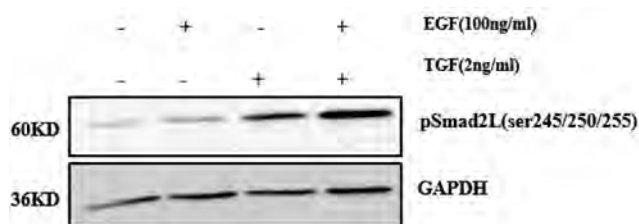
The results are presented as mean \pm SEM of three individual experiments. Statistical significance was estimated by one-way ANOVA, followed by the least significant difference post-hoc analysis (LSD). $P < 0.05$ or $P < 0.01$ considered as statistically significant. Fold change was calculated by dividing all the measured values from the intensity of each area by their controls (for both target and internal control). The areas were obtained using Image J software program. Then, the values of target groups were divided by the values of their control. Graph Pad Prism software program was used for drawing the graphs.

Results

TGF and EGF induced Smad2L phosphorylation in BAEC

To investigate the role of TGF β and EGF in phosphorylation of Smad2L (ser245/250/255), BAECs were incubated with TGF β (2 ng/ml) and EGF (100 ng/ml) for 1 hour and 5 minutes, respectively, once alone and once in combination with each other. TGF β ($P < 0.05$) and EGF ($P < 0.05$) stimulated Smad2L phosphorylation, and the effects of combination of TGF and EGF could be additive to Smad2L phosphorylation ($P < 0.01$, Fig.1). This data demonstrates that both EGF and TGF β are individually involved in the phosphorylation of Smad2L through two distinct pathways.

A



B

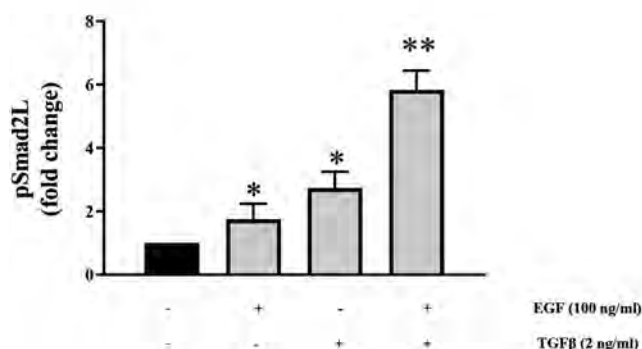


Fig.1: TGF β and EGF lead to phosphorylation of Smad2L. BAECs were incubated with TGF β (2 ng/ml) and EGF (100 ng/ml) for 1 hour and 5 minutes, respectively. Values are presented as mean \pm SEM of three individual experiments. TGF β ; Transforming growth factor beta, EGF; Epidermal growth factor, *, $P < 0.05$, and **, $P < 0.01$ vs. untreated.

ET-1 stimulated Smad2L phosphorylation in BAECs

The effects of ET-1 on phosphorylation of Smad2L (ser245/250/255) were investigated in different times. BAECs were exposed to ET-1 (100 nM) and phosphorylation of Smad2L measured in a period of 5 minutes to 8 hours. ET-1 induced the phosphorylation of Smad2L (ser245/250/255) ($P < 0.01$, Fig.2). This result showed that ET-1 strongly stimulates Smad2L phosphorylation in BAEC.

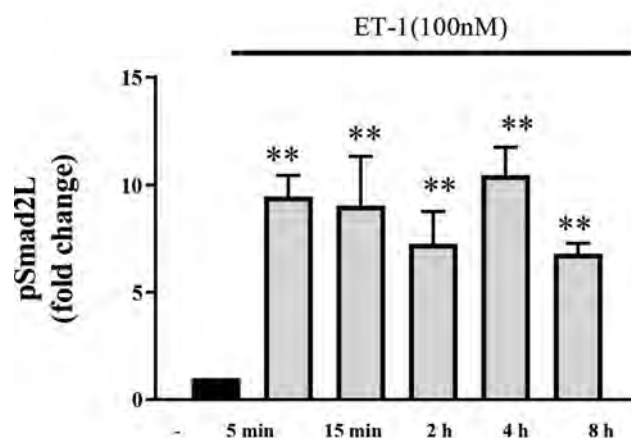
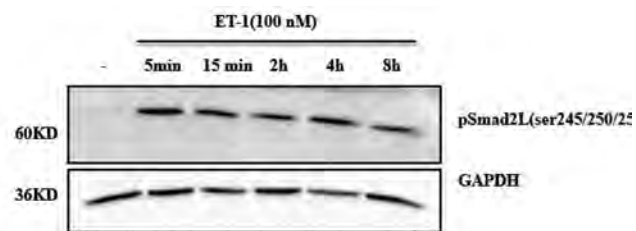


Fig.2: ET-1 stimulates the phosphorylation of Smad2L. BAECs were incubated with ET-1 (100 nM) for periods of 5 minutes up to 8 hours. Values are presented as mean \pm SEM of three individual experiments. ET-1; Endothelin-1, **, $P < 0.01$ vs. untreated, min; Minutes, and h; Hours.

ET-1 mediated dual transactivation of EGFR and TGF β in BAECs

The question here is that whether there is evidence that the transactivation signaling pathways induced by GPCR are directly involved in phosphorylation of Smad2L? In order to evaluate the role of ET-1 in TGF β transactivation, the phosphorylation of Smad2C (Ser465/467) was investigated as the instant downstream mediator of TGF β activation. BAECs were treated with ET-1 (100 nM) in a period of 1-4 hours. ET-1 led to time-dependent increase in Smad2C phosphorylation at hours two ($P < 0.05$) and four ($P < 0.01$, Fig.3A). These results demonstrated that by induction of TGF β transactivation, ET-1 can stimulate Smad2C phosphorylation in BAEC in a time-dependent manner. Moreover, to examine the role of ET-1 in EGFR transactivation, the phosphorylation of ERK1/2 was investigated as the instant downstream mediator of EGFR. BAECs were incubated with ET-1 (100 nM) in certain intervals in a period from 5 minutes to 8 hours. ET-1 stimulated ERK1/2 phosphorylation in different points in time between 5 minutes and 1 hours ($P < 0.01$) and between 2 and 8 hours ($P < 0.05$, Fig.3B). These results suggest that by transactivation of EGFR, ET-1 can lead to phosphorylation of ERK1/2 in BAEC.

ET-1 stimulates Smad2L phosphorylation through dual transactivation of TGF β and EGFR, as well as ROCK activity in BAECs

Subsequently, to explore the role of ET-1 induced transactivation pathways in phosphorylation of Smad2L, cells were evaluated in the presence of EGFR antagonist, AG1478 (10 μ M) and TGF β antagonist, SB431542 (10 μ M)

for 30 minutes prior to treatment with ET-1 (100 nM) for 4 hours. Phosphorylation of Smad2L (ser245/250/255) was markedly alleviated in the presence of AG1478 and SB431542 ($P < 0.05$, Fig.4A). The results of this experiment indicate that ET-1 can induce the phosphorylation of Smad2L via transactivation of EGFR and TGFR. Furthermore, the roles of ROCK and PLC were examined in ET-1-induced phosphorylation of Smad2L (ser245/250/255). Neomycin (100 μ M), the specific inhibitor of PLC β , was used as the

downstream mediator of G α_q for 1 hours prior to treatment with ET-1 (100 nM) for 4 hours, and Y27632 (10 μ M), a potent inhibitor of ROCK was used as the downstream mediator of G12/13 for 30 minutes prior to treatment with ET-1 (100 nM) for 4 hours. The results of this work showed that Y27632 can reduce Smad2L phosphorylation ($P < 0.05$), but neomycin cannot do the same (Fig.4B). This shows that stimulation of Smad2L phosphorylation by ET-1 is dependent on ROCK activity.

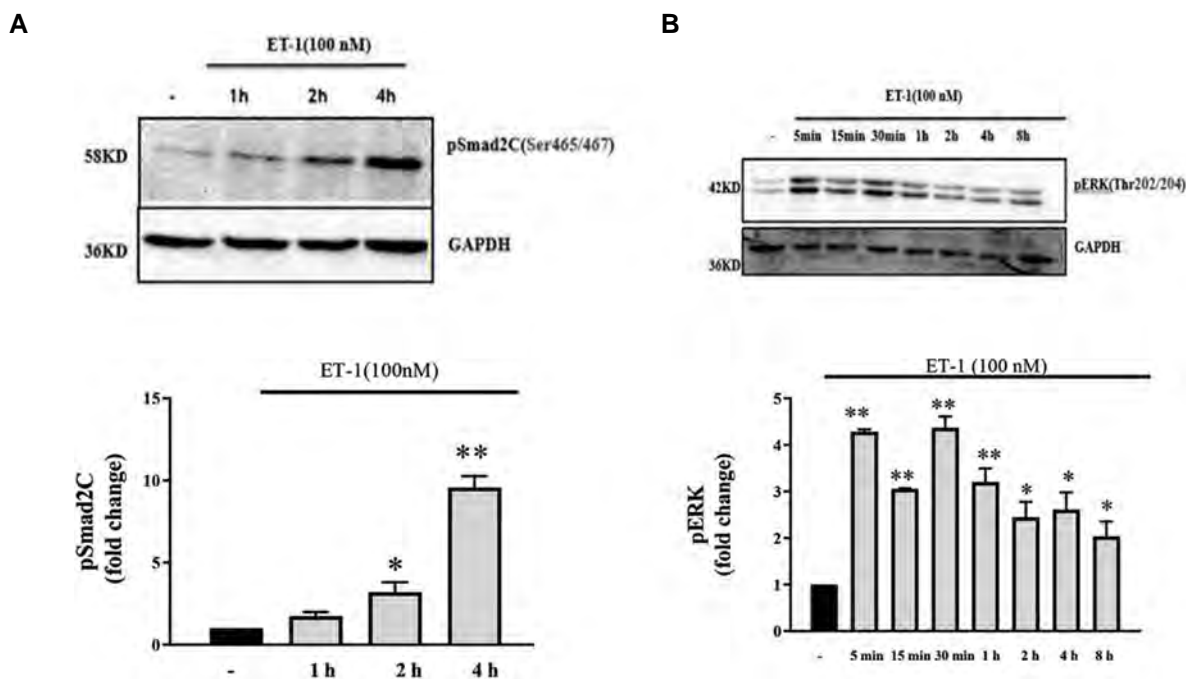


Fig.3: ET-1 leads to phosphorylation of Smad2C and ERK1/2. BAECs were incubated with ET-1 (100 nM). ET-1; Endothelin-1, *; $P < 0.05$, **; $P < 0.01$ vs. untreated, min; Minutes, and h; Hours. Values are presented as mean \pm SEM of three individual experiments.

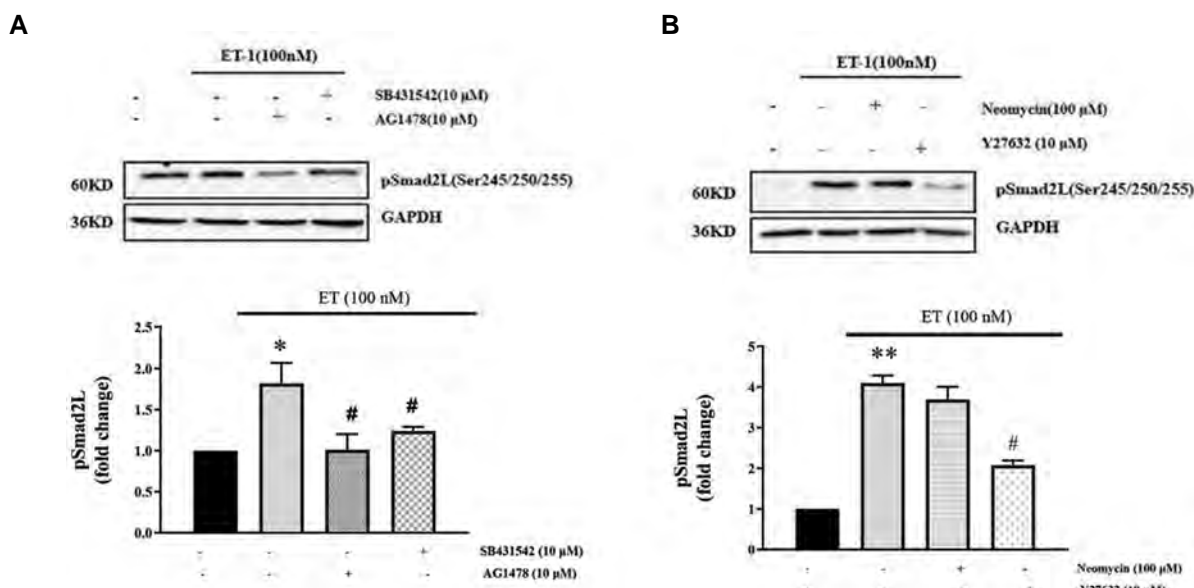


Fig.4: ET-1 leads to phosphorylation of Smad2L via both dual transactivation and the ROCK activity. **A.** BAECs were preincubated with SB431542 (10 μ M) for 30 minutes and AG1478 (10 μ M) for 5 minutes before stimulation with ET-1 (100 nM) for 4 hours. **B.** BAECs were preincubated with neomycin for 1 hours (100 μ M) and with Y27632 (10 μ M) for 30 minutes before stimulation with ET-1 (100 nM) for 4 hours. ET-1; Endothelin-1, *; $P < 0.05$ vs. untreated, #; $P < 0.05$ vs. ET-1 treated. Values are presented as mean \pm SEM of three individual experiments.

ET-1 stimulated the protein expression of PAI-1 in BAEC

The effects of ET-1 were examined on the protein expression of PAI-1. BAECs were exposed to ET-1 (100 nM) at certain points in time from 30 minutes to 8 hours. ET-1 induced the protein expression of PAI-1 at hours one and two ($P<0.05$) and four ($P<0.01$, Fig.5). Overall, the results showed that ET-1 increases the protein expression of PAI-1 in BAEC. we chose four hours' incubation time with ET-1 for the next experiments.

ET-1 stimulates the protein expression of PAI-1 in BAECs through dual transactivation of TGFR and EGFR, as well as the ROCK activity

To assess whether ET-1 leads to an increase in protein expression of PAI-1 via its receptor with induction of dual transactivation, AG1478 (10 μ M) and SB431542 (10 μ M) as EGFR and TGFR inhibitors, respectively, and Bosentan (10 μ M) as ET receptor inhibitor were

utilized for 30 minutes prior to treatment with ET-1(100 nM) for 4 hours. The results showed that ET-1-increased protein expression of PAI-1 was reduced in the presence of AG1478 ($P<0.05$), SB431542 ($P<0.05$), and Bosentan ($P<0.05$, Fig.6A). The present work's data showed that via its receptor, ET-1 can transactivate EGFR and TGFR in order to stimulate the protein expression of PAI-1. Moreover, in order to study the roles of ROCK and PLC as mediators of the transactivation pathway in protein expression of PAI-1, neomycin (100 μ M) for 1 hours and Y27632 (10 μ M) for 30 minutes as inhibitors of PLC β and ROCK were used before being stimulated with ET-1 (100 nM) for 4 hours. The results showed the significant reduction of the protein expression of PAI-1 in the presence of Y27632 ($P<0.05$), while neomycin could not inhibit the protein expression of PAI-1 (Fig.6B). From this data, it was concluded that ET-1 increased the protein expression of PAI-1, which was dependent on ROCK activity.

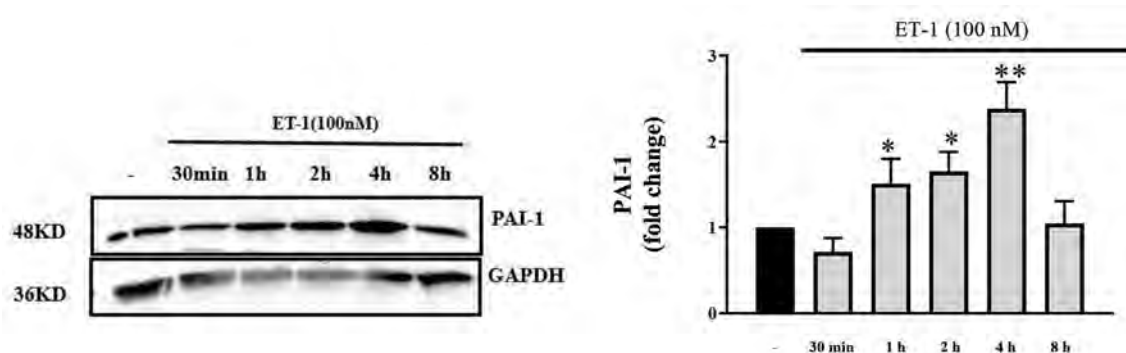


Fig.5: ET-1 leads to an increase in the protein level of PAI-1. BAECs were incubated with ET-1 (100 nM) for 30 minutes to 8 hours. Values are presented as mean \pm SEM of three individual experiments. ET-1; Endothelin-1, *; $P<0.05$, **; $P<0.01$ vs. untreated, min; Minutes, and h; Hours.

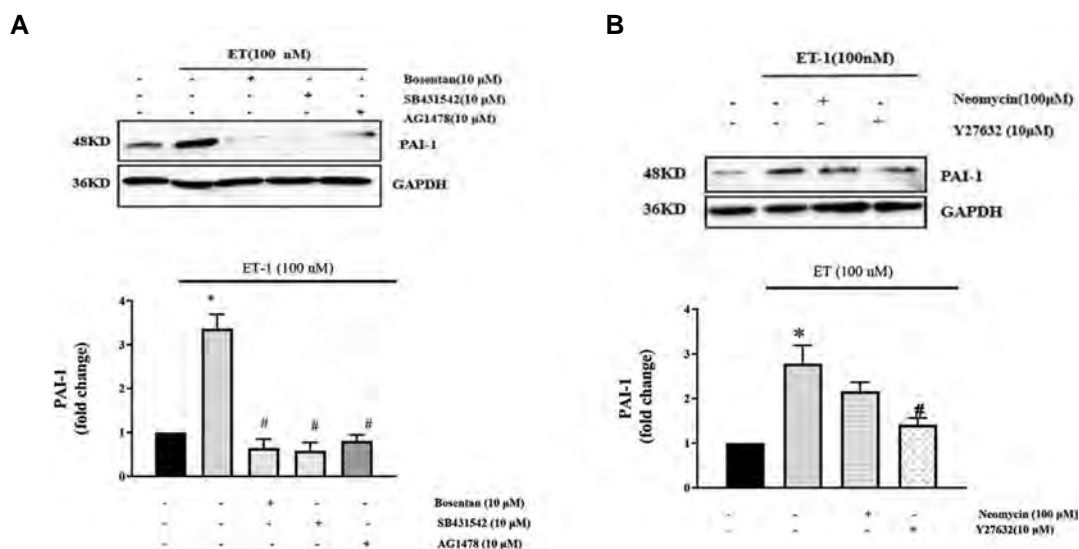


Fig.6: ET-1 leads to an increase in the protein level of PAI-1 via induction of dual transactivation pathways, as well as the ROCK activity. **A.** BAECs were preincubated with SB431542 (10 μ M), AG1478 (10 μ M), and Bosentan (10 μ M) 30 minutes before being stimulated with ET-1 (100 nM) for 4 hours. **B.** BAECs were preincubated with neomycin (100 μ M) for 1 hours and Y27632 (10 μ M) for 30 minutes before stimulation with ET-1 (100 nM) for 4hours. ET-1; Endothelin-1, *; $P<0.05$ vs. untreated, #; $P<0.05$ vs. ET-1 treated. Values are presented as mean \pm SEM of three individual experiments.

Discussion

In this study, the role of ET-1-induced dual transactivation pathways of EGFR and TGF β R were investigated in phosphorylation of Smad2L, as well as the protein expression of PAI-1. Here, it was demonstrated that ET-1 stimulates Smad2L phosphorylation and increases the level of PAI-1 protein through transactivation of EGFR and TGF β R, and that ROCK has a central role in this pathway. TGF- β 1, alone and in combination with EGF, induced the phosphorylation of Smad2L, which is consistent with the data put out by Kamato et al. (10). Phosphorylation of Smad2L was increased by EGF and TGF- β , indicating the presence of the active pathways of these growth factors in induction of Smad2L phosphorylation. Recent studies have shown that in addition to EGF and TGF- β , GPCR agonists result in activation of kinases such as NOX, P38, and ERK through induction of TGF β R and EGFR transactivation (27). Our results showed that ET-1 increased the phosphorylation of Smad2L in BAECs. Kamato et al. (10) presented the evidence that thrombin leads to phosphorylation of Smad2L in VSMCs via transactivation-dependent signaling pathways. In this study, the focus was on the signaling pathways causing the phosphorylation of Smad2L. It was demonstrated that ET-1 stimulated the phosphorylation of Smad2C via TGF β R transactivation, as well as ERK1/2 via EGFR transactivation, in BAEC. In a study recently published by the authors, it has been shown that ET-1 stimulates the phosphorylation of Smad2C via TGF β R transactivation in BAEC (13). Burch et al. (28) showed that via PAR-1, thrombin can not only lead to EGFR transactivation, but also TGF β R transactivation in VSMCs.

It was found that AG1478 (EGFR antagonist) and SB431542 (TGF β R antagonist) reduced the effect of ET-1 on phosphorylation of Smad2L, suggesting that ET-1 mediated the phosphorylation of Smad2L through dual transactivation of EGFR and TGF β R. Kamato et al. (24) demonstrated that thrombin stimulated the phosphorylation of Smad2L through transactivation of both EGFR and TGF β R in VSMC. GPCRs are the biggest cell-surface receptors without any enzymatic activity. These receptors associate with G proteins including G α , G β , and G γ . Activated G proteins interact with diverse mediators and can regulate signaling responses (8). Signaling pathways that are activated by G proteins are comprised of the following: phospholipase C β , adenylate cyclase (AC), and cyclic adenosine monophosphate (cAMP) pathways, as well as Rho kinase (ROCK) (29).

There have been several studies on the roles of these mediators in transactivation pathways. EGFR transactivation is stimulated by Ang II via increasing intracellular Ca²⁺ and activation of PLC/IP3 pathway (30). On the other hand, another study concluded that EGFR transactivation was induced by Ang II, independent of intracellular calcium concentration and PLC/IP3 pathway (31). ROCK signaling leads to transactivation of RSTK in the epithelial cells of mouse lung (32). Therefore, in this study the roles of ROCK and PLC

were assessed in Smad2L phosphorylation. It was found that Y27632 (ROCK antagonist) decreased the phosphorylation of Smad2L that was induced by ET-1, but neomycin (PLC antagonist) had no effect on Smad2L phosphorylation. According to the previous studies, ROCK leads to phosphorylation of Smad2C through TGF β R transactivation (13, 28, 33). Therefore, based on the results of this study, it is suggested that ROCK has an important role in ET-1 transactivation pathways and subsequently Smad2L phosphorylation. This result is consistent with earlier studies, showing that thrombin stimulated the phosphorylation of Smad2L which is dependent on MMP and ROCK activities in VSMCs (23). Wang et al. (34) showed that PAI-1 is a remarkable prognosticator of cardiovascular disease -dependent death. PAI-1 is a significant factor in the pathophysiology of vascular sclerosis. PAI-1 is mostly expressed by endothelial cells as well as tissues with elevated TGF- β 1 (35). Multiple studies have confirmed that TGF- β 1-induced PAI-1 expression occurs via stimulation of EGFR transactivation in vascular, epithelial, and endothelial cells (35, 36). The current study demonstrated that ET-1 increased the level of PAI-1 expression in BAECs in four hours after treatment with ET-1; however, this response was decreased eight hours after the treatment. Therefore, it is possible that deactivation of ET-1 occurred in eight hours. The same pattern can be seen in Smad2L phosphorylation, thus verifying that these pathways are related together. Cell lines alter in morphology, response to stimuli, growth rates, gene and protein expression in different passage numbers (37). The changes observed in the protein expression particularly in the control group in various experiments, may be influenced by different passage numbers, which can be considered as a limitation of this study. In addition, Cockell et al. (38) showed that thrombin induces antigen, natural activity, and mRNA expression of PAI-1 in baboon aortic smooth muscle cells (BASMC). Kerins et al. (39) indicated that Ang IV can stimulate the endothelial expression of PAI-1 via induction of an endothelial receptor.

The protein expression of PAI-1 that is stimulated by ET-1 is decreased in the presence of SB431542 and AG1478. It is suggested that induction of PAI-1 by ET-1 is intervened by transactivation of EGFR and TGF β R. Chaplin et al. (33) reported that thrombin transactivated EGFR and TGF β R, which can phosphorylate Smad2L and ERK1/2, increase the gene expression of CHSY1 enzymes in VSMCs. The ET-1-stimulated protein expression of PAI-1 was blocked in the presence of ET receptor antagonist (bosentan), strongly suggesting that this response is mediated via the ET-1 receptor. This study has been the first attempt to scrutinize the significant role of ROCK in protein expression of PAI-1 in BAECs. To examine the importance of ROCK and PLC as mediators of activated G proteins, the level of PAI-1 protein was investigated in the presence of Y27632 (ROCK antagonist) and neomycin (PLC antagonist). In a previous study by the authors, it was shown that ET-1 receptor can transactivate the TGF β R and then phosphorylate Smad2C.

It was demonstrated that Rho/ROCK kinase plays an important role in mediating the transactivation of TGFR and phosphorylation of Smad2C (Ser465/467) induced by ET-1 (13). Moreover, in another study by the authors that has not yet been published, the role of Rho/ROCK kinase is investigated in ET-1-induced EGFR transactivation. In the current study, a decrease in PAI-1 protein expression was observed in the presence of Y27632 (ROCK antagonist) that could inhibit Smad2L phosphorylation. Based on the results obtained from this study, Rho/ROCK kinase (as a mediator of the transactivation pathway) has a role in Smad2L phosphorylation and PAI-1 protein expression.

In this study, it was shown that ROCK is involved in PAI-1 protein expression for the first time. Observations of the current work strongly suggest that ROCK induced Smad2L phosphorylation via transactivation and affected the enhancement of PAI-1 protein expression. TGF- β 1 increases the PAI-1 expression in aortic endothelial cells via P38 and CDK activations, resulting in phosphorylation of Smad2L (16). Similarly, Talati et al. (40) described that thrombin induced the phosphorylation of the linker region of Smad2 and the increase of the mRNA expression of PAI-1 via transactivation of EGFR in keratinocytes. The results showed that EGFR and TGFR transactivation pathways that are induced by ET-1 are in fact independent pathways. Whereas, Smad2L phosphorylation is the common pathway between dual transactivation pathways. Therefore, this study suggests that Smad2L can be considered as a therapeutic target. However, further studies are required in order to identify GPCRs signaling more comprehensively.

Conclusion

The current study demonstrated that ET-1 stimulated the phosphorylation of Smad2L, and this reaction was blocked by AG1478 and SB431542, suggesting that ET-1 leads to Smad2L phosphorylation via induction of dual transactivation of EGFR and TGFR. According to the results of previous studies, ROCK has a key role in inducing transactivation pathways. Hence, induction of Smad2L phosphorylation through dual transactivation of EGFR and TGFR is dependent on ROCK signaling. Furthermore, it was demonstrated that ET-1 increased the level of PAI-1 protein via transactivation of EGFR and TGFR, which is associated with promoting the intravascular thrombosis and atherosclerosis. Moreover, this cellular response is also dependent on ROCK signaling. Therefore, it can be concluded that Smad2L phosphorylation and promotion of PAI-1 protein level may be related together. However, further studies are needed to identify this signalling.

Acknowledgements

This study was financially supported by Ahvaz Jundishapur University of Medical Sciences (Grant No.: HLRC-9605). The authors declare that there are no conflicts of interest related to the subject matter or materials discussed in this manuscript.

Authors' Contributions

F.S.; Performed all *in vitro* experiments, analyzed the data, and wrote the manuscript. H.B.-R., A.Kh.; Contributed to concept and design, financial support, and final approval of the manuscript. All the authors read and approved the final manuscript.

References

- Babaahmadi-Rezaei H, Kheirollah A, Rashidi M, Seif F, Niknam Z, Zamanpour M. EGF receptor transactivation by endothelin-1 increased CHSY-1 mediated by NADPH oxidase and phosphorylation of ERK1/2. *Cell J*. 2021; 23(5): 510-515.
- Donato AJ, Gano LB, Eskurza I, Silver AE, Gates PE, Jablonski K, et al. Vascular endothelial dysfunction with aging: endothelin-1 and endothelial nitric oxide synthase. *Am J Physiol Heart Circ Physiol*. 2009; 297(1): H425-H432.
- Li MW, Mian MOR, Barhoumi T, Rehman A, Mann K, Paradis P, et al. Endothelin-1 overexpression exacerbates atherosclerosis and induces aortic aneurysms in apolipoprotein E knockout mice. *Arterioscler Thromb Vasc Biol*. 2013; 33(10): 2306-2315.
- Seif F, Kheirollah A, Babaahmadi-Rezaei H. Efficient isolation and identification of primary endothelial cells from bovine aorta by collagenase P. *Immunopathol Persa*. 2020; 6(2): e15.
- Zhang C, Wang X, Zhang H, Yao C, Pan H, Guo Y, et al. Therapeutic monoclonal antibody antagonizing endothelin receptor A for Pulmonary arterial hypertension. *J Pharmacol Exp Ther*. 2019; 370(1): 54-61.
- Bassilana F, Nash M, Ludwig MG. Adhesion G protein-coupled receptors: opportunities for drug discovery. *Nat Rev Drug Discov*. 2019; 18(11): 869-884.
- Burch ML, Ballinger ML, Yang SNY, Getachew R, Itman C, Loveland K, et al. Thrombin stimulation of proteoglycan synthesis in vascular smooth muscle is mediated by protease-activated receptor-1 transactivation of the transforming growth factor beta type I receptor. *J Biol Chem*. 2010; 285(35): 26798-26805.
- Duc NM, Kim HR, Chung KY. Recent progress in understanding the conformational mechanism of heterotrimeric G protein activation. *Biomol Ther (Seoul)*. 2017; 25(1): 4-11.
- Kamoto D, Thach L, Bernard R, Chan V, Zheng W, Kaur H, et al. Structure, function, pharmacology, and therapeutic potential of the G protein, G α_q ,11. *Front Cardiovasc Med*. 2015; 2: 14.
- Kamoto D, Thach L, Getachew R, Burch M, Hollenberg MD, Zheng W, et al. Protease activated receptor-1 mediated dual kinase receptor transactivation stimulates the expression of glycosaminoglycan synthesizing genes. *Cell Signal*. 2016; 28(1): 110-119.
- Little PJ, Burch ML, Getachew R, Al-aryahi S, Osman N. Endothelin-1 stimulation of proteoglycan synthesis in vascular smooth muscle is mediated by endothelin receptor transactivation of the transforming growth factor- β type I receptor. *J Cardiovasc Pharmacol*. 2010; 56(4): 360-368.
- Sharifat N, Mohammad Zadeh G, Ghaffari MA, Dayati P, Kamato D, Little PJ, et al. Endothelin-1 (ET-1) stimulates carboxy terminal Smad2 phosphorylation in vascular endothelial cells by a mechanism dependent on ET receptors and de novo protein synthesis. *J Pharm Pharmacol*. 2017; 69(1): 66-72.
- Seif F, Little PJ, Niayesh-Mehr R, Zamanpour M, Babaahmadi-Rezaei H. Endothelin-1 increases CHSY-1 expression in aortic endothelial cells via transactivation of transforming growth factor β type I receptor induced by type B receptor endothelin-1. *J Pharm Pharmacol*. 2019; 71(6): 988-995.
- Rezaei HB, Kamato D, Ansari G, Osman N, Little PJ. Cell biology of Smad2/3 linker region phosphorylation in vascular smooth muscle. *Clin Exp Pharmacol Physiol*. 2012; 39(8): 661-667.
- Hough C, Radu M, Doré JJ. Tgf-beta induced Erk phosphorylation of smad linker region regulates smad signaling. *PLoS One*. 2012; 7(8): e42513.
- Kamoto D, Rostam MA, Piva TJ, Babaahmadi Rezaei H, Getachew R, Thach L, et al. Transforming growth factor β -mediated site-specific Smad linker region phosphorylation in vascular endothelial cells. *J Pharm Pharmacol*. 2014; 66(12): 1722-1733.
- Kamoto D, Burch ML, Piva TJ, Rezaei HB, Rostam MA, Xu S, et al. Transforming growth factor- β signalling: role and consequences of Smad linker region phosphorylation. *Cell Signal*. 2013; 25(10): 2017-2024.

18. Mehr RNM, Kheirollah A, Seif F, Dayati PM, Babaahmadi-Rezaei H. Reactive oxygen species and p38MAPK Have a role in the Smad2 linker region phosphorylation induced by TGF- β . *Iran J Med Sci*. 2018; 43(4): 401-408.
19. Rabieian R, Boshtam M, Zareei M, Kouhpayeh S, Masoudifar A, Mirzaei H. Plasminogen activator inhibitor type-1 as a regulator of fibrosis. *J Cell Biochem*. 2018; 119(1): 17-27.
20. Samarakoon R, Higgins SP, Higgins CE, Higgins PJ. The TGF- β 1/p53/PAI-1 signaling axis in vascular senescence: role of caveolin-1. *Biomolecules*. 2019; 9(8).
21. Cesari M, Pahor M, Incalzi RA. Plasminogen activator inhibitor-1 (PAI-1): a key factor linking fibrinolysis and age-related subclinical and clinical conditions. *Cardiovasc Ther*. 2010; 28(5): e72-e91.
22. Mkaouer H, Akermi N, Kriaa A, Abraham AL, Jablaoui A, Soussou S, et al. Serine protease inhibitors and human wellbeing interplay: new insights for old friends. *PeerJ*. 2019; 7: e7224.
23. Eitzman DT, Westrick RJ, Xu Z, Tyson J, Ginsburg D. Plasminogen activator inhibitor-1 deficiency protects against atherosclerosis progression in the mouse carotid artery. *Blood*. 2000; 96(13): 4212-4215.
24. Kamato D, Ta H, Afroz R, Xu S, Osman N, Little PJ. Mechanisms of PAR-1 mediated kinase receptor transactivation: Smad linker region phosphorylation. *Cell Commun Signal*. 2019; 13(4): 539-548.
25. Shah BH, Baukal AJ, Chen HD, Shah AB, Catt KJ. Mechanisms of endothelin-1-induced MAP kinase activation in adrenal glomerulosa cells. *J Steroid Biochem. Mol Biol*. 2006; 102(1-5): 79-88.
26. Hu GF. Neomycin inhibits angiogenin-induced angiogenesis. *Proc Natl Acad Sci USA*. 1998; 95(17): 9791-9795.
27. Schafer AE, Blaxall BC. G protein coupled receptor-mediated transactivation of extracellular proteases. *J Cardiovasc Pharmacol*. 2017; 70(1): 10.
28. Burch ML, Getachew R, Osman N, Febbraio MA, Little PJ. Thrombin-mediated proteoglycan synthesis utilizes both protein-tyrosine kinase and serine/threonine kinase receptor transactivation in vascular smooth muscle cells. *J Biol Chem*. 2013; 288(10): 7410-7419.
29. Kamato D, Burch ML, Osman N, Zheng W, Little PJ. Therapeutic implications of endothelin and thrombin G-protein-coupled receptor transactivation of tyrosine and serine/threonine kinase cell surface receptors. *J Pharm Pharmacol*. 2013; 65(4): 465-473.
30. Murasawa S, Mori Y, Nozawa Y, Gotoh N, Shibuya M, Masaki H, et al. Angiotensin II type 1 receptor-induced extracellular signal-regulated protein kinase activation is mediated by Ca²⁺/calmodulin-dependent transactivation of epidermal growth factor receptor. *Circ Res*. 1998; 82(12): 1338-1348.
31. Wang D, Yu X, Cohen RA, Brecher P. Distinct effects of N-acetylcysteine and nitric oxide on angiotensin II-induced epidermal growth factor receptor phosphorylation and intracellular Ca²⁺ levels. *J Biol Chem*. 2000; 275(16): 12223-12230.
32. Gieseler F, Ungefroren H, Settmacher U, Hollenberg MD, Kaufmann R. Proteinase-activated receptors (PARs)—focus on receptor-receptor-interactions and their physiological and pathophysiological impact. *Cell Commun Signal*. 2013; 11(1): 1-26.
33. Chaplin R, Thach L, Hollenberg MD, Cao Y, Little PJ, Kamato D. Insights into cellular signalling by G protein coupled receptor transactivation of cell surface protein kinase receptors. *Cell Commun Signal*. 2017; 11(2): 117-125.
34. Wang TJ, Gona P, Larson MG, Tofler GH, Levy D, Newton-Cheh C, et al. Multiple biomarkers for the prediction of first major cardiovascular events and death. *N Engl J Med*. 2006; 355(25): 2631-2639.
35. Samarakoon R, Higgins SP, Higgins CE, Higgins PJ. TGF- β 1-induced plasminogen activator inhibitor-1 expression in vascular smooth muscle cells requires pp60c-src/EGFR^{Y845} and Rho/ROCK signaling. *J Mol Cell Cardiol*. 2008; 44(3): 527-538.
36. Kutz SM, Higgins CE, Samarakoon R, Higgins SP, Allen RR, Qi L, et al. TGF- β 1-induced PAI-1 expression is E box/USF-dependent and requires EGFR signaling. *Exp Cell Res*. 2006; 312(7): 1093-1105.
37. Kwist K, Bridges W, Burg K. The effect of cell passage number on osteogenic and adipogenic characteristics of D1 cells. *Cytotechnology*. 2016; 68(4): 1661-1667.
38. Cockell KA, Ren S, Sun J, Angel A, Shen GX. Effect of thrombin on release of plasminogen activator inhibitor-1 from cultured primate arterial smooth muscle cells. *Thromb Res*. 1995; 77(2): 119-131.
39. Kerins DM, Hao Q, Vaughan DE. Angiotensin induction of PAI-1 expression in endothelial cells is mediated by the hexapeptide angiotensin IV. *J Clin Invest*. 1995; 96(5): 2515-2520.
40. Talati N, Kamato D, Piva TJ, Little PJ, Osman N. Thrombin promotes PAI-1 expression and migration in keratinocytes via ERK dependent Smad linker region phosphorylation. *Cell Signal*. 2018; 47: 37-43.

MiRNA-16-1 Suppresses Mcl-1 and Bcl-2 and Sensitizes Chronic Lymphocytic Leukemia Cells to BH3 Mimetic ABT-199

Nooshin Ashofteh, M.Sc.¹, Amir Sayed Ali Mehdod, Ph.D.², Mohammad Bayat, Ph.D.³, Hadi Karami, Ph.D.^{1*}

1. Department of Molecular Medicine and Biotechnology, Faculty of Medicine, Arak University of Medical Sciences, Arak, Iran

2. Department of Parasitology and Mycology, School of Medicine, AJA University of Medical Sciences, Tehran, Iran

3. Department of Anatomy, Faculty of Medicine, Arak University of Medical Sciences, Arak, Iran

*Corresponding Address: P.O.Box: 3848176941, Department of Molecular Medicine and Biotechnology, Faculty of Medicine, Arak University of Medical Sciences, Arak, Iran
Email: h.karami@arakmu.ac.ir

Received: 05/June/2021, Accepted: 19/October/2021

Abstract

Objective: Chronic lymphoid leukemia (CLL) is the most common type of leukemia among adults. Increased levels of Mcl-1 and Bcl-xL is linked to resistance to Bcl-2 inhibitors including ABT-199. In this study, we investigated the effect of *miRNA-16-1* on apoptosis and sensitivity of the CLL cells to ABT-199.

Materials and Methods: In this experimental study, the Mcl-1 and Bcl-2 expression were measured using qualitative reverse transcription-polymerase chain reaction (qRT-PCR) and western blotting. The effect of treatments on cell survival and growth were explored with MTT assay and Trypan blue assay, respectively. The drug interaction was evaluated using combination index analysis. Apoptosis was assessed by ELISA cell death and caspase-3 activity assays.

Results: *MiRNA-16-1* markedly inhibited the expression of Mcl-1 and Bcl-2 in a time dependent manner ($P < 0.05$, relative to blank control). Pretreatment with *miRNA-16-1* synergistically suppressed the cell growth and survival and reduced the half-maximal inhibitory concentration (IC_{50}) value of ABT-199. Moreover, *miRNA-16-1* markedly augmented the apoptotic effect of ABT-199 in CLL cells ($P < 0.05$).

Conclusion: Our findings propose that *miRNA-16-1* act in concert with ABT-199 to exert synergistic anticancer efficacy against CLL, which is attributed to the inhibition of Bcl-2 and Mcl-1. This may propose a promising strategy for CLL resistant patients.

Keywords: ABT-199, Bcl-2, Chronic Lymphocytic Leukemia, Mcl-1

Cell Journal (Yakhteh), Vol 24, No 8, August 2022, Pages: 473-480

Citation: Ashofteh N, Sayed Ali Mehdod A, Bayat M, Karami H. MiRNA-16-1 suppresses Mcl-1 and Bcl-2 and sensitizes chronic lymphocytic leukemia cells to BH3 mimetic ABT-199. Cell J. 2022; 24(8): 473-480. doi: 10.22074/cellj.2022.8101.

This open-access article has been published under the terms of the Creative Commons Attribution Non-Commercial 3.0 (CC BY-NC 3.0).

Introduction

Chronic lymphoid leukemia (CLL) is the most common type of leukemia among adults with a median age of diagnosis 72 years (1, 2). Despite recent advances in treatments over single-agent chemotherapy such as fludarabine or chemo-immunotherapy combinations, CLL remains an incurable disease (2). A variety of parameters such as deregulated production of survival signals or intrinsic defects in apoptotic machinery contribute to the therapy resistance in CLL patients (3-5). As a result, there remains a need for understanding the detailed molecular pathophysiology of CLL as well as the development of new drugs for clinical treatment of CLL (6).

Apoptosis is induced by the two extrinsic and intrinsic pathways. The intrinsic pathway cell death is controlled by the Bcl-2 family proteins members, including the proapoptotic and the antiapoptotic proteins (5, 7). Over-expression of some antiapoptotic proteins such as Mcl-1 and Bcl-2 is correlated with shorter overall survival and chemoresistance in CLL patients. Accordingly, many targeted strategies have been developed to the Bcl-2 and Mcl-1 to overcome drug-resistance of CLL patients (8, 9).

The Bcl-2-specific antagonist ABT-199 or venetoclax has showed improved clinical efficacy in patients with

CLL (10, 11). ABT-199 is demonstrated high cytotoxicity against CLL cells *in vitro* but is much less effective against CLL cells that have expressed high levels of Mcl-1. Therefore, combination therapy of CLL cell with Mcl-1 inhibitors and ABT-199 have been suggested for improvement of apoptosis-based therapies in CLL resistance cells (12-14).

MicroRNAs (miRNAs) are a small family of endogenous, single-stranded, non-coding RNAs with 20-22 nucleotides in length that are involved in numerous cellular processes such as cell survival, cell death, differentiation and proliferation. They act by directly binding to the specific target mRNA, causing inhibition of the gene expression (15, 16). Several studies have demonstrated that miRNAs are recognized as important diagnostic and therapeutic biomarkers in numerous types of cancers, such as colon and breast cancer (17, 18). Furthermore, miRNAs are involved in almost all hematological processes, suggesting the important role of miRNAs in CLL (19-21). Genetic abnormalities have been observed in the majority of CLL cases. These aberrations include the 11q deletion with intermediate risk, the 13q deletion with low risk, and the 17p deletion with high risk (22). The 13q14 deletion is the most common genetic aberrations observed in more than

50% of CLL cases. The results of previous studies have clarified that the *miRNA-16-1* gene was absent or down-regulated in CLL cases with 13q14 deletion. *MiRNA-16-1* is a tumor suppressor gene that involved in the regulation of cell proliferation and cell death via targeting of several molecules (cyclin-dependent kinase 6, cyclin D1, cyclin D3, and Bcl-2) (23). In addition, the results of experimental studies show that there is a significant relationship between *miRNA-16-1* and Mcl-1 expression levels in samples of CLL patient (19, 24). However, the exact role of miRNA-16-1 in pathogenesis and drug resistance of CLL has not been fully investigated.

We hypothesized that reducing the expression of the *miRNA-16-1* gene could lead to increased expression of Bcl-2 and Mcl-1, and subsequently resistance to the ABT-199 in CLL cells. Therefore, we investigated the combination effect of *miRNA-16-1* and ABT-199 on survival and apoptosis of the CLL cells.

Materials and Methods

Cell culture conditions

The CLL-CII leukemia cells (Pasteur Institute, Iran) were cultured in RPMI-1640 medium (Sigma-Aldrich, St. Louis, MO, USA) containing 10% (vol/vol) heat-inactivated fetal bovine serum (FBS, Sigma Aldrich, USA), streptomycin (100 mg/ml), penicillin (100 U/ml), 1% (v/v) Glutamax (Sigma Aldrich, USA), and 1% sodium pyruvate at 37°C in 5% CO₂ (25). The cells were seeded in suspension at a concentration of 1×10⁵ cells/ml with the medium changed every two days.

This research was ethically wise approved from Deputy of Research and Technology, Arak University of Medical Sciences, Arak, Iran (IR.ARAKMU.REC.1395.185).

Transfection of miRNA

The *miRNA-16-1* mimics with the sense strand sequence 5'-UAG CAG CAC GUA AAU AUU GGC G-3' and the negative control (NC) miRNA sense strand sequence 5'-ACU ACU GAG UGA CAG UAG A-3' were 5'-ACU ACU GAG UGA CAG UAG A-3' bought from Dharmacon (Lafayette, CO, USA) and used in transient transfection of CLL-II cells. Cell transfection was executed with using Lipofectamine™2000 transfection reagent (Invitrogen, Carlsbad, CA, USA) and Opti-MEM I reduced serum medium (Invitrogen, USA) according to the manufacturer's recommendation. In brief, the cells were cultured at 40-50% confluence in culture medium without serum and antibiotics one day before transfection. To make the transfection complex, we diluted *miRNA-16-1* mimics or NC miRNA (50 nM) with Lipofectamine™2000 (4 µl/ml of transfection medium) in Opti-MEM I. The diluted solutions were thoroughly mixed and incubated for 15-20 minutes at room temperature. Next, the mixture was added to the culture medium. After 6 h of incubation, medium was replaced with a complete growth medium (10% FBS). At different time points after transfection, the

CLL-II cells were harvested and various experiments performed.

MTT assay

The cytotoxic effects of *miRNA-16-1* and ABT-199 (Sigma- Aldrich, USA) on CLL cells was evaluated using 3-(4, 5-Dimethylthiazol-2-yl)-2, 5-Diphenyltetrazolium Bromide (MTT) assay (25). The experiment was divided into eight groups: ABT-199, *miRNA-16-1* mimics, NC miRNA, *miRNA-16-1* mimics and ABT-199, NC miRNA and ABT-199, miRNA blank control, ABT-199 blank control and combination blank control. Briefly, the cells were cultivated in 96-well tissue plates at a density of 5×10⁴ cells per well, and then transfected with miRNAs. Six hours later, the cells were treated with different concentrations of ABT-199 (0, 0.05, 0.1, 0.2, 0.4, 0.8, 1.6 and 3.2 µM). After 24 and 48 hours of incubation, the cytotoxicity was determined using a MTT assay kit (Roche Diagnostics GmbH, Mannheim, Germany) according to the manufacturer's instructions. The absorbance (A) was measured spectrophotometrically at 570 nm with a microplate reader (Awareness Technology, Palm City, FL, USA). Half-maximal inhibitory concentration (IC₅₀) (drug concentration that reduced 50% survival rate) value of the ABT-199, alone or in combination with miRNA, was calculated with Prism 6.01 software (GraphPad Software Inc., San Diego, CA, USA). In the next experiments, the IC₅₀ doses of fludarabine were used.

Combination effect analysis

The combination index (CI) analysis was performed to explore the interaction between ABT-199 and *miRNA-16-1* (25-27). The results obtained from the MTT experiment were converted to Fraction affected (Fa, where Fa=0 is 100% cell survival and Fa=1 is 0% cell survival) and analyzed by CompuSyn 1.0 software from Combosyn (Paramus, NJ, USA). Additive, synergistic and antagonistic effects are indicated by CI=1, CI<1 and CI>1, respectively.

Quantitative real time polymerase chain reaction

After treatments, total RNA was extracted by using AccuZol™ reagent (Bioneer, Daedeokgu, Daejeon, Korea) according to the manufacturer's instructions. Then, reverse transcription of 1 µg of purified total RNA was performed by use of PrimeScript RT reagent kit (Promega, Madison, WI, USA), following the manufacturer's protocol. Relative gene expression was measured by qualitative reverse transcription-polymerase chain reaction (qRT-PCR) using SYBR Premix Ex Taq (Takara Bio, Otsu, Shiga, Japan) and the LightCycler 96 System (Roche Diagnostics GmbH). RT-PCR carried out in a final volume of 20 µl containing 1 µl of cDNA template, 10 µl of SYBR green reagent and 0.2 µM of each of the primers. The sequences of PCR primers were as follows:

β-actin-

F: 5'-TCC CTG GAG AAG AGC TAC G-3'
 R: 5'-GTA GTT TCG TGG ATG CCA CA-3'

Mcl-1-

F: 5'-TAA GGA CAA AAC GGG ACT GG-3'
 R: 5'-ACC AGC TCC TAC TCC AGC AA-3'

Bcl-2-

F: 5'-ATC GCC CTG TGG ATG ACT GAG T-3'
 R: 5'-GCC AGG AGA AAT CAA ACA GAG GC-3'

The protocol parameters were as follows: initial incubation at 95°C for 3 minutes followed by 40 cycles of denaturation at 95°C for 10 seconds and annealing and extension at 60°C for 50 seconds. The relative mRNA levels were determined using the comparative CT method, $2^{-\Delta\Delta Ct}$ (26, 27), and *β-actin* as an endogenous control.

Immunoblotting analysis

After treatments, the cells were washed with phosphate-buffered saline (PBS, Sigma-Aldrich, USA) and cell lysates prepared by disrupting cells in lysis buffer (1% NP-40, 0.1% sodium dodecyl-sulfate (SDS, Sigma-Aldrich, USA), 0.5% sodium deoxycholate, 1 mM ethylenediaminetetraacetic acid (EDTA, Sigma-Aldrich, USA), 50 mM Tris-HCl pH=7.4, 150 mM NaCl) containing protease inhibitor cocktail (Roche Diagnostics GmbH). Protein samples (fifty micrograms) were separated on 10% sodium dodecyl-sulfate polyacrylamide gel electrophoresis (SDS-PAGE, Sigma-Aldrich, USA) gels and transferred onto PVDF membrane (GE Healthcare, Amersham, Buckinghamshire, UK). Mouse primary monoclonal antibodies for Mcl-1 (Abcam, Cambridge, MA, UK), Bcl-2 (Abcam) and *β-actin* (Abcam) were used at 1:1000 dilutions. HRP-conjugated secondary antibodies (Abcam) were used at 1:4000 dilutions. The blot signals were detected using ECL plus western blotting detection Kit (GE Healthcare) and X-ray film (Estman Kodak, Rochester, NY, USA) and quantified via ImageJ 1.62 software (National Institutes' of Health, Bethesda, Maryland, USA).

Cell growth assay

The effect of *miRNA-16-1* and ABT-199 on tumor cell growth was assessed by the trypan blue staining. CLL-CII cells (1×10^5 cells/well) were treated with *miRNA-16-1* and ABT-199 in 6-well culture plates for 5 days as described previously. At the end of each day, the cells were collected and cell suspensions stained with 0.4% trypan blue dye (Merck KGaA, Darmstadt, Germany). After 2 minutes of incubation, the number of viable cells was measured using a hemocytometer and an inverted microscope (Nikon Instrument Inc., Melville, NY, USA). The percentage of cell viability in control group was considered as 100%.

Apoptosis ELISA assay

Cell death was determined with an ELISA apoptosis

kit (Roche Diagnostics GmbH) that determines mono- and oligonucleosomes released into the cytoplasm of apoptotic cells (25). The CLL-CII cells were cultivated at a density of 1×10^5 cells/well in 6-well culture plates and exposed to *miRNA-16-1* and ABT-199, as described previously. After 24-48 hours of incubation, the cells were lysed and ELISA assay was performed according to the manufacturer's instructions. Briefly, 20 μ l of the supernatants and 80 μ l of immunoreagent containing DNA-peroxidase and histone-biotin antibodies were added to each well of a streptavidin-coated plate and the plate was incubated for 2 hours at room temperature. After washing with incubation buffer, 100 μ l of ABTS solution was added. Finally, the reactions were stopped with ABTS stop solution and absorbance was quantified immediately by an ELISA reader (Awareness Technology, Palm City, FL, USA) at 405 nm. Data were calculated as the fold increase in the absorbance of test groups relative to the control group.

Caspase-3 activity assay

The *in vitro* induction of caspase-3 activity was determined using a colorimetric caspase assay Kit (Abnova, Taipei, Taiwan) (25). Briefly, the treated cells were resuspended in 50 μ l cooled lysis buffer and then centrifuged in 10,000 g for 1 minute. Then, 5 μ l of the 4 mM DEVD-pNA substrate and 50 μ l of 2X reaction buffer (containing 10 mM DTT) were added to each sample. After 2 hours incubation at 37°C the absorbance was quantified using a microplate plate reader (Awareness Technology, Palm City, FL, USA) at 405 nm.

Statistical analysis

All results in this study are demonstrated as mean \pm standard deviation (SD) of three experiments. ANOVA followed by Bonferroni's test was used to determine the significant differences between groups. A $P < 0.05$ was considered significant. All results were analyzed using Prism 6.01 software (GraphPad Software Inc., San Diego, CA, USA).

Results**MiRNA-16-1 inhibited the expression of Mcl-1 and Bcl-2 mRNA and protein in CLL-CII cells**

First, we explored the effect of *miRNA-16-1* on Mcl-1 and Bcl-2 levels in CLL-CII leukemic cells by qRT-PCR and western blotting. As shown in Figure 1A and 1B, transfection of *miRNA-16-1* markedly reduced both *Mcl-1* and *Bcl-2* mRNA levels in a time-dependent way ($P < 0.05$, relative to the blank control). At 24 and 48 hours after treatment with ABT-199, the relative Mcl-1 mRNA expression levels were significantly enhanced, while the expression levels of Bcl-2 mRNA did not change. In *miRNA-16-1* and ABT-199 combination group, the expression of Bcl-2 mRNA was similar to the cells transfected with only *miRNA-16-1*. In addition, the expression of Mcl-1 mRNA in the combination group was

higher and lower than the cells treated with only *miRNA-16-1* or ABT-199, respectively. However, NC miRNA had a negligible effect on mRNA expression compared to the blank control ($P>0.05$). The results of western blotting were in agreement with the PCR results (Fig.1C-F).

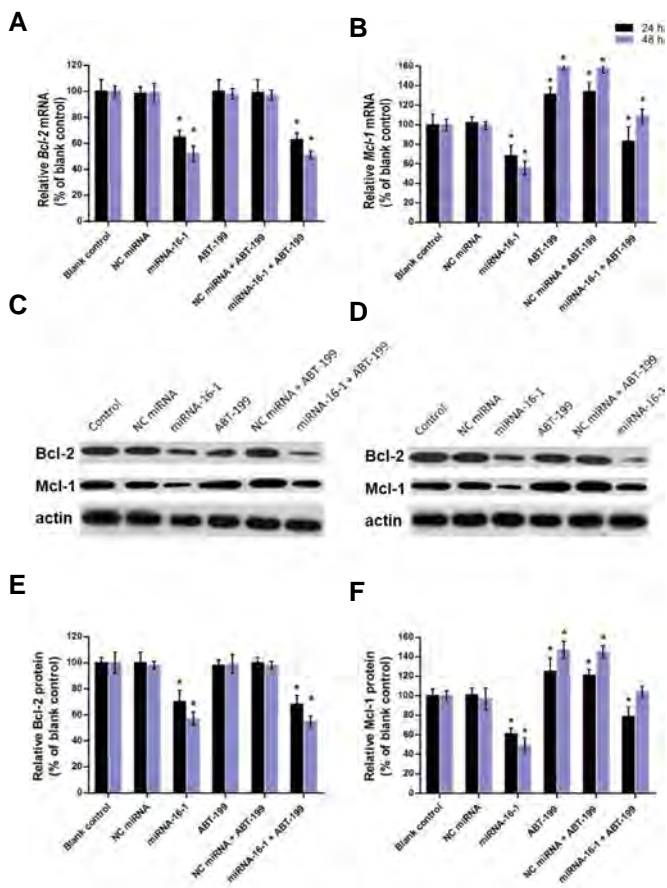


Fig.1: Bcl-2 and Mcl-1 expression analysis in CLL-CII cells treated with *miRNA-16-1* and ABT-199. The cells were treated with *miRNA-16-1*, ABT-199 and combination of them for 24 and 48 hours, and then relative **A.** *Bcl-2* and **B.** *Mcl-1* mRNA expression was measured using RT-qPCR. Representative western blots of Mcl-1, Bcl-2 and β -actin after **C.** 24 and **D.** 48 hours. The density of **E.** Bcl-2 and **F.** Mcl-1 protein bands was measured and normalized to the corresponding β -actin. The data are presented as mean \pm SD of the results of three experiments. *, $P<0.05$ versus corresponding blank control or NC miRNA transfected cells, RT-qPCR; Reverse transcription qualitative-polymerase chain reaction, and NC; Negative control.

MiRNA-16-1 increased ABT-199 sensitivity in CLL-CII leukemia cells

To explore whether suppression of Mcl-1 and Bcl-2 by *miRNA-16-1* could increase the sensitivity of leukemia cells to ABT-199, a combination study with *miRNA-16-1* and ABT-199 was done. The results of MTT assay showed that single treatment with ABT-199 reduced the cell survival in a dose-dependent way. Moreover, transfection of *miRNA-16-1* at 24 and 48 h markedly reduced the cell survival to 87.10% and 83.162% respectively, relative to the control (Fig.2, $P<0.05$). Combination treatment with *miRNA-16-1* and ABT-199 further reduced the survival rate of the CLL cells compared with *miRNA-16-1* or ABT-

199 monotreatment ($P<0.05$). Furthermore, in the presence of *miRNA-16-1*, the IC_{50} values of ABT-199 dramatically decreased from 0.37 μ M to 0.22 μ M and 0.24 μ M to 0.14 μ M after 24 and 48 hours, respectively (Table 1). Notably, NC miRNA had a minimal effect on survival and chemosensitivity of the cells ($P>0.05$, Fig2, Table 1).

Table 1: IC_{50} of ABT-199 in combination with miRNAs, in CLL cells

Treatment	IC_{50} (μ M)	
	24 hours	48 hours
ABT-199	0.37 \pm 1.33	0.24 \pm 1.30
NC miRNA and ABT-199	0.33 \pm 1.54 [#]	0.22 \pm 0.80 [#]
<i>miRNA-16-1</i> and ABT-199	0.22 \pm 2.41 [*]	0.14 \pm 1.53 [*]

IC_{50} of ABT-199 was calculated by GraphPad Prism 6.01 software and sigmoidal dose-response model. Data expressed as the mean \pm SD of three independent experiments. CLL; Chronic lymphoid leukemia, ^{*}; $P<0.05$ relative to the corresponding ABT-199, [#]; $P>0.05$ relative to the corresponding ABT-199, and IC_{50} ; Half-maximal inhibitory concentration.

MiRNA-16-1 synergistically enhanced the effect of ABT-199 on CLL-CII cells

To assess whether the combination of *miRNA-16-1* and ABT-199 on CLL-CII cells is synergistic, the combination analysis using the Chou-Talalay method was carried out. The results showed that the effects of *miRNA-16-1* (50 nM) and ABT-199 (0.05-3.2 μ M) were synergistic with the CI values of >1 in all concentrations of ABT-199 (Fig.2B, D). CI-Fa curved demonstrated that the most synergistic effects of 24 hours (CI=0.77) and 48 hours (CI=0.72) of treatment were seen at 0.4 and 0.2 μ M of ABT-199 with Fa values of 0.61 and 0.49, respectively (Table 2).

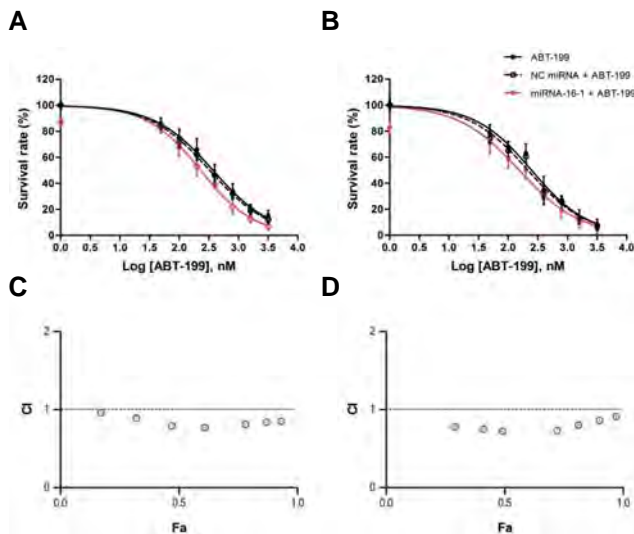


Fig.2: The effect of *miRNA-16-1* on ABT-199 sensitivity of the CLL-CII cells. The leukemia cells were exposed to *miRNA-16-1* (50 nM) and different concentrations of ABT-199 for **A,** **B.** 24 hours and **C,** **D.** 48 hours. Next, the cell survival rate was evaluated using MTT assay. Cell survival curves were plotted by GraphPad Prism software. The results are shown as mean \pm SD (n=3). Chou and Talalay method and CalcuSyn software were used to plot the CI vs. Fa. Dashed lines represent CI value equal to 1. CI; Combination index and Fa; Fraction affected.

Table 2: CI analysis of *miRNA-16-1* and ABT-199 in CLL cells

ABT-199 concentration (μM)	24 hours			48 hours		
	Fa	CI	Combined effect	Fa	CI	Combined effect
0.05	0.17	0.96	S	0.29	0.78	S
0.1	0.32	0.89	S	0.41	0.75	S
0.2	0.47	0.79	S	0.49	0.72	S
0.4	0.61	0.77	S	0.72	0.73	S
0.8	0.78	0.81	S	0.81	0.80	S
1.6	0.86	0.84	S	0.90	0.86	S
3.2	0.93	0.85	S	0.97	0.91	S

The CI analysis was measured using CompuSyn software and combination index method of Chou-Talalay. CLL; Chronic lymphoid leukemia, CI value >1 , $=1$ and <1 show antagonistic, additive and S effects, respectively, CI; Combination index, S; Synergistic, and Fa; Fraction affected.

MiRNA-16-1 enhanced the effect of ABT-199 on CLL cell growth

As over-expression of Mcl-1 and Bcl-2 is linked to the cell growth; we therefore explored whether *miRNA-16-1* could inhibit the proliferation of the CLL-CII cells. The CLL-CII cells were treated with *miRNA-16-1* (50 nM), ABT-199 (IC_{50} of 25 hours) and combination of them for 1-5 days and the percent of the viable cells was counted every day by trypan blue staining assay. Data showed that in comparison with the control group, treatment with *miRNA-16-1* or ABT-199 significantly suppressed the growth of CLL-CII cells over a period of 5 days. At 24 hours after treatment with *miRNA-16-1* or ABT-199, the cell viability dropped to 83.30% and 62.23% respectively, and then to a further 54.15% and 25.67% at the end of the experiment (day 5). Moreover, combination therapy with *miRNA-16-1* and ABT-199 had a stronger effect on inhibition of cell growth compared to single therapy ($P<0.05$). However, no significant difference in cell growth was seen between the NC miRNA and the blank control groups (Fig.3).

Increased levels of *miRNA-16-1* enhanced ABT-199-induced apoptotic

To explore whether the observed sensitizing effect of the *miRNA-16-1* was associated with the increased amount of apoptosis, the effects of *miRNA-16-1* and ABT-199 alone and in combination on apoptosis, were assessed using an ELISA apoptosis assay. Results demonstrate that 24 h treatment with *miRNA-16-1* or ABT-199 increased apoptosis by 1.93 fold and 4.30 fold, respectively, compared to the control group (Fig.4A, $P<0.05$). Furthermore, combination treatment enhances the extent of cell death to 7.44 fold ($P<0.05$, compared with either ABT-199 alone or *miRNA-16-1* alone). Moreover, 48 h exposure of the cells with *miRNA-16-1* or ABT-199 alone, increased apoptosis by 2.46 and 5.12 fold, respectively, relative to the control

group ($P<0.05$). Also, the combination of *miRNA-16-1* and ABT-199 further augmented the induction of apoptosis to 8.56 fold during same period of time ($P<0.05$, compared with the blank control or monotreatment). However, NC miRNA (alone or in combination with ABT-199) showed no significant effect on extents of apoptosis compared with the *miRNA-16-1* or ABT-199, respectively (Fig.4A, $P>0.05$). The results of ELISA apoptosis assay shows that *miRNA-16-1* sensitizes the chronic lymphocytic leukemia cells to ABT-199 partially via enhancement of apoptosis.

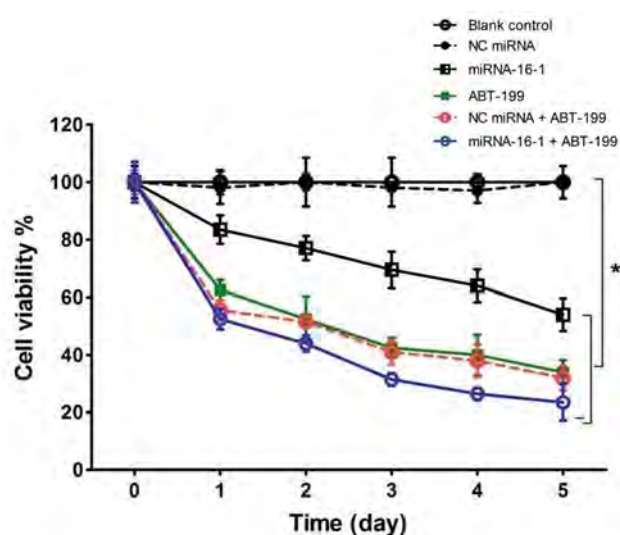


Fig.3: Cell growth curve of CLL-CII cells after treatment with *miRNA-16-1* and ABT-199. Cell viability was measured using trypan blue staining over a period of 24-120 hours. Results are expressed as mean \pm SD (n=3). *, $P<0.05$ versus blank control or NC miRNA and NC; Negative control.

MiRNA-16-1 enhanced the effect of ABT-199 on caspase-3 activity in CLL-CII cells

To explore the mechanism by which apoptosis occurred

in the treated cells, changes in the activation of the caspases-3 were determined by using caspase-3 activity assay Kit. Figure 4B shows the changes in caspases-3 activity in the CLL cells treated with the *miRNA-16-1*, ABT-199 (IC₅₀) and their combination for 24 hours, that show the caspase-3 activity was enhanced by 1.65, 3.42, and 6.21 times, respectively, relative to the blank control group (P<0.05). As indicated in Figure 4B, *miRNA-16-1* alone and in combination with ABT-199 activated caspase-3 activity in a time dependent way. However, treatment with NC miRNA did not show a notable effect on caspase-3 activity relative to the blank control group (P>0.05).

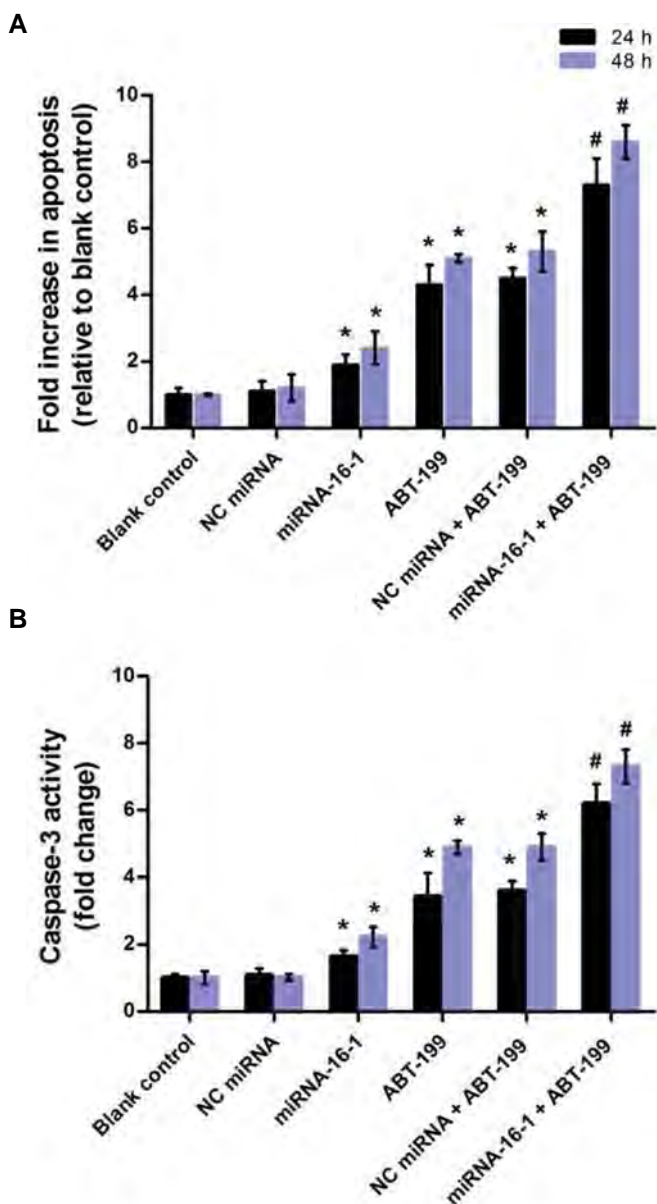


Fig.4: The effects of *miRNA-16-1* and ABT-199 on apoptosis of CLL cells. Cells were treated with *miRNA-16-1* (50 nM), NC miRNA (50 nM) and ABT-199 (IC₅₀ doses of 24 and 48 hours), alone and in combination. **A.** Next, the cell death was assessed using ELISA cell death assay. **B.** Caspase-3 activity of CLL cells was measured using a caspase-3 activity assay Kit. The data are showed as mean ± SD (n=3). CLL; Chronic lymphoid leukemia, IC₅₀; Half-maximal inhibitory concentration, NC; Negative control, *; P<0.05 relative to the control, and #; P<0.05 versus *miRNA-16-1* or ABT-199 monotreatment.

Discussion

Although ABT-199 has shown high clinical activity against CLL, some patients do not respond or become resistant to this Bcl-2 inhibitor. It has been reported that genetic factors such as Bcl-2 and Bax mutations have been associated with ABT-199 resistance. Sustained activation of B-cell receptor and AKT as well as up-regulation of Mcl-1 and Bcl-xL levels is also related to this process (12-14). However, the exact mechanisms of resistance are not fully known. Our findings propose that *miRNA-16-1* act in concert with ABT-199 to exert synergistic anticancer efficacy against CLL, which is attributed to the inhibition of Bcl-2 and Mcl-1.

Our study demonstrated that inhibition of Mcl-1 and Bcl-2 by *miRNA-16-1* was associated with inhibition of cell proliferation and increased the sensitivity of the CLL cells to ABT-199 in a synergistic way. So far, various studies have investigated the role of apoptotic proteins, especially Mcl-1, in the sensitivity of tumor cells to ABT-199. For example, Wang et al. (28) showed that Mcl-1-dependent AML cells were resistant to ABT-199 and Mcl-1-specific inhibitors such as A-1210477 that could counteract these resistance *in vitro* and *in vivo*. Other study indicated that treatment with A-1592668, a small-molecule inhibitor of CDK9, resulted in the loss of Mcl-1 expression and apoptosis in Mcl-1 dependent lymphoma and AML cell lines. Moreover, the A-1592668 plus ABT-199 combination showed efficacy superior to either agent alone with minimal toxicity in mouse models (29). In addition, Choudhary et al. (13) explored the mechanisms of resistance to ABT-199 in CLL and non-Hodgkin lymphoma cell lines. Their study demonstrated persistent activation of AKT as well as over-expression of Bcl-xL and Mcl-1 levels in the acquired and inherent ABT-199 resistant cells. Moreover, treatment with specific inhibitor of AKT pathway reduced Mcl-1 levels and sensitized the tumor cells to ABT-199. However, our data further confirms the results of the above studies and suggests that downregulation of Mcl-1 by *miRNA-16-1* can enhance the ABT-199 sensitivity in CLL cells that depend on Mcl-1 for survival.

MiRNA-16-1 acts as a tumor suppressor by targeting critical molecules in CLL cells. However, few studies have been performed on the role of this miRNA in the chemoresistance of CLL (30). In our study, transfection of *miRNA-16-1* increased the ABT-199 sensitivity of the CLL cells. So far, several investigations have been performed to show the relationship of miRNA with chemoresistance. Zhu et al. (31) reported that *miRNA-15a*, *miRNA-16-1*, *miRNA-34* and *miRNA-181a/b* sensitized the CLL cells to fludarabine-induced apoptosis through the inhibition of Mcl-1 and Bcl-2. Some other studies of miRNA expression reported that *miRNA-221* and *miRNA-181a* were significantly up-regulated and *miRNA-29a* strongly down-regulated in fludarabine-resistant cells *in vitro* (24, 32). Since the increased expression of Mcl-1 is associated with resistance of tumor cells to Bcl-2-specific inhibitors, other investigations have been performed to

explore the effect of miRNAs on Mcl-1 expression and the sensitivity of tumor cells to these inhibitors. *MiRNA-193b* is down-regulated in melanoma cells, and induced expression of this miRNA restores ABT-737 sensitivity of the resistant cells by targeting Mcl-1 (33, 34). Similarly Lam et al. (34) recognized a panel of 12 miRNAs that were linked to the reduced Mcl-1 protein levels that can sensitize melanoma cells to the apoptosis induced by ABT-263. In accordance with the above reports, our findings showed that *miRNA-16-1* increases ABT-199 sensitivity of the CLL cells. No other study has been done on the relationship between miRNAs and sensitivity to ABT-199 in cancer cells.

We also examined the effects of *miRNA-16-1* and ABT-199 on cellular apoptosis. Our results demonstrated that ABT-199 significantly triggered apoptosis and enhanced caspase-3 activity in CLL cells. Moreover, suppression of Mcl-1 and Bcl-2 by *miRNA-16-1* was associated with the induction of apoptosis and enhancement of the ABT-199-mediated apoptosis. The intrinsic pathway of apoptosis is induced with different stimuli such as DNA damage, oxidative stress, cytotoxic drugs and radiation. This pathway is under the control of Bcl-2 family of pro- and anti-apoptotic proteins (35, 37). The pro-apoptotic members Bcl-2 family such as Bak and Bax when activated lead to protein hemodimerization, change in the mitochondrial outer membrane permeability (MOMP), release of cytochrome c, and ultimately the downstream activation of the caspases 3, 6 and 7. The anti-apoptotic members such as Bcl-2 and Mcl-1 inhibit apoptosis by heterodimerising with Bax and Bak (5, 9). ABT-199 induces intrinsic pathway of apoptosis in CLL cells by inhibiting Bcl-2. It has been shown that caspase-3 activation is induced by the ABT-199. Moreover, it has been shown that the tumor cells which over-expressed Bcl-2, Mcl-1 and Bcl-xL were resistant to ABT-199 (9, 28, 29). The above reports are in accordance with our results and propose that targeting of anti-apoptotic family members would be a promising strategy to enhance the activity of ABT-199 in various malignancies including CLL.

Conclusion

The data presented here indicate that *miRNA-16-1* act in concert with ABT-199 to exert synergistic anticancer efficacy against CLL, attributed to the inhibition of Bcl-2 and Mcl-1. Moreover, our study demonstrated that *miRNA-16-1* could augment the execution of apoptosis induced by ABT-199. The intrinsic pathway of apoptosis and caspase activation may be a part of the underlying mechanisms involved in this process. Collectively, our findings show that the combination of *miRNA-16-1* and ABT-199 can efficaciously induce the apoptosis of CLL cells, and may offer a promising strategy for patients with CLL.

Acknowledgments

This work is part of M.Sc. thesis of Nooshin Ashofteh

that was supported by a grant from the Faculty of Medicine, Arak University of Medical Sciences, Arak, Iran (grant number 1206). The authors would like to thank Dr. Bahman Yousefi for his technical support in western blotting experiment. The authors have no conflict of interest to declare.

Authors' Contributions

H.K.; Study concept and design. N.A., A.S.A.M., M.B.; Acquisition of data. N.A., H.K., M.B., A.S.A.M.; Analysis and interpretation of data. N.A., H.K., M.B.; Drafting of the manuscript. N.A., H.K., A.S.A.M.; Critical revision of the manuscript for important intellectual content. H.K., A.S.A.M.; Funding recipients. All authors read and approved the final manuscript.

References

- Danilov AV. Targeted therapy in chronic lymphocytic leukemia: past, present, and future. *Clin Ther*. 2013; 35(9): 1258-1270.
- Khan M, Siddiqi T. Targeted therapies in CLL: monotherapy versus combination approaches. *Curr Hematol Malig Rep*. 2018; 13(6): 525-533.
- Chen R, Plunkett W. Strategy to induce apoptosis and circumvent resistance in chronic lymphocytic leukaemia. *Best Pract Res Clin Haematol*. 2010; 23(1): 155-166.
- Hertlein E, Byrd JC. Signalling to drug resistance in CLL. *Best Pract Res Clin Haematol*. 2010; 23(1): 121-131.
- Masood A, Shahshahan MA, Jazirehi AR. Novel approaches to modulate apoptosis resistance: basic and clinical implications in the treatment of chronic lymphocytic leukemia (CLL). *Curr Drug Deliv*. 2012; 9(1): 30-40.
- Nana-Sinkam SP, Croce C M. MicroRNA in chronic lymphocytic leukemia: transitioning from laboratory-based investigation to clinical application. *Cancer Genet Cytogenet*. 2010; 203(2): 127-133.
- Arnason JE, Brown JR. Targeted therapy for chronic lymphocytic leukemia: current status and future directions. *Drugs*. 2015; 75(2): 143-155.
- Billard C. Design of novel BH3 mimetics for the treatment of chronic lymphocytic leukemia. *Leukemia*. 2012; 26(9): 2032-2038.
- Fegan C, Pepper C. Apoptosis deregulation in CLL. *Adv Exp Med Biol*. 2013; 792: 151-171.
- D'Rozario J, Bennett SK. Update on the role of venetoclax and rituximab in the treatment of relapsed or refractory CLL. *Ther Adv Hematol*. 2019; 10: 2040620719844697.
- Lasica M, Anderson MA. Review of venetoclax in CLL, AML and multiple myeloma. *J Pers Med*. 2021; 11(6): 463.
- Bojarczuk K, Sasi BK, Gobessi S, Innocenti I, Pozzato G, Laurenti L, et al. BCR signaling inhibitors differ in their ability to overcome Mcl-1-mediated resistance of CLL B cells to ABT-199. *Blood*. 2016; 127(25): 3192-3201.
- Choudhary GS, Al-Harbi S, Mazumder S, Hill BT, Smith MR, Bodo J, et al. MCL-1 and BCL-xL-dependent resistance to the BCL-2 inhibitor ABT-199 can be overcome by preventing PI3K/AKT/mTOR activation in lymphoid malignancies. *Cell Death Dis*. 2015; 6(1): e1593.
- Thijssen R, Slinger E, Weller K, Geest CR, Beaumont T, van Oers MH, et al. Resistance to ABT-199 induced by microenvironmental signals in chronic lymphocytic leukemia can be counteracted by CD20 antibodies or kinase inhibitors. *Haematologica*. 2015; 100(8): e302-306.
- Alamdari-Palangi V, Amini R, Karami H. MiRNA-7 enhances erlotinib sensitivity of glioblastoma cells by blocking the IRS-1 and IRS-2 expression. *J Pharm Pharmacol*. 2020; 72(4): 531-538.
- Alamdari-Palangi V, Karami Z, Karami H, Baazm M. MiRNA-7 replacement effect on proliferation and tarceva-sensitivity in U373-MG cell line. *Asian Pac J Cancer Prev*. 2020; 21(6): 1747-1753.
- Amri J, Molaee N, Baazm M, Karami H. Targeting epidermal growth factor receptor by MiRNA-145 inhibits cell growth and sensitizes NSCLC cells to erlotinib. *Asian Pac J Cancer Prev*. 2019; 20(9): 2781-2787.
- Amri J, Molaee N, Karami H. Up-Regulation of miRNA-125a-5p inhibits cell proliferation and increases EGFR-TKI induced apop-

- tosis in lung cancer cells. *Asian Pac J Cancer Prev.* 2019; 20(11): 3361-3367.
19. Calin GA, Cimmino A, Fabbri M, Ferracin M, Wojcik SE, Shimizu M, et al. MiR-15a and miR-16-1 cluster functions in human leukemia. *Proc Natl Acad Sci USA.* 2008; 105(13): 5166-5171.
 20. Lv M, Zhu S, Peng H, Cheng Z, Zhang G, Wang Z. B-cell acute lymphoblastic leukemia-related microRNAs: uncovering their diverse and special roles. *Am J Cancer Res.* 2021; 11(4): 1104-1120.
 21. Mardani R, Jafari Najaf Abadi M H, Motieian M, Taghizadeh-Boroujeni S, Bayat A, Farsinezhad A, et al. MicroRNA in leukemia: tumor suppressors and oncogenes with prognostic potential. *J Cell Physiol.* 2019; 234(6): 8465-8486.
 22. Hallek M. Chronic lymphocytic leukemia: 2020 update on diagnosis, risk stratification and treatment. *Am J Hematol.* 2019; 94(11): 1266-1287.
 23. Lia M, Carette A, Tang H, Shen Q, Mo T, Bhagat G, et al. Functional dissection of the chromosome 13q14 tumor-suppressor locus using transgenic mouse lines. *Blood.* 2012; 119(13): 2981-2990.
 24. Calin GA, Ferracin M, Cimmino A, Di Leva G, Shimizu M, Wojcik SE, et al. A microRNA signature associated with prognosis and progression in chronic lymphocytic leukemia. *N Engl J Med.* 2005; 353(17): 1793-1801.
 25. Karami H, Baradaran B, Esfehiani A, Sakhinia M, Sakhinia E. Down-regulation of Mcl-1 by small interference RNA induces apoptosis and sensitizes HL-60 leukemia cells to etoposide. *Asian Pac J Cancer Prev.* 2014; 15(2): 629-635.
 26. Shahverdi M, Amini R, Amri J, Karami H. Gene therapy with MiRNA-mediated targeting of Mcl-1 promotes the sensitivity of non-small cell lung cancer cells to treatment with ABT-737. *Asian Pac J Cancer Prev.* 2020; 21(3): 675-681.
 27. Shahverdi M, Amri J, Karami H, Baazm M. Knockdown of myeloid cell leukemia-1 by microRNA-101 increases sensitivity of A549 lung cancer cells to etoposide. *Iran J Med Sci.* 2021; 46(4): 298-307.
 28. Wang Q, Wan J, Zhang W, Hao S. MCL-1 or BCL-xL-dependent resistance to the BCL-2 antagonist (ABT-199) can be overcome by specific inhibitor as single agents and in combination with ABT-199 in acute myeloid leukemia cells. *Leuk Lymphoma.* 2019; 60(9): 2170-2180.
 29. Phillips DC, Jin S, Gregory GP, Zhang Q, Xue J, Zhao X, et al. A novel CDK9 inhibitor increases the efficacy of venetoclax (ABT-199) in multiple models of hematologic malignancies. *Leukemia.* 2020; 34(6): 1646-1657.
 30. Zhou XX, Wang X. Role of microRNAs in chronic lymphocytic leukemia (Review). *Mol Med Rep.* 2013; 8(3): 719-725.
 31. Zhu DX, Zhu W, Fang C, Fan L, Zou ZJ, Wang YH, et al. miR-181a/b significantly enhances drug sensitivity in chronic lymphocytic leukemia cells via targeting multiple anti-apoptosis genes. *Carcinogenesis.* 2012; 33(7): 1294-1301.
 32. Moussay E, Palissot V, Vallar L, Poiriel HA, Wenner T, El Khoury V, et al. Determination of genes and microRNAs involved in the resistance to fludarabine in vivo in chronic lymphocytic leukemia. *Mol Cancer.* 2010; 9: 115.
 33. Chen J, Zhang X, Lentz C, Abi-Daoud M, Paré GC, Yang X, et al. miR-193b regulates Mcl-1 in melanoma. *Am J Pathol.* 2011; 179(5): 2162-2168.
 34. Lam LT, Lu X, Zhang H, Lesniewski R, Rosenberg S, Semizarov D. A microRNA screen to identify modulators of sensitivity to BCL2 inhibitor ABT-263 (navitoclax). *Mol Cancer Ther.* 2010; 9(11): 2943-2950.
 35. Beroske L, Van den Wyngaert T, Stroobants S, Van der Veken P, Elvas F. Molecular imaging of apoptosis: the case of caspase-3 radiotracers. *Int J Mol Sci.* 2021; 22(8): 3948.
 36. Bertheloot D, Latz E, Franklin BS. Necroptosis, pyroptosis and apoptosis: an intricate game of cell death. *Cell Mol Immunol.* 2021; 18(5): 1106-1121.
 37. Pan Y, Cheng A, Wang M, Yin Z, Jia R. The dual regulation of apoptosis by flavivirus. *Front Microbiol.* 2021; 12: 654494.

Genetic and Epigenetic Evaluation of Human Spermatogonial Stem Cells Isolated by MACS in Different Two and Three-Dimensional Culture Systems

Maria Zahiri, Ph.D.^{1,2}, Mansoureh Movahedin, Ph.D.^{1*}, Seyed Javad Mowla, Ph.D.³, Mehrdad Noruzinia, Ph.D.⁴, Morteza Koruji, Ph.D.⁵, Mohammad Reza Nowroozi, Ph.D.⁶, Fatemeh Asgari, Ph.D.⁷

1. Anatomical Science Department, Faculty of Medical Sciences, Tarbiat Modares University, Tehran, Iran
2. The Persian Gulf Marine Biotechnology Research Center, The Persian Gulf Biomedical Sciences Research Institute, Bushehr University of Medical Sciences, Bushehr, Iran
3. Department of Molecular Genetics, Faculty of Biological Sciences, Tarbiat Modares University, Tehran, Iran
4. Department of Medical Genetics, School of Medicine, Tarbiat Modares University, Tehran, Iran
5. Department of Anatomical Sciences, School of Medicine, Iran University of Medical Sciences, Tehran, Iran
6. Department of Urology, Uro-Oncology Research Center, Tehran University of Medical Sciences, Tehran, Iran
7. Clinical Research Development Unit of Nekouei-Hedayati-Forghani Hospital, Qom University of Medical Sciences, Qom, Iran

*Corresponding Address: P.O.Box: 14115-175, Anatomical Science Department, Faculty of Medical Sciences, Tarbiat Modares University, Tehran, Iran
Email: movahed.m@modares.ac.ir

Received: 05/December/2020, Accepted: 17/May/2021

Abstract

Objective: Epigenetic and genetic changes have important roles in stem cell achievements. Accordingly, the aim of this study is the evaluation of the epigenetic and genetic alterations of different culture systems, considering their efficacy in propagating human spermatogonial stem cells isolated by magnetic-activated cell sorting (MACS).

Materials and Methods: In this experimental study, obstructive azoospermia (OA) patient-derived spermatogonial cells were divided into two groups. The MACS enriched and non-enriched spermatogonial stem cells (SSCs) were cultured in the control and treated groups; co-culture of SSCs with Sertoli cells of men with OA, co-culture of SSCs with healthy Sertoli cells of fertile men, the culture of SSCs on PLA nanofiber and culture of testicular cell suspension. Gene-specific methylation by MSP, expression of pluripotency (*NANOG*, *C-MYC* and *OCT-4*), and germ cells specific genes (*Integrin α6*, *Integrin β1*, *PLZF*) evaluated. Cultured SSCs from the optimized group were transplanted into the recipient azoospermic mouse.

Results: The use of MACS for the purification of human stem cells was effective at about 69% with the culture of the testicular suspension, being the best culture system. Upon purification, the germ-specific gene expression was significantly higher in testicular cell suspension and treated groups ($P \leq 0.05$). During the culture time, gene-specific methylation patterns of the examined genes did not show any changes. Our data from transplantation indicated the homing of the donor-derived cells and the presence of human functional sperm.

Conclusion: Our *in vivo* and *in vitro* results confirmed that culture of testicular cell suspension and selection of spermatogonial cells could be effective ways for purification and enrichment of the functional human spermatogonial cells. The epigenetic patterns showed that the specific methylation of the evaluated genes at this stage remained constant with no alteration throughout the entire culture systems over time.

Keywords: Azoospermia, Genetic and Epigenetic, Spermatogonial Stem Cells

Cell Journal (Yakhteh), Vol 24, No 8, August 2022, Pages: 481-490

Citation: Zahiri M, Movahedin M, Mowla SJ, Noruzinia M, Koruji M, Nowroozi MR, Asgari F. Genetic and epigenetic evaluation of human spermatogonial stem cells isolated by MACS in different two and three-dimensional culture systems. Cell J. 2022; 24(8): 481-490. doi: 10.22074/cellj.2022.7888.

This open-access article has been published under the terms of the Creative Commons Attribution Non-Commercial 3.0 (CC BY-NC 3.0).

Introduction

Male infertility is a disorder with complex and multifactorial etiology that caused researchers have been trying to achieve *in vitro* spermatogenesis (IVS) for a century (1). Epigenetic and genetic modifications roles are essential in spermatogenesis and embryogenesis of clinical approaches (2). *In vitro* culture and transplantation are two techniques of spermatogonial stem cells (SSCs) resuscitation after cryopreservation that could have a risk to change genetics and epigenetics (3). Consequently, SSCs grown *in vitro* due to exposure to growth factors and maturation processes can have a higher risk of becoming genetically modified. Therefore, special attention must be paid to the status of *in vitro* culture and post-transplantation (4).

A low number of SSCs about 0.03% of all germ cells in the rodents and no specific markers for identifying them have hampered rapid success in scientific development (5). Two major developments in SSCs culture include the establishment of the spermatogonial transplantation technique and the identification of glial cell derived neurotrophic factor (GDNF) as a key growth factor for the proliferation of SSCs *in vitro* (6).

Researchers have used different techniques for the proliferation of SSCs isolated from testis of azoospermic men, such as using human Sertoli cells as a monolayer in the absence of exogenous growth factors (7). Two-dimensional culture systems (2D) resulted in the incomplete proliferation and differentiation stages of SSCs. Thus, three-dimensional (3D) cultures have been

introduced very recently and have been hypothesized to be able to mimic seminiferous epithelium developing male germ cells better (3). Therefore, due to the improvement of culture conditions, one of the most widely used methods in tissue engineering is nanofibers. Poly(lactic acid) (PLA) is a form of an organic polymer obtained from lactic acid dissolved in water and carbon dioxide. Its most important properties are mechanical tensile strength, biocompatibility, and biodegradability. It contributes to mesenchymal stem cells and has chemical and mechanical properties similar to the extracellular matrix (8). In this study, the effect of culturing spermatogonia stem cells with a suspension of testicular cells, Sertoli cells, and culture on PLA nanofiber coated with laminin will be investigated.

Various techniques have been proposed for the isolation of very pure human SSCs (9, 10). Purification is suggested by fluorescence-activated cell sorting (FACS) or magnetic-activated cell sorting (MACS) (11). Panda et al. (12) used Ficoll gradient centrifugation chased by MACS and Thy1 surface marker for extraction of SSCs from growing *L. rohita* testis. Nevertheless, since there are enormous differences in spermatogenesis details between rodents and mammals, further studies are essential, especially on humans.

In this study, for the first time, the genetic and epigenetic data on the effect of different *in vivo* and *in vitro* conditions evaluated. We aimed to examine genetic and epigenetic changes of human SSCs isolated by MACS and *GFR α -1* marker on their proliferation and purification capacity in various cultural systems. SSCs of azoospermic men who had obstructive azoospermia (OA) were cultured in five experimental groups; as a control group, with healthy Sertoli cells of fertile men, with Sertoli cells from men with OA, 3D culture system by PLA nanofiber and suspension groups evaluated. Finally, the SSCs function of the selected culture system after xenograft was considered to evaluate the effect of the length and nature of the culture system on the methylation pattern by the Methylation-specific polymerase chain reaction (PCR) (MSP) method.

Material and Methods

Sample collection

In this experimental study, human research specimens for four experimental groups were taken from men with OA via the intra-cytoplasmic sperm injection (ICSI) program from Shayanmehr Clinic (Tehran, Iran), whose remaining tissue was used for this study. Testicular samples from a fertile man who had an orchidectomy for reasons other than testicular problems were used to obtain healthy Sertoli cells. Testicular samples and the experimental procedure were authorized by Tarbiat Modares University's National Research Council guidelines (Tehran, Iran). The study goals were clarified to the contributors, and informed consent was taken from patients willing to take part in the research (52/12037). Inclusion criteria for a patient to enter the research are FSH levels between 15-1mIU/

ml, testicular volume 6-15 ml, dynamic biopsy with motile sperm, and pathology assessment is positive for spermatogenic cells (13).

Spermatogonial stem cells isolation and *in vitro* culture

Ten azoospermic men testicular biopsy samples for each experimental group were used and the biopsies specimens were transferred to the laboratory in a medium, within 60 minutes. They were broken into small pieces and placed in Dulbecco's Modified Eagle medium (DMEM, Gibco, Paisley, UK), got in touch with 14 mm NaHCO₃ (Sigma, St Louis, MO, USA), non-essential amino acids, 100 IU/mL penicillin, and 100 μ g/mL streptomycin. The broken pieces of the testis were placed in DMEM, which included 0.5 mg/mL collagenase, 0.5 mg/mL trypsin, 0.5 mg/mL hyaluronidase, and 0.05 mg/mL DNase, for 30 minutes, at 37°C. The gradient of gravity caused the spermatogenic tubules and cells to sediment. After three DMEM washes and the elimination of most interstitial cells, the next digestion step (45 minutes at 37°C) was done in by adding fresh enzymes and media to the fragments of the seminiferous tubule. With centrifugation at 1500 rpm for 4 minutes at 37°C, the cells were separated from the remaining tubule fragments.

Finally, the suspension of testicular cells was incubated in DMEM with FCS 10% and cultured overnight at 37°C and 5% CO₂. Sertoli cells stuck to the bottom of the container faster. In this way, after this period, the top cell suspension containing more germ cells and SSCs was collected.

In the first stage, a total of 2×10^5 cells were cultured per 12-well plate in five groups for two weeks. You can see the results in our previous study (13). After enrichment of SSCs to enough count, suitable conditions were provided for SSCs purification with MACS. Then we cultured SSCs with and without MACS isolation for one week. Therefore, the cells of each experimental group were divided into two groups part was cultured as before for another week, and part was purified by MACS:

1. Control group, SSCs cultured in the culture dish.
2. Culture of SSCs with men's own Sertoli cells (Sertoli cells of men with OA). A testicular biopsied specimen was cultured at 37°C after digestion of the second enzymatic period. After 24 hours, the supernatant was removed and the bottom of the dish containing Sertoli cells was cultured with men's own sorted SSCs.
3. Culture of SSCs with normal Sertoli cells. To provide Sertoli cells for this group, a testicular sample from a fertile man who had an orchidectomy for reasons other than testicular issues was used to achieve healthy Sertoli cells. A testicular specimen was cultured at 37 °C after digestion of the second enzymatic period. After 24 hours, the supernatant was removed and the bottom of the dish containing Sertoli cells was cultured with SSCs (13).
4. Culture of SSCs on PLA nanofiber, covered with Laminin.

5. The suspension of biopsied testicular cells from biopsy cultured without separation of SSCs.

Three repetitions of each experimental group were cultured in 34-StemPro for one week with its complement (Invitrogen), 25 µg/ml human insulin, 100 µg/ml transferrin, 60 µM putrescine, 30 nM sodium selenite, 6 mg/ml -D (±) glucose, 30 µg/ml Pyruvic acid, 1 µM -DL lactic acid, 5 mg/ml bovine serum albumin, 2 µM L-glutamine, -25×10^{-5} Mercaptoethanol, MEM soluble vitamins, 10^{-4} Ascorbic acid, 10 µg/ml -d biotin, 30 ng/ml beta-estradiol, 60 ng/ml Progesterone, 20 ng/ml human epidermal growth factor, 10 ng/ml derived neurotrophic factor class of glial cell and Humanities (GDNF), 10 ng/ml human leukemia inhibitory factor (LIF), 10 ng/ml basic fibroblast growth factor (bFGF), 5% FCS, 100 IU/ml penicillin, 100 µg/ml Streptomycin (Sigma), and the cells incubated at 37°C with 5% CO₂. We changed the cell culture medium every two days.

Purification of spermatogonial stem cells by MACS

To purify cultured cells, the cells in the plates were washed once with MACS buffer and then an appropriate volume of MACS buffer (based on the plate's level, number of cells, and the manufacturer's guideline) was added, and cells were mechanically isolated from the base by a cell scraper and centrifuged. After cell counting, cells were cultured in two groups with and without purification. In the second group, 200 µL buffer was added for all 2×10^6 cells, and antibodies against GFR α -1 (SC-10716) diluted in 1:50 were added to the cells. Cells were refrigerated for 15 minutes. The column type was chosen based on the number of cells. The column was placed in a separator magnetic field. After washing the column and diluting buffer cells, secondary antibodies attached to Microbead (Milteny Biotec) diluted in 1:10 were added and incubated for half an hour at 4°C on the shaker. After washing with buffer twice and centrifuge, cells were labeled and poured into columns with buffer. Negative cells crossed the column while the GFR α -1 positive cells remained attached.

PLA nanofiber and Laminin preparation

The PLA fibers were made sterile by sinking in ethanol 70% for 2 hours or ultraviolet (14) radiation. Then, 20 µg/mL laminin (Sigma-Aldrich, USA) was poured on them and incubated at 37°C for 2 hours until one night. Before use, it was rinsed with phosphate buffer solution (PBS) and prepared for cell culture. Spermatogonial cell suspension prepared after one-night incubation of the second enzyme lysis was used in this group. The cell load was as follows: first, the cells were suspended in 30 µl of culture medium and a concentration of 3.5×10^5 cells/mL. The fiber was added to the fiber dropwise and put in an incubator. After two hours, the rest of the culture medium was added. The cell medium was changed every other day.

Spermatogonial and sertoli cells confirmation

The Sertoli cells and SSCs were evaluated for vimentin

and GFR α 1 markers by immunocytochemistry. The cells were treated with an anti-vimentin antibody. The cells were fixed with 4% formaldehyde and became permeable by 0.2% Triton X100 and clogging with 10% goat serum (Vector, Burlingame, CA) for 30 minutes. The utilized primary antibody (mouse monoclonal anti-vimentin antibody with a dilution, 1:200; Sigma Company, USA) and the rabbit anti-human GFR α 1 antibody (dilution 1:100) were added at 4°C and the dishes were incubated 24 hours. The fluorescent-labeled second antibody (1:100, Sigma) was added and incubated for 2 hours at 4°C in darkness. The cells were finally mounted with a mounting medium (Vector Laboratories Inc., Burlingame, CA) after three washes with PBS and examined under a fluorescence microscope (IX-71, Olympus).

Quantitative analysis of gene expression

Total RNA was isolated from SSCs derived from all groups, using an RNX-Plus TM (Cinnagen, Iran). RNA concentrations were evaluated by a UV spectrophotometer (Eppendorf, Germany). RevertAidTM first-strand cDNA synthesis kit (Fermentase) with oligo dT primer was used for reverse-transcription of treated RNA. Oligonucleotide PCR primers specific for alpha-6-integrin, beta-1 integrin, *PLZF*, *C-MYC*, *NANOG*, *OCT-4*, and *TBP* (internal control) genes were adapted from other primers and synthesized by GenFanAvaran Company.

The Thermal Cycler used SYBR Green and PCR master mix (Cinnagen) for PCR reactions (Applied Biosystems, StepOne TM, USA). Cycling conditions were initiated with a melting period at 95°C for 5 minutes, chased by 40 cycles of melting 30 seconds at 95°C, annealing 30 seconds at 58-60°C and extending 30 seconds at 72°C. Melt curve analysis was performed, and the standard curve for each gene was prepared using serial cDNA dilution from the testis to determine the output. The same run amplified the target gene and the reference gene. The ratio of gene expression was determined using the comparative cycle threshold (CT) method (n=3).

Epigenetic assessment

DNA extraction of spermatogonial stem cells

DNAs of the SSCs in all groups were extracted using a DNA extraction kit (Roche Co) based on the suggested guideline at the end of the culture. The cultured cells were isolated by trypsin and suspended after rinsing in 200 mL PBS. Then, 200 mL binding buffer and 40 µL K proteinase were added and incubated at 70°C. Then, 100 µL isopropanol was added, then centrifuged after being transformed into a filtered tube. Finally, 50 µL elution buffer was added after centrifuge. The quality of DNA extraction was tested on agarose gel by absorption at 260-280 nm wavelengths.

DNA methylation by SSS1 enzyme

SSS1 methylase enzyme (Biolabs Co, New England) was used to guide the methylate primers to DNA, according to the instructions. After treatment with sodium

bisulfate (SBS), methylated primers were used for PCR. Enzyme stock 32 mmol was converted to 1600 μ mol and incubated at 37°C for 1.5 hours. Heating up to 65°C for 20 minutes would stop the reaction. Then, methylated DNA was treated with SBS, before methylation-specific PCR (MSP) with M primer. Finally, methylated DNA was used as a positive control in MSP with methylated M primer.

Methylation-specific PCR

MSP was done by M primer with methylated DNA-modified sequence with SBS, and U primer with non-methylated DNA-modified sequence with SBS. Amplification with M primer showed methylation in CpG zones inside primer sequences, amplification with U primer showed no methylation, and amplification with both primers showed partial methylation in CpG zones inside primer sequences. In the present research, MSP with methylated and unmethylated primers was performed on *Integrin $\alpha 6$* , *Integrin $\beta 1$* , *PLZF*, *C-MYC*, and *OCT-4*.

Spermatogonial stem cells labeling and transplantation

To confirm spermatogonial cell identity and function in spermatogenesis, SSCs resulting from cultures were transplanted to twelve NMRI mice, aged 6–8 weeks, with a mean weight of 25 g, kept in separate cages in fair conditions. Initially, the innate spermatogenesis was stopped by an intra-peritoneal injection of 40 mg/kg busulfan. After 4 weeks, the mice were azoospermic. For developing the azoospermia model, 40 mg/kg (Sigma, USA) of Busulfan was injected into each mouse for 4 weeks (15).

To detect and monitor the transplanted cells, spermatogonial colonies were mechanically extracted from culture plates under a reverse microscope. Then, after rinsing with PBS, they were exposed to Dil dye (2 μ g Dil per 1 mL of PBS) for 5 minutes at room temperature. Next, they were kept at 4°C in darkness for 20 minutes. After confirming the cell dye under a fluorescent microscope, and three times rinsing in a culture medium, they were transplanted to the recipient mice. The technique used was similar to Brinster's technique (16). Before transplantation, the recipient mice anesthesia was performed through intraperitoneal injection of 10% ketamine and 20% xylazine. Then, the prepared SSCs were diluted at 10^5 cells per testis in a 10 μ L culture medium (17) and micro-injected by 30 Gauge under stereomicroscope guide (Olympus SZ1145, Japan) at a concentration of $10^5/10 \mu$ L DMEM to rete testis and finally to the left seminiferous tubule of the mice. To ensure the entrance of the cells to rete testis, 10% trypan-blue dye was simultaneously injected which makes the path visible to the naked eye. The right testis was chosen as the control. After 4, 8, and 16 weeks, the transplanted recipient animals were sacrificed and their testes were separated for assessments under a fluorescence microscope. The cell showing Dil staining was considered transplanted cells. The right testis is considered as the control group without transplantation of donor cells. Also, right side pictures are as phase contrast.

Assessment of the mouse testes' weight and epididymis sperms

The weight of testes was measured by an accurate digital scale after 16 weeks of transplantation in azoospermic mice (n=3). After separating the epididymis of both sides, they were placed in phosphate buffer solution with a pH of 7.4 which had been normalized in the incubator previously. They were then cut for the sperm to exit the epididymis. The phosphate buffer solution containing epididymis parts was incubated at 37°C and 5% CO₂ pressure for 30–45 minutes to increase the capacitated nature of the sperms. Finally, the number of sperms was counted by a hemocytometer under a light microscope and compared between the transplanted and control side.

Histological studies

For this part, samples were fixed in Bouin's fixative solution (Sigma-Aldrich, USA), dehydrated by 70–100% alcohol, and elucidated by xylene twice. Then, the samples were dipped with paraffin twice for 1.5 hours, sectioned by microtome with a type C fixed blade (Leitz, Germany), and stained with hematoxylin-eosin (Merck, Germany). The technique was performed in accordance with the manufacturer's instructions (n=3 per condition). A total of 50 seminiferous tubes were chosen and the number of germ cells (spermatogonia, spermatocyte, and spermatid), as well as the number of cells per surface, were counted in 15 random fields with $\times 400$ magnification under a light microscope.

Human *CatSper* expression gene in transplanted mice

To confirm the presence of human SSCs, quantitative PCR was used to detect human *CatSper* gene expression in cDNA of the transplanted testis of the mice after 16 weeks (n=3).

Statistical analysis

The statistical software SPSS version 16.0 for windows (SPSS Inc., Chicago, IL) was used and graphs were prepared by Microsoft Excel software version 2010. To analyze the data of real-time PCR, first, the raw data were converted to reportable data through available formulas and then analyzed by One-way ANOVA. P values of 0.05 are considered significant.

Results

Confirmation of spermatogonia cells

The immunohistochemical staining of the isolated Sertoli cells obtained from the seminiferous tubules of testes biopsies of azoospermic men who had OA contained mostly two different cell types: First Sertoli cells which proliferated and formed a monolayer of cells as a feeder layer defined by vimentin. It was observed in the cytoplasm of the Sertoli cells (Fig.1A) around the nucleus (Fig.1B) and merged (Fig.1C). The second type with a spherical outline and two or three exocentric nuclei were spermatogonial cells creating colonies after proliferation (Fig.1D). *GFR α -1*, which is a spermatogonial stem cell nuclear marker, was found in the obtained colonies (n=3, Fig.1E).

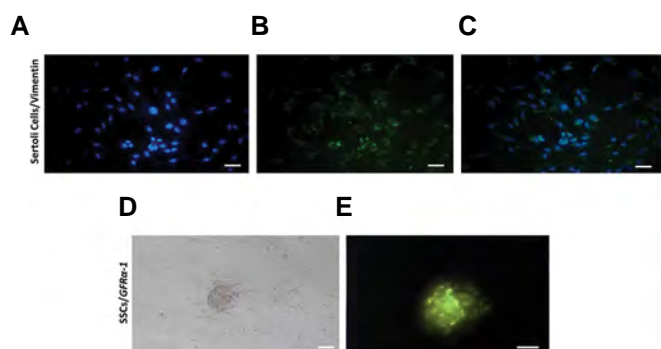


Fig.1: Spermatogonial and Sertoli cells confirmation. **A-C.** The immunohistochemical staining of the isolated Sertoli cells obtained from the human testes with detected Vimentin. **D.** Human spermatogonial stem cell colony. **E.** Immunofluorescent staining of spermatogonial stem cells (SSCs), detected *GFRα1* positive under an immune fluorescence microscope (scale bar: 200 μm).

Isolation of spermatogonial stem cells by MACS

After two phases of crossing the column (repeat separation), Figure 2 shows the immunohistochemistry of expression of *GFRα-1* before and after cell isolation with MACS (Fig.2A, a-d). The percentage of *GFRα-1*-positive cells by the second isolation phase fraction of MACS was significantly higher than the percentage of positive cells after one isolation phase and before isolation (respectively, $69.01 \pm 3.54\%$ to $58.14 \pm 2.26\%$ and 37.7 ± 1.53 , $P < 0.05$, Fig.2.B).

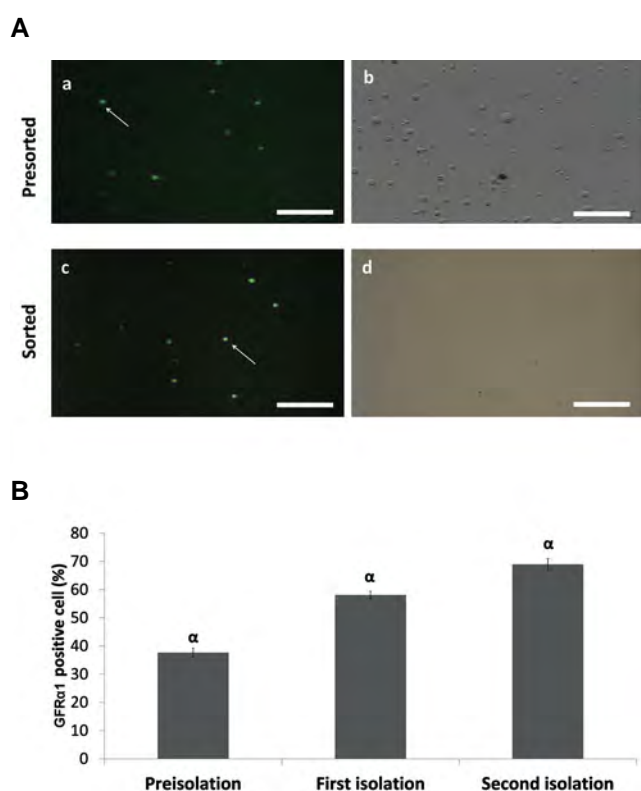


Fig.2: Isolation of spermatogonial stem cells (SSCs) by MACS. **A.** *GFRα-1* immunohistochemistry to evaluate the expression of markers of spermatogonial cells before (a and b) and after (c and d) cell isolation by MACS. **B.** Expression of *GFRα-1* marker of human spermatogonial stem cells derived from cultures after the two-step flowcytometry by MACS. α : Significant differences with the first time (mean \pm SD, $n=3$, $P < 0.05$) (scalr bar: 400 μm).

Results of quantitative polymerase chain reaction

Integrin α6, *Integrin β1*, and *PLZF* gene

Without MACS isolation, *Integrin-α6*, *Integrin β1*, and *PLZF* genes expression were significantly higher in testicular suspension cells than in other groups during culture ($P < 0.05$). After cell isolation, the highest *Integrin α6*, *Integrin β1*, and *PLZF* expressions were observed in testicular suspension cells ($P < 0.05$). Also, a comparison of cells isolated with and without MACS showed significantly higher expression of these genes in the isolated groups ($P < 0.05$, Fig.3A).

NANOG, *C-MYC*, and *OCT-4* gene expression

The expression of the *C-MYC* gene was lowest in the testicular suspension cells group without isolation of MACS than in healthy Sertoli, simple culture, and nanofiber after one week ($P < 0.05$), but this difference was not statistically significant from men's own Sertoli cells group ($P > 0.05$). After MACS isolation, it was significantly lowest in testicular suspension cells ($P < 0.05$). Also, a comparison of cells isolated with and without MACS showed lower expression in the isolated groups ($P < 0.05$).

The expression of Nanog after one week, without isolation of MACS, was lowest in testicular suspension and highest in simple culture ($P < 0.05$), but this difference was not statistically significant between the men's own Sertoli cells group and nanofiber groups ($P > 0.05$). After isolation with MACS, the expression of *NANOG* was lowest in testicular suspension and highest in the control group ($P > 0.05$). The gene expression was lower in isolated than in non-isolated groups.

OCT-4 gene expression was highest in the simple culture, with and without cell isolation ($P < 0.05$). The comparison of cells isolated with and without MACS showed no difference in gene expression ($P > 0.05$, Fig.3).

Epigenetic results of MSP in different groups during culture

MSP results with methylated primer for *Integrin α6*, *β1*, and *PLZF* gene in all cultured cells had a similar pattern in all culture systems and remained non-methylated. The size of the proliferation fragment for *Integrin α6* for methylated primers was 100 bp and for non-methylated primers 101 bp. They were 203, and 205 bp for *Integrin β1* gene, while for *PLZF* gene they were 125, and 130 bp, respectively. Methylation pattern did not change in *C-MYC* and *OCT-4* gene during culture and it remained in partial methylation. The size of the proliferation fragment was 140 bp for methylated and non-methylated primers in *PLZF* gene and 105 bp for *OCT-4* (Fig.4).

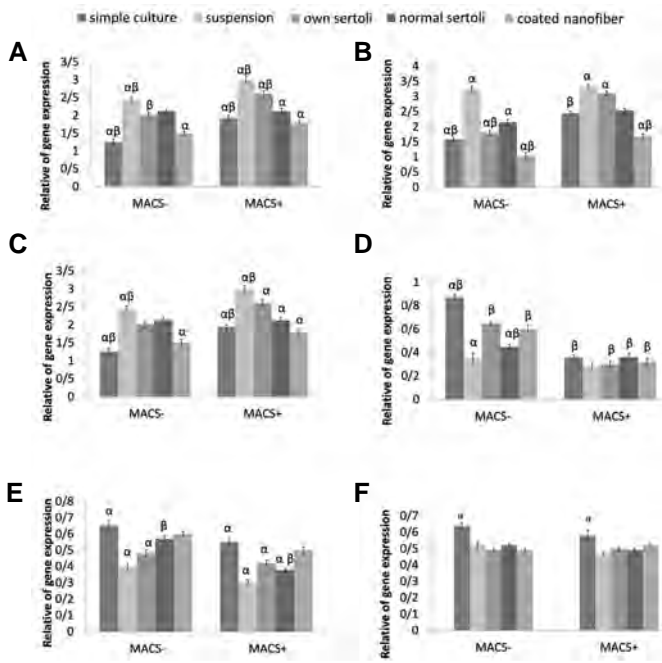


Fig.3: Quantitative gene expression analysis by qRT-PCR. **A.** *Integrin α6*, **B.** *β1*, **C.** *PLZF*, **D.** *NANOG*, **E.** *C-MYC*, and **F.** *OCT-4*, during spermatogonial cells culture in the studied groups. In each group, the expression level of a gene in each sample is normalized to *TBP*, as an internal control. The level of expression of each sample is also calibrated to a calibrator (the cells derived from second enzymatic digestion). α; Significant differences with other groups each time ($P \leq 0.05$), β; Significant differences between MACS⁺ and MACS⁻ groups ($n=3$, $P < 0.05$, $P \leq 0.05$).

The results of *in vivo* assessment

Regarding the culture results of the previous steps as well as epigenetic studies, the suspension culture group was considered the best group, and the resulting cells were selected for transplantation. The azoospermic status of the mice before transplantation was confirmed (Fig.5A).

Monitoring the transplanted cells

The results of the sections' assessment showed that after 4 weeks, the cells were placed at the base of seminiferous tubes (Fig.5B); after 8 weeks, the tracked cells were shown in the diameter of seminiferous tubes (Fig.5C); and after 16 weeks, some seminiferous tubes of the transplanted testis (Fig.5D, left side) contained spermatozoa. Also, endogenous spermatogenesis was observed in the control testis (right side, Fig.5B-D).

Comparison of the testes' weight and number of sperms in epididymis between the transplanted and control testis

The mean testis weight of the azoospermic SSCs transplanted and control mice showed a significantly higher mean weight than azoospermic (sham group: without SSCs transplantation) and the opposite side testis of the transplanted azoospermic mice that were not transplanted after 16 weeks (0.08 ± 0.00058 , 0.095 ± 0.0015 , 0.057 ± 0.0032 , 0.063 ± 0.0051 g respectively, $P < 0.05$). The mean

testis weight of the transplanted group was significantly lower than the mean testis weight of normal healthy adult mice ($P < 0.05$, Fig.6A).

Assessment of the number of sperms in epididymis revealed that the transplanted and control testis had significantly higher mean sperms than the sham and opposite side testis groups after 16 weeks (26 ± 5 , 31 ± 9 , 18.7 ± 4 , 16.3 ± 5 respectively, $P < 0.05$). The mean sperm count of the transplanted group was significantly higher than the mean sperm count of the sham and opposite side testis groups ($P < 0.05$). The mean number of sperms in the control testis of the transplanted mouse was similar to the transplanted group ($P > 0.05$, Fig.6B).

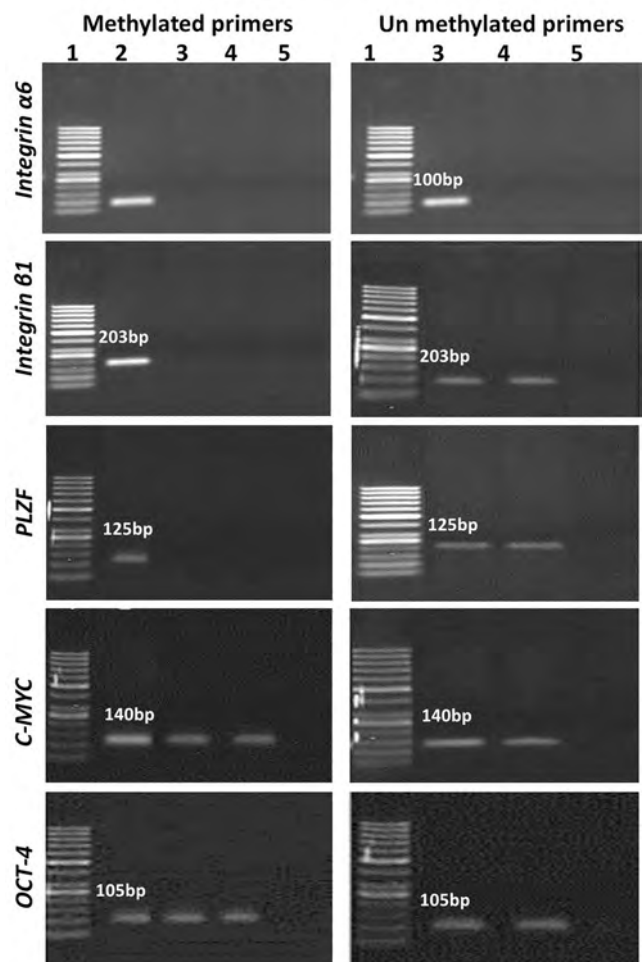


Fig.4: Results of MSP-PCR for methylation of genes *Integrin α6*, *β1*, *PLZF*, *C-MYC*, and *OCT-4*. Left image: MSP with methylated primer. Right image: MSP with non-methylated primer. Column 1; Ladder 50 bp, Column 2; Positive control of methyl primer, Column 3; The group MACS⁻ one week after *in vitro* culture, Column 4; Group MACS⁺ one week after *in vitro* culture, and Column 5; Negative control.

Histopathology of testis sections in the transplanted and control testis

Based on Figure 6C-E, the mean number of spermatogonia, spermatocytes, and spermatids was higher in the transplanted testis than in the control and sham ($P < 0.05$), but it was

significantly lower than that of normal healthy adult mice ($P < 0.05$). The mean number of cells in the control testis of the transplanted mouse was similar to that of the sham group ($P > 0.05$).

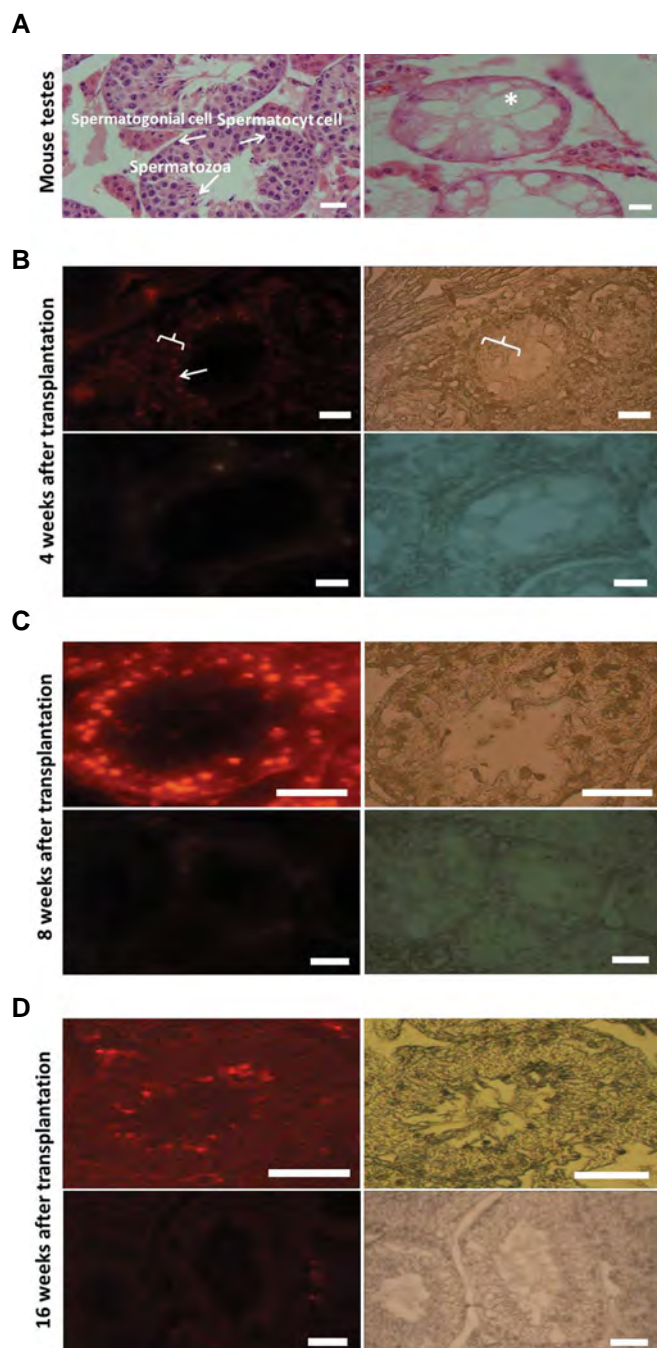


Fig.5: The results of *in vivo* assessment. **A.** Histological examination of seminiferous tubules in mouse testes before and after busulfan injection. **B-D.** Tracking human spermatogonial cells 4, 8, and 16 weeks after transplantation. **B.** Human SSCs on the base of the mouse seminiferous tubules after 4 weeks of transplantation. **C.** Human SSCs within the mouse seminiferous tubules 8 weeks after transplantation. **D.** Derived sperm were observed in the mouse testes 16 weeks after transplantation. The cell showing Dil staining was considered transplanted cells. The top figures in each group (A-D) are the sections of the testicular seminiferous tubules transplanted and the bottom figures are related to the opposite testicle as a control (the right testis is considered as the control group without transplantation of donor). The figures on the left side are fluorescent and the figures on the right side are phase contrast (scale bars: 20 μ m).

Assessment of *CatSper* gene in the transplanted testis

CatSper gene was evaluated after 16 weeks of transplantation in the azoospermic mouse model. The expression of this gene in the transplanted testis showed proliferation and presence of the human *CatSper* gene in the transplanted testis. Nevertheless, the results showed significantly lower *CatSper* gene expression in the transplanted testis than in the human testis ($P < 0.05$). The expression of this gene was zero in the control testis (Fig.6F).

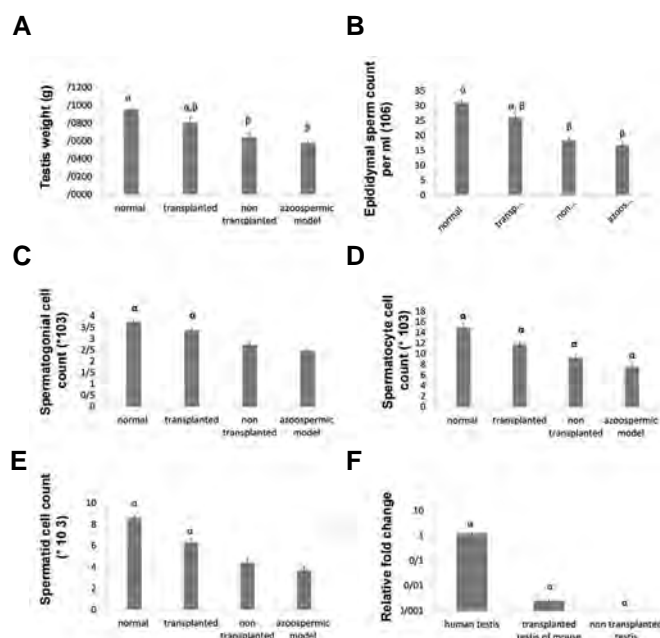


Fig.6: Comparison between the transplanted and control testis. **A.** Mean testis' weight (s), **B.** Mean the number of sperms in the epididymis among the groups. **C.** Mean the number of spermatogonia, **D.** Spermatocytes, **E.** Spermatids in seminiferous tubes among the study groups. **F.** The pattern of *CatSper* gene expression after 16 weeks of transplantation in the azoospermic mouse model. α and β ; Significant differences with others ($P \leq 0.05$).

Discussion

Optimization of a system for the proliferation and differentiation of male germ cells is a valuable tool for managing male infertility and spermatogenesis regulation (18). One of the important regulators in different spermatogenesis processes is epigenetic modifications (19). Genetic and epigenetic structures of chromatin are essential for fertile sperm production (20). Hence, we used MACS for human SSCs purification by *GFR- α* positive marker. *GFR α* is a self-renewal-related or pre-meiotic gene, expressed in undifferentiated SSCs such as A_{single} , A_{paired} and spermatogonia $A_{alleled}$ (21). The MACS⁺ isolated SSCs were cultured in different culture systems and compared for genetic and epigenetic expression between five experimental groups; i. Control two dimensional culture, ii. Co-culture of SSCs with

Sertoli cells of men with OA, iii. Co-culture of SSCs with healthy Sertoli, iv. Culture of SSCs on PLA nanofiber, and v. Culture of testicular cell suspension. Researchers have similarly investigated the isolation of human SSCs through the FACS method (9, 22). Meanwhile, the high costs and time-consuming nature of FACS may limit its application in cell isolation. Thus, we used two-step enzyme lysis and incubation of the resulting cells for one night and isolation of suspended spermatogonial cells on the next day, as required in different groups. The results of the present study confirmed *GFR- α 1* (GDNF receptor) as an effective marker in improving SSCs isolation, which has been previously suggested by Godmann et al. (23) as well. It has been confirmed that GDNF supplies the necessary items for the growth and maintenance of human SSCs in the medium and generally shows the suitability of MACS with *GFR- α 1* for isolation and enrichment of human SSCs (24). Miltenyi et al. (25) suggesting MACS as a fast and simple separation system for large immunologic cells. Baert et al. (26) cultured MACS-enriched epithelial cells in the interstitial cell-laden scaffolds (CD49f+/CLS). They observed double-cell compartment testicular constructs. Cell spheres showed in the pores after cell seeding on CFS and CLS. The elongated spermatids were observed in 66% of TC/CFS. Differentiation was achieved in all and 33% of CD49f+/CLS constructs, respectively.

The MACS enriched and non-enriched (SSCs cultured without MACS sorting) SSCs were cultured in the control and treated groups; co-culture of SSCs with Sertoli cells of men with OA, co-culture of SSCs with healthy Sertoli cells, the culture of SSCs on PLA nanofiber, and culture of testicular cell suspension. We observed significantly the highest expression of *Integrin α 6* and *PLZF* genes in the testicular suspension cells group and lowest expression in the simple culture group than in other groups. *Integrin β 1* gene expression was highest in testicular suspension cells and lowest in the PLA nanofiber group, which confirmed that testicular suspension cells could effectively purify and enrich the functional human spermatogonial cells. *Integrin α 6* and *Integrin β 1* are premeiotic markers and they have a connection to laminin and collagen proteins in the base membrane of seminiferous tubes (6). Nevertheless, the expression of *OCT-4* gene was not significantly different among groups. The gene expression of *OCT-4* and *PLZF* is related to GDNF and affects the self-renewal of SSCs (27, 28). The three-dimensional culture, with the aid of an extracellular matrix, enables cells to organize properly and imitate the spermatogonial epithelium (29). The use of three-dimensional culture on PLA nanofiber with a laminin layer in the present study showed the superiority of this method over simple culture, regarding germ-cell specific gene expression. We used PLA, because of their biodegradability and biocompatibility, which is quickly made by electrospinning and creates a three-dimensional non-woven grid. Eslahi et al. (8) cultured SSCs seeded on PLLA with the control groups and suggested that PLLA increases the colony formation of human SSCs in the culture system. Also in the present study, a superior co-culture with Sertoli cells in comparison with the control

group was observed. It might be SSCs culture with GDNF-secreting Sertoli cells acting as spermatogonial cell renewal regulator. Koruji et al. (30) co-cultured human SSCs and Sertoli cells and observed an increase in the count and diameter of SSC colonies. The gene expression of pluripotency genes showed minimum expression of *C-MYC* gene and Nanog in testicular suspension cells, especially after isolation with MACS with increased gene expression during culture in all isolated groups. Rajpert-De Meyts et al. (31) could isolate multivalent germ cells from the adult human testis by using suitable culture conditions to isolate embryonic stem cells. They observed that these cells express *OCT-4* proteins but do not express *NANOG*.

According to our previous study, the suspension culture group is regarded as most similar to testes' micro-environment (13). We observed that the other culture groups, such as Sertoli and PLA nanofiber, which kept the nature of human SSCs also confirms the importance of the presence of extracellular matrix, micro-environment, and their signaling. On the other hand, germ cells often show genetic and epigenetic changes *in vitro*, and SSCs seem to maintain relative genetic stability. SSCs characteristics did not change and cells were not differentiated suggesting the stability of this culture technique, which could be due to the protective effect of GDNF against differentiation (32). It can be a reason for prolonged epigenetic changes after culture among different groups with and without MACS. This may limit the assessment of gene expression and DNA methylation to only some printed genes. Because of this, comparative genomic hybridization is not able to detect small genetic changes. Goossens et al. (33) evaluated the DNA methylation pattern in a paternally methylated gene (*Igf2*), a maternally methylated gene (*Peg1*), and a non-imprinted gene (*α -Actin*). The spermatids obtained from the 3D-I system have similarities in global gene profile and DNA methylation compared to *in vivo* spermatids. They used MACS for human spermatogenesis *in-vitro*, by isolating GPR125⁺ spermatogonia from the testes of OA patients.

Transplantation of SSCs is a fertility restoration option that has already been introduced as a convenient method in animals (16). Studies on the imprinting situation after SSCs transplantation are limited but show that implantation does not change. The results of the present study on transplantation of human SSCs, cultured with healthy Sertoli cells to seminiferous tubes of a recipient mouse, showed that it can result in spermatogenesis with a donor origin. Although transplantation of human SSCs is not likely to produce sperm in mice, it may activate endogenous spermatogenesis-stimulating factors. Thus, we evaluated sperm production in mice after 16 weeks. When the SSCs from the donor are transplanted to the seminiferous tubes of an infertile recipient, the germ cells of the donor migrate to the lateral base of the tubes in the seminiferous tubes of the recipient, then proliferate, produce new colonies, and start spermatogenesis

with a donor origin (35). Although initial studies have experimented with mice models (16), this technique can be useful in spermatogenesis studies of other animals as well. Indeed, some studies have reported successful heterografts from mouse testis to hamsters that resulted in spermatogenesis of mouse and hamster (36). There are several studies that transplanted human SSCs into the mouse testis and reported that SSCs adhere to the seminiferous tubules after 2 weeks (22, 34). Mohaqiq et al. (34) isolated human SSCs and confirmed them by *PLZF* protein. They transplanted SSCs to adult azoospermia mouse testes and studied them after two weeks. The results revealed that the number of SSCs was significantly more than those in the control group. IHC studies and qRT-PCR indicated that the *PLZF* was only expressed in the transplantation groups. The results of SSCs transplantation in our study were similar to others (9, 34).

GCT, as the ultimate goal of these cellular studies, could successfully restore spermatogenesis in animal models and resolve infertility, which is considered the gold standard (37). Further research continues to elucidate different aspects of GCT for successful experiments on humans. Despite the scientific development in stem cells, human SSCs culture is still a controversial issue. The results of the present study can dynamically add to the knowledge of researchers and clinicians and is an important step toward future clinical use for male infertility, which was the strongest strength of the present study. In addition, we could successfully achieve an appropriate number of cells through a two-phase culture which was an important limitation in previous studies (38). Yet, the current study had some limitations, including the fact that the transplantation experimented on mice and thus, the results cannot easily be generalized to humans. Further research on mammals can add to the results of the present study.

Conclusion

The epigenetic pattern showed that the specific methylation of the evaluated genes at this stage remained constant throughout the entire culture system over time and the culture conditions did not alter the methylation pattern. Also, MACS could increase the efficiency of human SSCs isolation and purification by 69% with the testicular suspension group showing the highest expression of germ cell genes (*Integrin α6, β1*, and *PLZF*), and lowest gene expression of *C-MYC* gene and *NANOG*, among the tested groups. Further, the proposed culture systems could maintain the cell-specific genetic and epigenetic contain and the suspension cells group known as the best system for SSCs culture *in vitro*. Thus, the results indicate the ability of purification and proliferation of functional cells in the suspension culture.

Acknowledgements

Financial support of this work was provided by the Research Council of Tarbiat Modares University, Iran.

The authors declare no conflict of interest in this project.

Authors' Contribution

M.Z.; Performed the experiments, data acquisition, data analysis and interpretation, and drafting the manuscript. M.M.; Was the conductor of the study, participated in study design, edited the manuscript, also participated in the finalization of the manuscript, and also approved the final draft. S.J.M., M.N.; Advised for genetic and epigenetic assessment, real-time PCR technique, extracted mRNA and produced cDNA. M.R.N; Advised sample collection and separated SSC from samples. M.K., F.A.; Performed transplantation and participated in statistical analysis, and edited the manuscript. All authors were involved in the drafting and revision of the draft manuscript.

References

1. Martinovitch P. The development in vitro of the mammalian gonad. Ovary and ovogenesis. Proc R Soc B: Biol Sci. 1938; 125(839): 232-249.
2. Ge SQ, Lin SL, Zhao ZH, Sun QY. Epigenetic dynamics and interplay during spermatogenesis and embryogenesis: implications for male fertility and offspring health. Oncotarget. 2017; 8(32): 53804-53818.
3. Topraggaleh TR, Valojerdi MR, Montazeri L, Baharvand H. A testis-derived macroporous 3D scaffold as a platform for the generation of mouse testicular organoids. Biomater Sci. 2019; 7(4): 1422-1436.
4. Bahadur G. Ethics of testicular stem cell medicine. Hum Reprod. 2004; 19(12): 2702-2710.
5. Galdon G, Atala A, Sadri-Ardekani H. In vitro spermatogenesis: how far from clinical application? Curr Urol Rep. 2016; 17(7): 49.
6. Hofmann M-C. Gdnf signaling pathways within the mammalian spermatogonial stem cell niche. Mol Cell Endocrinol. 2008; 288(1-2): 95-103.
7. Hwang K, Lamb DJ. New advances on the expansion and storage of human spermatogonial stem cells. Curr Opin Urol. 2010; 20(6): 510-514.
8. Eslahi N, Hadjighassem MR, Joghataei MT, Mirzapour T, Bakhtiyari M, Shakeri M, et al. The effects of poly L-lactic acid nanofiber scaffold on mouse spermatogonial stem cell culture. Int J Nanomed. 2013; 8: 4563-4576.
9. He Z, Kokkinaki M, Jiang J, Dobrinski I, Dym M. Isolation, characterization, and culture of human spermatogonia. Biol Reprod. 2010; 82(2): 363-372.
10. Aslam I, Robins A, Dowell K, Fishel S. Isolation, purification and assessment of viability of spermatogenic cells from testicular biopsies of azoospermic men. Hum Reprod. 1998; 13(3): 639-645.
11. Nagano MC. Techniques for culturing spermatogonial stem cells continue to improve. Biol Reprod. 2011; 84(1): 5-6.
12. Panda RP, Barman H, Mohapatra C. Isolation of enriched carp spermatogonial stem cells from Labeo rohita testis for in vitro propagation. Theriogenology. 2011; 76(2): 241-251.
13. Zahiri M, Mowla SJ, Noruzinia M, Koruji M, Nowroozi MR, Bashiri Z. The epigenetic assessment and proliferation of human spermatogenic cells derive from obstructive azoospermic patients in different culture systems. Urol J. 2020: 6092.
14. Rameshbabu AP, Ghosh P, Subramani E, Bankoti K, Kapat K, Datta S, et al. Investigating the potential of human placenta-derived extracellular matrix sponges coupled with amniotic membrane-derived stem cells for osteochondral tissue engineering. J Mater Chem B. 2016; 4(4): 613-625.
15. Goodyear S, Brinster R. Spermatogonial stem cell transplantation to the testis. Cold Spring Harb Protoc. 2017; 2017(4): pdb-prot094235.
16. Brinster RL, Zimmermann JW. Spermatogenesis following male germ-cell transplantation. Proc Natl Acad Sci USA. 1994; 91(24): 11298-11302.
17. Kadam P, Ntemou E, Onofre J, Van Saen D, Goossens E. Does co-transplantation of mesenchymal and spermatogonial stem

- cells improve reproductive efficiency and safety in mice? *Stem Cell Res Ther.* 2019; 10(1): 310.
18. Gholami K, Pourmand G, Koruji M, Sadighilani M, Navid S, Izadyar F, et al. Efficiency of colony formation and differentiation of human spermatogenic cells in two different culture systems. *Reprod Biol.* 2018; 18(4): 397-403.
 19. Carrell DT, Hammoud SS. The human sperm epigenome and its potential role in embryonic development. *Mol Hum Reprod.* 2010; 16(1): 37-47.
 20. Jenkins TG, Carrell DT. The paternal epigenome and embryogenesis: poisoning mechanisms for development. *Asian J Androl.* 2011; 13(1): 76-80.
 21. Ziloochi Kashani M, Bagher Z, Asgari HR, Najafi M, Koruji M, Mehraein F. Differentiation of neonate mouse spermatogonial stem cells on three-dimensional agar/polyvinyl alcohol nanofiber scaffold. *Syst Biol Reprod Med.* 2020; 66(3): 202-215.
 22. Mirzapour T, Movahedin M, Koruji M, Nowroozi M. Xenotransplantation assessment: morphometric study of human spermatogonial stem cells in recipient mouse testes. *Andrologia.* 2015; 47(6): 626-633.
 23. Godmann M, May E, Kimmins S. Epigenetic mechanisms regulate stem cell expressed genes *Pou5f1* and *Gfra1* in a male germ cell line. *PLoS One.* 2010; 5(9): e12727.
 24. Kossack N, Meneses J, Shefi S, Nguyen HN, Chavez S, Nicholas C, et al. Isolation and characterization of pluripotent human spermatogonial stem cell-derived cells. *Stem Cells.* 2009; 27(1): 138-149.
 25. Miltenyi S, Müller W, Weichel W, Radbruch A. High gradient magnetic cell separation with MACS. *Cytometry.* 1990; 11(2): 231-238.
 26. Baert Y, Dvorakova-Hortova K, Margaryan H, Goossens E. Mouse *in vitro* spermatogenesis on alginate-based 3D bioprinted scaffolds. *Biofabrication.* 2019; 11(3): 035011.
 27. Shams A, Eslahi N, Movahedin M, Izadyar F, Asgari H, Koruji M. Future of spermatogonial stem cell culture: application of nanofiber scaffolds. *Curr Stem Cell Res Ther.* 2017; 12(7): 544-553.
 28. Hamidabadi HG, Bojnordi MN. Co-culture of mouse spermatogonial stem cells with sertoli cell as a feeder layer, stimulates the proliferation and spermatogonial stemness profile. *Middle East Fertil Soc J.* 2018; 23(2): 107-111.
 29. Asgari F, Khosravimelal S, Koruji M, Ahovan ZA, Shirani A, Hashemi A, et al. Long-term preservation effects on biological properties of acellular placental sponge patches. *Mater Sci Eng.* 2021; 121: 111814.
 30. Koruji M, Movahedin M, Mowla S, Gourabi H, Arfaee A. Efficiency of adult mouse spermatogonial stem cell colony formation under several culture conditions. *In Vitro Cell Dev Biol Anim.* 2009; 45(5-6): 281-289.
 31. Rajpert-De Meyts E, Bartkova J, Samson M, Hoei-Hansen CE, Frydelund-Larsen L, Bartek J, et al. The emerging phenotype of the testicular carcinoma in situ germ cell. *APMIS.* 2003; 111(1): 267-279.
 32. Sada A, Hasegawa K, Pin PH, Saga Y. NANOS2 Acts downstream of glial cell line-derived neurotrophic factor signaling to suppress differentiation of spermatogonial stem cells. *Stem Cells.* 2012; 30(2): 280-291.
 33. Goossens E, De Rycke M, Haentjens P, Tournaye H. DNA methylation patterns of spermatozoa and two generations of offspring obtained after murine spermatogonial stem cell transplantation. *Hum Reprod.* 2009; 24(9): 2255-2263.
 34. Mohaqiq M, Movahedin M, Mazaheri Z, Amirjannati N. Successful human spermatogonial stem cells homing in recipient mouse testis after *in vitro* transplantation and organ culture. *Cell J.* 2019; 20(4): 513.
 35. Ohta H, Yomogida K, Yamada S, Okabe M, Nishimune Y. Real-time observation of transplanted 'green germ cells': proliferation and differentiation of stem cells. *Dev Growth Differ.* 2000; 42(2): 105-112.
 36. Honaramooz A, Behboodi E, Blash S, Megee S, Dobrinski I. Germ cell transplantation in goats. *Mol Reprod Dev.* 2003; 64(4): 422-428.
 37. Brinster RL. Germline stem cell transplantation and transgenesis. *Science.* 2002; 296(5576): 2174-2176.
 38. Huleihel M, Fadlon E, Abuelhija A, Piltcher Haber E, Lunenfeld E. Glial cell line-derived neurotrophic factor (GDNF) induced migration of spermatogonial cells *in vitro* via MEK and NF-kB pathways. *Differentiation.* 2013; 86(1-2): 38-47.
-